DOCTORAL SCHOOL IN ENGINEERING
SECTION SCIENCES OF CIVIL ENGINEERING

SCUOLA DI DOTTORATO IN INGEGNERIA
SEZIONE SCIENZE DELL'INGEGNERIA CIVILE

XXV DOCTORAL CYCLE

XXV CICLO DI DOTTORATO

STRESS-CORROSION AND LIFETIME IN GLASS: INFLUENCE OF ENVIRONMENTAL CONDITIONS

CORROSIONE SOTTO SFORZO E TEMPO VITA NEL VETRO:
INFLUENZA DELLE CONDIZIONI AMBIENTALI

PhD student: Costanza Ronchetti

Supervisor: Professor Ginevra Salerno

Doctoral school coordinator: Professor Leopoldo Franco

Series of PhD thesis
Sciences of Civil Engineering
Università degli Studi Roma Tre
Thesis n° 40

Collana delle tesi di Dottorato di Ricerca
In Scienze dell'Ingegneria Civile
Università degli Studi Roma Tre
Tesi n° 40

Abstract

The problem of glass strength arises from the increasingly spread use of the material in building. Due to its high transparency, glass has been always used as closure element, but in recent years a tendency of using it for structural purpose is growing rapidly. In addition, glass provides challenging solutions for conservation of archaeological heritage. These reasons require a deep investigation on failure mechanisms of glass and above all on its resistance to tensile stress.

Since 1920, linear elastic fracture mechanics allowed understanding the reasons of the low tensile strength values registered in glass. It seems that this is due to the propagation, even very slow, of surface microdefects induced by manufacturing processes. Later, physical theories empirically founded further investigated on the processes of rupture in glass, observing that microdefects may evolve up to structural failure not only for a stress increase but also as consequence of chemical-physical interaction with surrounding environment.

Most of prediction models which aim at evaluating a glass element lifetime are based on empirical laws. The parameters of those theories are related to the influence of environment but their values are provided by the literature only within limited ranges. However, the influence of environmental variables is complex and not secondary. In addition, in recent years, glass is being used in building even in non favorable climatic conditions. This latter is a challenging aim, considering the high aesthetic qualities of glass.

For these reasons, the present thesis considered necessary to investigate on the microphysics and chemistry which determine the phenomenon of environmental corrosion, and this allowed identifying the physical variables which play the most influent role. Secondarily, an expression of failure time as explicit function of environmental variables is provided, focusing on temperature and relative humidity. Through parameter calibration, on the basis of four-point beam-bending tests, a lifetime curve is obtained for a given environment.

This work arises on the one hand from a physical interest and it shows a scientific coherence, considering the strong influence of environmental variables, and on the other hand it is strictly connected to

design purposes, since glass is being used in increasingly disparate climatic conditions. For this latter reason, to be able to express failure time as function of environment becomes a non negligible need.

Keywords : stress-corrosion, physical variables, temperature, relative humidity, lifetime.

Sommario

Il problema della resistenza del vetro nasce dall'uso sempre più diffuso del materiale in ambito edilizio. Grazie all'elevata trasparenza, il vetro è da sempre utilizzato come elemento di chiusura, ma negli ultimi anni si sta diffondendo una tendenza ad un uso anche strutturale del medesimo. Inoltre, il vetro garantisce soluzioni ottimali in contesti archeologici. Tutto questo implica una necessità di investigare i meccanismi di rottura del materiale ed in particolare la sua resistenza a sforzi di trazione.

A partire dagli anni venti, la meccanica della frattura lineare elastica ha consentito negli anni di comprendere la ragione dei bassi valori di resistenza a trazione riscontrati nel vetro, insita nella propagazione anche lenta di microdifetti superficiali indotti dai processi di manifattura. Successivamente, teorie fisiche empiricamente fondate hanno investigato ulteriormente sui processi di rottura nel vetro, osservando come i microdifetti evolvono sino a portare al collasso strutturale non solo per un aumento dello stress applicato ma anche per via dell'interazione chimico-fisica con l'ambiente.

La maggior parte dei modelli predittivi che consentono di valutare il tempo vita di un elemento di vetro si basa su leggi di tipo empirico. I parametri di tali leggi si riferiscono all'influenza dell'ambiente ma sono forniti dalla letteratura entro dei range limitati. Tuttavia, il peso delle variabili ambientali è complesso e non di secondo piano. Va inoltre detto che il vetro, recentemente, viene usato in ambito edilizio in situazioni climatiche anche poco favorevoli. Quest'ultimo è un obiettivo intrigante, considerando le alte qualità estetiche del materiale.

Per queste ragioni, la presente tesi ha visto necessario un approfondimento della microfisica e della chimica che sono alla base del fenomeno di corrosione ambientale, e ciò ha consentito di individuare le variabili fisiche che hanno maggiore influenza. In un secondo momento, si è scelto di arrivare ad una espressione del tempo vita come funzione esplicita delle variabili ambientali, in particolare di temperatura ed umidità relativa. Attraverso una taratura dei parametri del problema, sulla base di prove di flessione su quattro punti, si ricava una curva di *lifetime* in funzione dell'ambiente.

Quest'obiettivo è da una parte spinto da un interesse fisico e mostra una coerenza scientifica, considerando la forte influenza delle variabili ambientali, e dall'altra è legato a scopi progettuali, dal momento che il vetro viene usato in condizioni climatiche sempre più diversificate e poter esprimere il tempo vita in funzione dell'ambiente diventa una esigenza non trascurabile.

Parole chiave : corrosione sotto sforzo, variabili fisiche, temperatura, umidità relativa, tempo vita.

Résumé

Le problème d'évaluer la résistance du verre nait à partir de l'utilisation de plus en plus diffusée du matériau dans le domaine de la construction. Grâce à sa grande transparence, le verre a toujours été utilisé comme élément de fermeture, mais récents il est aussi employé dans les parties structurelles des bâtiments. Cela implique la nécessité d'examiner les mécanismes de rupture du matériau et en détail sa résistance aux contraintes de traction.

A partir de 1920, la mécanique de la fracture linéaire élastique a permis pendant les ans de comprendre la raison des valeurs très faibles de résistance à traction qui étaient registrées dans le verre. La cause de ça est une évolution même lente de microdéfauts de surface qui sont produits par les procédés de fabrication.

En suite, des théories physiques empiriquement fondées ont examiné plus loin les processus de rupture dans le verre, en observant que les microdéfauts évoluent non seulement par l'augmentation de la contrainte appliquée mais aussi comme conséquence de l'interaction chimique-physique avec l'environnement.

La plupart des modèles prédictifs qui permettent d'évaluer le temps de vie d'un élément de verre est fondée sur des lois empiriques. Les paramètres de ces lois se réfèrent à l'influence de l'environnement mais ils sont donnés par la littérature dans une gamme limitée. Toutefois, l'influence des variables environnementales est complexe et elle ne peut pas être négligée. Par ailleurs, le verre est récents employé dans le domaine de bâtiment aussi dans des situations climatiques défavorables. Cela est un objectif intéressant si on considère les grandes qualités esthétiques du matériau.

Pour ces raisons, cette thèse a considéré nécessaire une étude de la microphysique et de la chimique qui sont à la base du phénomène de la corrosion environnementale, et cela a permit d'identifier les variables physiques qui ont la plus grande influence.

A un moment ultérieur, on est arrivé à exprimer les temps de vie comme fonction explicite de l'environnement, en particulier de la température et de l'humidité relative. Grâce à un calibrage des paramètres, fondé sur des essais expérimentaux de flexion quatre-points, on obtient

une courbe de temps de vie comme fonction de l'environnement.

Cet objectif est dérivé d'une partie de l'intérêt physique, et il montre une cohérence scientifique, en considérant la grande influence des variables environnementales, et de l'autre partie il est lié à des fins de conception, puisque le verre est utilisé en conditions climatiques toujours plus diversifiées, et donc exprimer le temps de vie en fonction de l'environnement devient une exigence qui ne peut pas être négligée.

Mots-clés : corrosion sous contrainte, variables physiques, temperature, humidité relative, temps de vie.

Acknowledgements

First of all, I would like to thank Professor Ginevra Salerno, supervisor of this thesis, for giving me the chance of improving the quality of my work and for supporting all my efforts during my studies.

I would like to thank Professor Nicola Rizzi, for giving me the idea of studying glass and for the useful suggestions.

Thanks are furthermore due to Professor Antonio Di Carlo, for giving me interesting suggestions during my PhD.

This work has been supported by an experimental investigation carried out at Steel Structures Laboratory Icom in EPFL (Lausanne, Switzerland). For this, I would like to thank Professor Jean-Paul Lebet, director of Icom Lab, for accepting me and allowing me performing tests. Further, special thanks go to Dr. Christian Louter, who supported my research in EPFL with useful suggestions and to Maria Lindqvist for her help.

I would also like to thank Dr. Tiziana Persichini of the Biology Department of Roma Tre University for having allowed the microscopic investigations that helped this work.

During my PhD studies, I had the opportunity of working within a very pleasant research environment. For this, special thanks go to Valerio, who helped me most of all at the beginning of my studies. I also thank Luciano, for his useful suggestions, and I thank Manuela for her support especially during these last months, and I thank Stefano, for giving me a clear idea of the difficulties I would find during PhD and for the great atmosphere that he can bring.

Of course I thank my family, my parents, my sister and my brother, for supporting me during my PhD studies and for their interest in my work. A very special thank goes to my sister-in-law Angela, who more than any other was close to me with her support and help.

Special thanks go to my close friends, Giulia, Carolina, Azzurra, Bruno, Serena, Paolo, Alessandra for their support and encouragement.

I finally greatly thank my partner, for all the time spent in supporting me during my studies and for understanding when I had to work in the evening and in the week-ends.

Contents

List of Figures

List of Tables

List of symbols

The following list shows the main symbols used in the present thesis:

Symbol	Description
θ	angle associated at a point close to the crack tip
μ	modulus of rigidity of the material
μ_B	chemical potential of an initial bond
μ_B^*	chemical potential of the activated state
ν	Poisson ratio
ρ	radius of curvature of the crack tip
σ_A	applied tensile stress
σ_c	critical stress
σ_{ch}	characteristic value of the loading history
σ_N	low-temperature strength based on tests in liquid nitrogen
σ_{tip}	tensile stress at the crack tip
σ_x	stress field at the crack tip in x direction
σ_y	stress field at the crack tip normal to the crack plane
$\overline{\sigma}$	equivalent static stress
$\dot{\sigma}$	constant stress rate
ψ	Airy stress function

Symbol	Description
a	crack length, or major semi-axis of elliptical crack
a_{cr}	critical crack length
a_F	crack length corresponding to failure
a_i	initial crack length
a_τ	crack length at $t = \tau$
A	Arrhenius pre-exponential kinetic factor
b	Wiederhorn activation volume considering the curvature of the tip
c	minor semi-axis of elliptical crack
$f_{ij}(\theta)$	generic function of θ describing the stress field at the tip
g	Mencik coefficient for equivalent stress
E_a	activation energy for the chemical reaction
E_a^*	activation energy including the effect of tip curvature
$E_a(0)$	ordinary zero-stress Arrhenius activation energy
h	specimen height
H_c	critical distance for water condensation
k	generic chemical reaction rate
K_I	stress intensity factor for fracture mode I
K_{Ic}	material toughness, i.e. critical value of the stress intensity factor
K_{I1}	stress intensity factor at initial conditions
K_P^0	ideal-gas equilibrium constant
K_{th}	crack growth threshold
L	capillary condensation critical length
n	empirical parameter referring to environmental conditions
OH^-	hydroxyl ion
p_{H_2O}	partial pressure of vapor
$p^o_{H_2O}$	saturation pressure
r	radial distance from the crack tip
R	perfect gas constant
RH	relative humidity
S	tensile stress
SiO_4	Silicon-Oxygen tetrahedron
$SiOH$	silanol
T	absolute temperature
t_F	failure time, i.e. lifetime
T_S	material surface tension
U	total energy of the system
U_M	mechanical energy term
U_S	surface energy term
V	activation volume for the chemical reaction
v_m	mean crack velocity
V_M	molar volume
v_x	corrosion rate in the x direction
v_0	pre-exponential kinetic factor
v_1	crack velocity at initial conditions
Y	defect geometry factor, or shape factor

Ad Ilaria e Angela

Chapter 1

Introduction

1.1 Preliminary considerations on glass

Even in the past, glass was considered a highly challenging material, since its almost total transparency provided relevant aesthetic qualities and natural illumination. For these reasons, glass was employed for building closure elements. In addition, its physical and chemical composition provided interesting optical effects, as witnessed by the *Lycurgus cup* shown in Fig. 1.1, which the Romans built in IV century B.C. by inserting gold and iron nanoparticles within the glass matrix. The use of additives induces interesting effects, since the cup changes colour whether the light is reflected (green) or absorbed (red).

In recent years, the use of glass in building has become more and more spread In addition, it is being used for covering increasingly larger spans. Hence, structural elements as beams and entire façades are made of glass. Some thermal treatments, as tempering, are used to increase glass strength, and the technique of laminating glass, i.e. producing elements made of several layers, provides more safe solutions. In the last ten years, many architectures made of glass have been constructed, as the Apple Store in New York or the glass architectures of the Sanaa group (see Fig. 1.2).

Although the existing techniques for improving glass strength, many research groups are still investigating on the complex behaviour of glass at rupture, aiming on the one hand at gaining a deep knowledge of failure mechanisms, including physical and chemical processes, and on the other hand at providing methods and models for predicting glass failure time, i.e. lifetime. This theme is strictly connected with a phenomenon occurring in glass as in other materials, that is a strong interaction between chemical environment and material structure. In the literature, this is known as stress-corrosion, since the chemical process is stress-dependent. The current lifetime models allow predicting how long a

Figure 1.1: Roman Lycurgus cup, IV century B.C.

structure will last, under a certain loading condition and for given environmental ranges. However, in recent years the use of glass is being increasing even in climatic regions presenting high levels of temperatures and relative humidity, which highly accelerate glass breakage. An explicit correspondence between lifetime and environmental variables is still lacking.

1.2 Aim of the thesis

The present thesis can be framed within this context, since it investigates on microcrack propagation in glass under stress-corrosion regime. On the one hand, physical and chemical processes of stress-corrosion are examined, on the other hand a lifetime prediction model is provided, as function of environmental variables.

The interest in glass arises from several reasons, which may be summarized as follows:

- Increasing structural use of glass requires both a deep knowledge of material fracture behaviour and correct lifetime prediction models;
- The strong influence of environmental variables makes it necessary to express lifetime models as explicit function of environment;

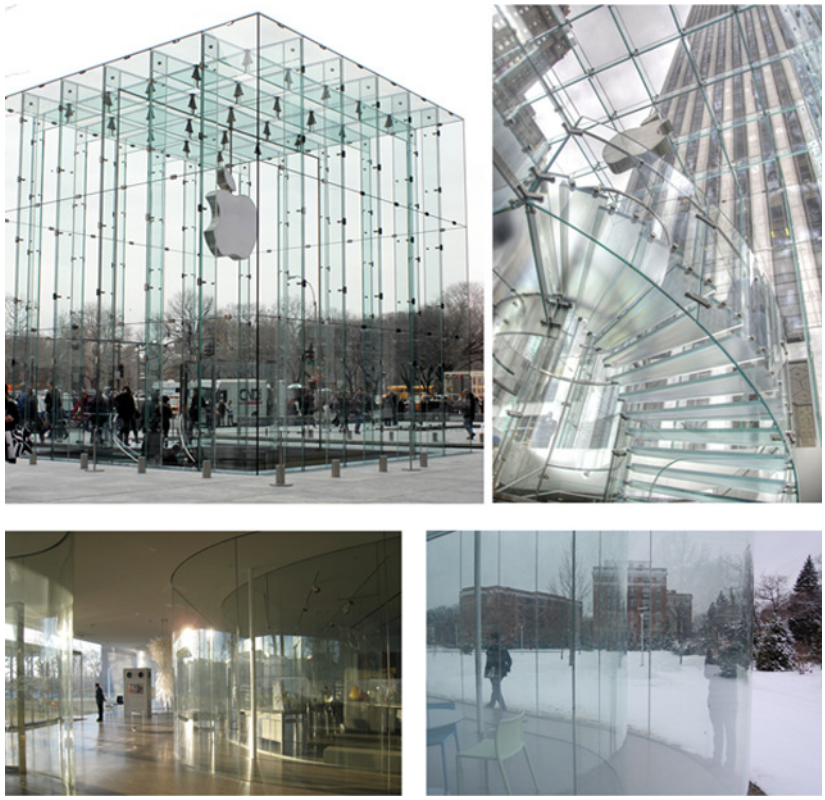

Figure 1.2: Apple Store in New York (top); Sanaa Glass Pavilion in Toledo (bottom).

- The phenomenon of stress-corrosion induces a strong interaction between different spatial scales and different physics, and this implies a multiscale and multiphysics approach;
- Physical-mathematical models for stress-corrosion in glass are still lacking, and an investigation on the physics of the phenomenon is necessary in order to identify the variables that could be included in a possible analytical model.

Indeed, the aim of this work is to provide a method for expressing material lifetime directly in function of temperature and relative humidity. The major part of predicting models are founded on empirical law, and they will be presented in order to frame this work in a current research context.

The proposed method is founded on the one hand on a deep knowledge of stress-corrosion theories, that will be examined, and on the

other hand on experimental investigation performed on small glass specimens. This work arises from a scientific interest but also has a design justification. In addition, the individuation of the environmental variables that mainly affect glass failure mechanisms has allowed selecting the parameters that could be included in a possible physical-mathematical model for glass. Considering the strong interaction between different scales and physics, which is due to glass nature and to the interaction with environment, glass appears as a possible application for a continuum model with microstructure. Some consideration on existing microstructure models will be provided for future developments.

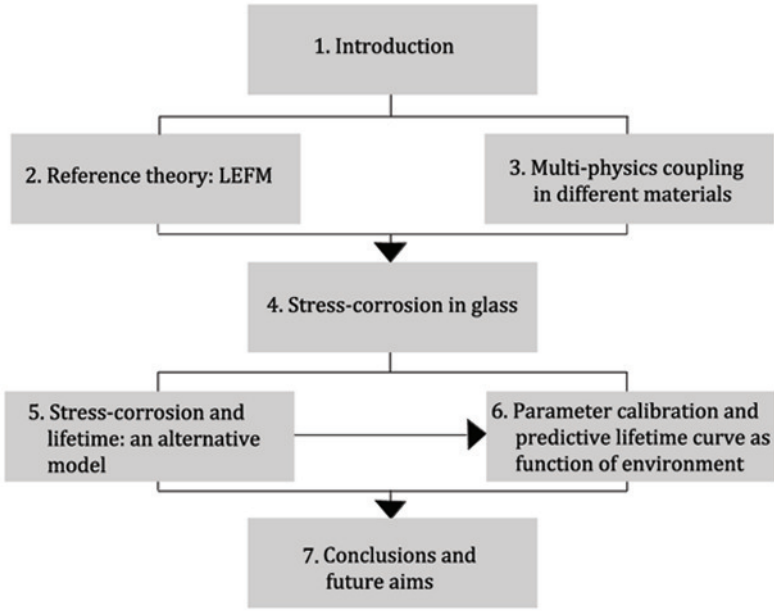

Figure 1.3: Organization of the thesis.

The thesis is composed as follows (see Fig. 1.3): in chapter 1, some considerations on glass failure behaviour are given. In chapter 2, linear elastic fracture mechanics (LEFM) is presented as an explanation of glass failure mechanisms, considering both macroscopic and microscopic scale. A complete comprehension needs to consider even the atomic scale, since microcrack propagation occurs by rupture of interatomic bonds, and stress-corrosion reactions occur at the very small scale, implying even a change of physics. For this reason, chapter 3 presents general cases of multi-physics coupling between mechanical

properties and environment for different material, including the interaction between different spatial scales. Chapter 4 represents the main literature part of the thesis, and it is entirely dedicated to the description of stress-corrosion mechanisms and of different stress-corrosion theories. Chapter 5 gives a design justification of this work, since it presents the strong relation between stress-corrosion and lifetime. Once that current prediction models have been introduced, chapter 6 shows the contribute of this work, presenting a simple methodology for lifetime evaluation, by using a physical relation based on chemical kinetics and by expressing glass failure time in function of temperature and relative humidity, which are the main environmental variables. In this section, the experimental investigation is presented as support of the theory, and lifetime curve for one environmental condition is given. In addition, the same methodology is applied to the case of non-constant stress, that is for linear stress history. Equivalently, a curve of strength as function of stress-rate and environment is provided. Once the effect of environment on stress-corrosion mechanisms and on glass failure time has been illustrated and quantified, it is possible to select the main environmental variables for a future micro-mechanical model. Hence, chapter 7 describes some of the microstructured models from the literature, showing how glass could be seen as an application of them. Finally, this section gives conclusions of the work.

1.3 Focus: mechanical behaviour of glass

In some works, glass is defined as a super-cooled liquid, in some others as a highly viscous solid. In each case, glass is a material which undergoes the phenomenon of vitreous transition, which separates amorphous and crystalline materials. As amorphous solids, glass does not present an ordered atomic structure, and this is one cause of its high transparency. However, its atomic bonds are not as weak as in liquids, even if they are not as strong as in solids.

In this thesis, glass will be treated as a continuum linear-elastic isotropic solid, whose physical atomic structure strongly affects macroscopic behaviour. It will be shown as the nature of the interatomic bonds has a relevant role in mechanical behaviour. In addition, glass chemical composition highly affects material response to stress, and differences between the different types of glass will be discussed. As an example, soda-lime silica glass, whose main structure of Silicon-Oxygen bonds is modified by the presence of other atoms, as Sodium and Calcium, has a low resistance to corrosion, even if it is the most widely used in glass architecture. On the contrary, Silica glass has a relevantly higher resistance, and it is the object of many recent research studies (Ciccotti, 2009). Glass main structure is composed on Silicon-Oxygen

tetrahedrons, and Fig. 1.4 shows the difference between silica glass and soda-lime silica glass.

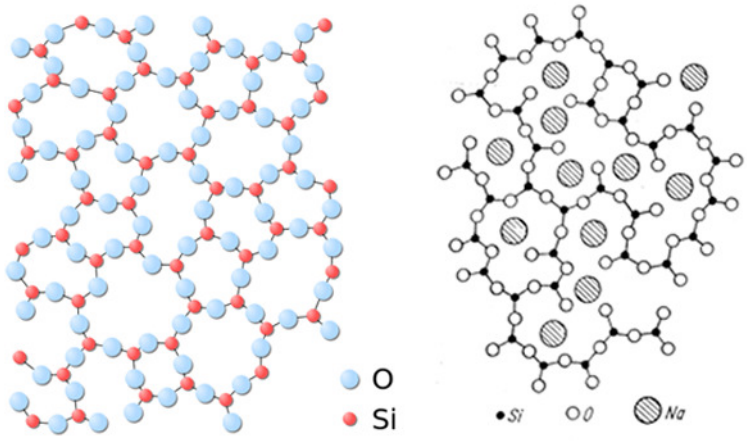

Figure 1.4: Glass atomic structure: silica glass (left) and soda-lime silica glass (right).

By analyzing glass phenomenology, it is normally considered as a brittle material, since non-elastic deformations are confined in very small regions (Pallares et al., 2011). Some recent works consider glass behaviour as quasi-brittle, stating that plastic phenomena are not negligible (Ferretti et al., 2011). In this thesis, glass is considered as perfectly linear-elastic until brittle fracture. As many other brittle materials, glass real tensile strength, evaluated through experiments, is relevantly lower than theoretical strength, considered as a material constant. In order to understand this incongruence, one has to go down from the specimen scale to a smaller scale, that is the microscopic scale. Indeed, microscopic investigations reveal on glass surface several defects as flaws, imperfections, which are normally due to the manufacturing processes and transportation. It seems that these microdefects are the cause of the lowering of real tensile strength. Glass triggered the studies of linear elastic fracture mechanics (LEFM), which considers the presence of microdefects within the elastic continuum material and allows describing behaviour of brittle solids containing flaws. In glass, these initial flaws can be of few micrometers up to hundred of micrometers, depending on the edge finishing used (Lindqvist et al., 2011). As will be discussed, these defects behave as stress concentrators, and this explains why real failure stress is lower than theoretical one. A part from

microscopic exogenous defects, glass atomic structure contains voids or imperfections which represent endogenous defects of nanometer dimensions. It is still open the question whether also atomic defects can affect macroscopic behaviour. A focus on LEFM appears necessary to understand glass fracture behaviour.

Some limits of LEFM arise from mechanisms occurring at the atomic scale. In addition, crack propagation normally occurs in chemically active environments, and not in vacuum. Therefore, in order to understand glass mechanical behaviour, one has to consider that a change of physics occurs. In a small region around the tip of the microcrack, corrosive reactions due to the interaction between environment and glass structure occur, with a relevant consequence on failure mechanisms. The thesis focuses on the problem of stress-corrosion in glass, which has an influence on macroscopic lifetime and shows a relevant interaction between scales and physics. It may be useful to give a glance of multi-physics coupling mechanisms between mechanical properties and environment, which affect not only glass but also many other materials. This will be briefly discussed in chapter 3.

1.4 Focal points

- Structural use of glass, more and more spread in building, requires a focus on material fracture behaviour and appropriate prediction models;
- The influence of environment and the use of glass in increasingly different climatic ranges require to take into account the dependence of material lifetime on environmental variables;
- Glass mechanical behaviour is strongly affected by the presence of microscopic surface defects;
- Linear elastic fracture mechanics (LEFM) provides explanation for the low tensile strength values registered in glass as in other brittle materials, as consequence of the evolution of microdefects;
- In this thesis, glass is modelled as linear-elastic until breakage, although some recent work consider the possibility of non-elastic behaviour;
- Defect evolution in glass is due not only to stress increase but also to a coupling effect between mechanical stress and chemical environment.
- The focus will be on stress-corrosion mechanisms, considering the strong interaction between different scales and physics.

Chapter 2

Reference theory: LEFM

2.1 The purpose of this theory

Since the last centuries, a purpose in design has been to provide criteria for material strength evaluation, in order to predict structural failure. Some first theories of fracture find their origin in XIX^{th} century, when a critical stress criterion was formulated. This criterion states that a material fails when the applied stress reaches a critical characteristic value. However, it was soon discovered that the critical stress criterion was not always appropriate for describing material strength. Indeed, fracture strength was shown to depend on several factors, such as temperature, load rate, environment, material. A simple stress criterion then could not take account of all these parameters.

Linear elastic fracture mechanics arises from these difficulties, and a wide explanation of its developments is given by Broek, who mentions several accidents that had occurred during the XIX^{th} century with metal structures (Broek, 1974). Some unexpected failures often occurred, even in conditions of low stress. An interesting example describes the case of several ships that failed suddenly while laying in the harbor, which is an evident effect of environment. It is clear that, in order to provide explanation for failure mechanisms occurring at levels of stress lower than the critical characteristic one, a new theory was needed. The basis of fracture mechanics is given by a pioneering work proposed by Griffith in 1920 (Griffith, 1920). In this work, he states that the unclear failure mechanisms observed in several brittle materials has to be attributed to the presence of small flaws. Indeed, he studies the case of an isolated crack in a solid under an applied stress and he formulates a criterion for crack propagation from the fundamental theorems of thermodynamics within a frame of linear elasticity. The presence of a flaw induces a stress concentration at its tip, and this is responsible for failure.

After '50s, the use of high strength materials widely increases. These materials are characterized by a low crack resistance, i.e. the residual strength under the presence of cracks is low. The diffusion of these materials runs parallel to new stress analysis methods, for more reliable determination of local stresses. The concept of local is crucial, since the strength of these materials is strongly affected by what locally occurs near the crack, which is a local stress concentrator. It is clear that a change of scale of observation is needed, in order to give correct explanation of macroscopic visible failure. The occurrence of low stress fracture in high strength materials due to small cracks induces the developments of fracture mechanics. This theory provides an alternative to the conventional design criteria based on tensile strength, which are inadequate when cracks are present. Strength appears to be related to the growth of the crack, and LEFM has the purpose of predicting this growth. Crack advance with time may be induced by the application of a cyclic load, or by a combination between loads and environmental attack, as evident in the above-mentioned example of the ship. Stress concentration induced by a crack increases when increasing crack length. This means that the rate of crack propagation increases with time, as shown in Fig. 2.1.

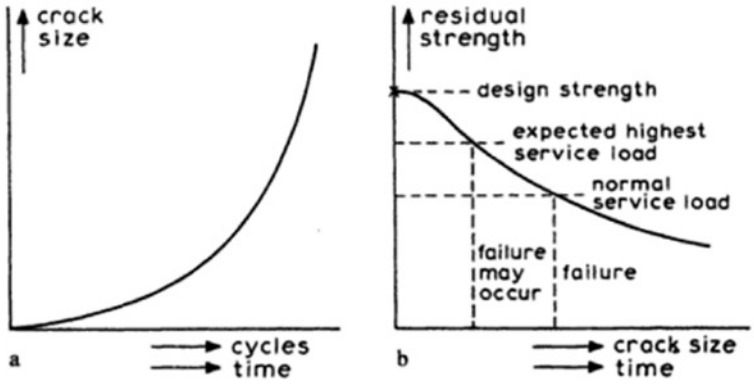

Figure 2.1: Crack length increase (left) and strength decrease (right) *versus* time, from Broek work (Broek, 1974).

Fracture mechanics allows predicting how fast cracks will grow and how fast the residual strength will decrease, and the final aim is to provide prediction models. In order to make some examples of applications, in several materials fracture behaviour is strongly affected by the evolution of microscopic flaws. One could think of ceramic materials as glass, or even metals, alloys, polymers, concrete. It is important to observe that fracture mechanics makes an effort in connecting two

different spatial scales, on the one hand the scale of the defect, which is of micrometer dimension, and on the other hand the scale of the visible breakage, i.e. the macroscopic scale. In these materials, macrofracture cannot be completely understood unless one considers what is occurring at the microscale. However, this theory has to take into account scales that go down at levels even lower than the microscale. Indeed, some physical-chemical processes may occur at the level of the molecule, or even lower at the level of the atom, and many of the mentioned materials contain defects at the very small scale, as imperfections of the atomic structure, vacancies, dislocations. This may appear as the field of molecular dynamics or quantum mechanics, and one has to remember that fracture mechanics develops as a continuation of continuum mechanics theories, by considering a microscopic defect within a continuum body. As an example, LEFM provides formulas for stress concentration near the crack, as discussed in the following section. However, this formula looses its validity at the exact point of the crack tip, where the stress would tend to infinite, which is not feasible. This is due to the fact that a consideration of levels even lower than the microscale would provide a correct modelling. We will see that cracks do not propagate only for a stress increase or stress cycles, but even for the combination of stress and environmental attack, which occurs through chemical reactions at the nanoscopic scale. It is then clear that fracture mechanics theory would need some further considerations at the very small scales in order to understand the complex behaviour of materials such as glass.

2.2 Fracture criteria: Griffith and Irwin

2.2.1 Griffith criterion

Griffith pioneering work of 1921 (Griffith, 1921) provides the basis for modern fracture mechanics and allows explaining why, in brittle materials, tensile strength theoretically evaluated is far from the value registered through experiments. This incongruence can be understood only considering the presence of microscopic surface defects, which play the role of stress concentrators.

That said, Griffith studies start from the mathematical work proposed by Inglis in 1913, where the flaw, considered as an elliptical cavity, was already seen as potential weakness of the material (Inglis, 1913). Both Griffith and Inglis fund their works on mathematical elasticity theory. However, in Inglis theory, strength does not depend on the defect dimension but only on its shape, and this is not conform with experimental results. Hence, it is evident that in cracked materials the ordinary hypotheses of rupture loose their applicability, and Griffith's aim is to formulate a criterion of rupture coherent with real behaviour.

Griffith treats the problem of rupture from a new point of view, taking into account even the intermolecular attractions. Starting from the theorem of minimum energy, he provides a new theoretical criterion for fracture, i.e. an energetic criterion for crack advancement, based on macroscopic thermodynamic variables and where potential energy is diminished by the presence of a crack. His criterion of rupture allows defining a breaking stress which strictly depends on the dimension of the flaw.

Theory *versus* experiments

Griffith's study applies to isotropic solids obeying to Hooke's law, within the framework of mathematical theory of elasticity. This latter loses its validity only within a small region around the crack tip, hence for sufficiently large cracks it may be correctly applied. In order to give consistency to his theoretical studies, Griffith chooses as real material glass, which obeys to Hooke's law and whose structure allows simple analysis.

Molecular theory states that rupture takes place at the value of the stress, i.e. breaking load, which corresponds to the maximum pull resultant force that can be exerted between the molecules of the material, i.e. the sum of the intermolecular attractions. Hence, applied stress must show maximum value at rupture, and this latter should imply large dissipative phenomena, but this is not registered in ordinary tensile tests of brittle materials. Theoretically estimated tensile strength, which is related to the energy of cohesive bonds, is a material constant, about ten times smaller than the elastic modulus.

However, experimentally observed strengths are only a small fraction of the values indicated by the molecular theory. Moreover, stress from the tests is far from being uniform, and elastic theory shows that stress must be uniform unless material is heterogeneous or discontinuous. At the very small scale, all substances are discontinuous since they contain molecules of finite size. However, this discontinuity cannot be sufficient to justify the above mentioned inconsistency between theory and real behaviour. Therefore, it may be deduced that the reduced strength of brittle materials registered in tests is due to the presence of a crack, which represents the most extreme type of discontinuity and heterogeneity of a material.

Tensile tests in glass show a value of tensile strength (175 MPa) more than ten times lower than the theoretical strength, which is of the order of several GPa. From the tests, Griffith deduces that a breakage stress of 175 MPa must be induced by a flaw of a dimension of at least $4{,}7\mu$m, which is of the order of 10^4 times higher than the molecular distance. Hence, it can be stated that the weakness of isotropic solids is due to the presence of discontinuities or flaws or other centers of

heterogeneities whose dimensions are large compared to the molecular distance.

Limits of previous theories

In Inglis's work, stress at the tip of an elliptical crack in an uniformly stressed plate is relevantly higher than the stress applied to the edges. The two major and minor semi-axes of the ellipse are defined a and c respectively. The case limit of an infinitively narrow ellipse represents the crack. It is a problem of linear elasticity, where the assumptions are Hooke's law validity, stress-free edges of the cavity, crack highly smaller compared to the plate size.

His theory is also valid, with a small error, for cracks which are elliptical only at their extremities, i.e. for sharp cracks. In such a case, for $c \ll a$, the flaw is nearly straight, and the following relation takes place:

$$\frac{\sigma_{tip}}{\sigma_A} = 2\sqrt{\frac{a}{\rho}} \tag{2.1}$$

where σ_{tip} is the maximum material tension at the crack tip, σ_A is the applied edge stress and a and ρ are respectively the semi-length and radius of curvature of the edge of the elliptical cavity. The ratio on the left side of Equation (2.1), which is normally > 1, is the elastic stress concentration factor and it depends more on the shape, i.e. the ratio a/ρ, than on the cavity dimension. Hence, Inglis provides an instrument for evaluating the potential weakness effect of a series of irregularities, included the crack. This weakness is due to the fact that a crack may increase the stress at the tip even six times, basing on its shape and on the nature of the stress but independently on its absolute dimension. This is in conflict with the experimental results, where the flaw dimension decreases the strength, and where large cracks propagate much more easily than small ones. Therefore, the ordinary hypotheses of rupture are not applicable and the mechanism of rupture is still unknown. Starting from this point, Griffith provides a criterion for fracture coherent with the real behaviour of brittle materials.

Energetic criterion of crack advancement

Griffith applies the mathematical theory of elasticity to the case of a homogeneous isotropic flat plate containing a straight flaw and subjected to an uniform tension at the edges. The edges of the crack are stress-free. In his model, differing from Inglis, he considers an infinitely narrow crack, i.e. $c \to 0$, of length $2a$ and, being the crack small compared to the plate dimension, the stress may be considered as applied to infinite.

The condition of crack propagation, i.e. the criterion of rupture, arises from the principle of minimum of potential energy, for which the equilibrium state of an elastic body deformed by surface forces implies that the potential energy of the total system is a minimum. By applying this principle to a cracked body, Griffith provides a new theoretical criterion of rupture, adding to the principle of minimum the statement that the equilibrium position is the one where rupture has occurred.

Firstly, he considers the total energy U of the system as the sum of a mechanical energy term U_M and a surface energy term U_S:

$$U = U_M + U_S \tag{2.2}$$

U_M is the potential energy of the crack surface, i.e. it corresponds to the work done against the cohesive forces of the molecules at the edges of the crack. This term decreases when crack propagates, since during crack evolution the attractive forces that need to be contrasted progressively reduce. Then, U_M favors crack extension. The term U_S represents the energy of intermolecular bonds that is released during crack propagation, since cohesive forces of molecular attraction are exceeded during the formation of new surfaces of fracture. Hence, this term increases during crack propagation and opposes it: in order to form a new surface of fracture, molecular forces, represented by U_S, must be overtaken. The higher is this term, the most difficult is propagation for the crack. By corresponding rupture with crack advancement, Griffith energetic criterion states that crack advances, i.e. material fails, when the following equilibrium condition is satisfied:

$$\frac{\partial}{\partial a}(U_S - U_M) = 0 \tag{2.3}$$

This means that the crack advances in unstable manner when the energy provided by the system, i.e. the energy released, is equal or more than the energy needed for crack propagation. The signs depend on whether the energy term opposes or favors crack propagation. Griffith observes that the configuration where the crack is at equilibrium is the one that minimizes the total energy of the system. At that point, the crack may extend. In particular, for the case of thin plate, i.e. in plane stress, the term U_S is given by the following expression:

$$U_S = \frac{4\nu\pi a^2 S^2}{(1+\nu)8\mu} \tag{2.4}$$

where ν is Poisson ration, S tensile stress and μ the modulus of rigidity of the material. The term U_M is given by:

$$U_M = 4aT_S \tag{2.5}$$

where T_S is the surface tension of the material. Equation (2.3) then becomes:

$$\frac{\nu\pi a S^2}{(1+\nu)\mu} - 4aT_S = 0 \tag{2.6}$$

From this latter Equation, in the case of plane stress, the stress at rupture is obtained:

$$S = \sqrt{\frac{2ET_S}{\pi\nu a}} \tag{2.7}$$

being $(1+\nu)\mu = E/2$. This expression is experimentally verified. The expression for the breaking stress S is true only for small cracks in large plates. A part from the tests performed on glass plates, Griffith tests glass fibers in order to verify his hypotheses. Thinner specimens show higher strength. The extreme case is to consider a single chain of molecules, which must have a strength equal to the theoretical value, since it cannot contain flaws. As an explanation of the presence of these cracks, Griffith provides the hypothesis of a localized rearrangement of molecules within glass network, with transformations from the amorphous state to a more dense crystalline phase.

2.2.2 Irwin tensional criterion: stress intensity factor

Starting from Griffith studies, fracture mechanics main developments are due to the later work of Irwin, who also gives a macroscopic and thermodynamic vision of crack propagation (Irwin, 1957). As discussed below, Griffith and Irwin theories may be seen as equivalent. Irwin states that comprehension of fracture mechanism requires an understanding of all processes occurring in a small region around the crack tip. Indeed, the presence of a crack induces a high stress concentration near its tip, depending on several factors. For the case of plane stress or plane strain of a continuum body subjected to tensile stress, the influence of geometry, boundary conditions and loading on the stress concentration at the tip may be expressed through a parameter called stress intensity factor, which allows simpler analysis. Irwin studies arise from the observation that a crack can propagate even for very low stresses. Both Orowan and Irwin propose a modified Griffith theory (Irwin, 1957). Irwin introduces the concept of strain-energy release rate and fracture work rate. This study is based on the idea that when a crack starts propagating, it is possible to equate the work of fracture per units of extension and the velocity of disappearance of the strain-energy of surrounding material. The strain-energy release rate controls crack extension velocity. His aim is to describe this relation through

elastic stresses and strains at the tip[1]. During crack extension, strain energy is converted into thermal energy, with a certain rate and with local plastic deformations. This energy release rate is called G, and determines the tensile stress at the tip. Irwin aims at evaluating the crack tip stress field. The model is a plate containing a straight crack, which is sufficiently large compared to the plate thickness, so the condition is plane stress. The assumption is that the crack evolves normal to the tension, that is shear components are zero.

Stress field at the crack tip as solution of elastic problem: Airy stress function

Irwin shows that the stress concentration at the crack tip is the solution of an elastic problem, as the one described by Westergaard (Westergaard, 1939). Considering a plane problem, the solution of the stress function can be found if a stress function ψ is known. This is called Airy stress function. In a stressed solid, in each point it is possible to define the stress components. A plane stress condition implies that $\sigma_z = \tau_{xz} = \tau_{yz} = 0$, while a plane strain condition means that $\epsilon_z = 0$, so that $\sigma_z = \nu(\sigma_x + \sigma_y)$. A plane problem may be described through the equilibrium equations

$$\frac{\partial \sigma_x}{\partial x} + \frac{\partial \tau_{xy}}{\partial y} = 0 \tag{2.8}$$

$$\frac{\partial \sigma_x}{\partial x} + \frac{\partial \tau_{xy}}{\partial y} = 0 \tag{2.9}$$

the cinematic equations

$$\epsilon_x = \frac{\partial u}{\partial x} \tag{2.10}$$

$$\epsilon_y = \frac{\partial v}{\partial y} \tag{2.11}$$

$$\gamma_{xy} = \frac{\partial u}{\partial y} + \frac{\partial u}{\partial x} \tag{2.12}$$

and constitutive laws

$$E\epsilon_x = \sigma_x - \nu\sigma_y \tag{2.13}$$

$$E\epsilon_y = \sigma_y - \nu\sigma_x \tag{2.14}$$

[1]Near the crack tip, some plasticity phenomena occur, but they are limited to very small regions.

$$\mu\gamma_{xy} = \tau_{xy} \tag{2.15}$$

being $\mu = E/2(1+\nu)$. By introducing the Airy stress function ψ, one can states that the equilibrium Equations (2.8) and (2.9) are satisfied if

$$\sigma_x = \frac{\partial^2\psi}{\partial y^2}, \quad \sigma_y = \frac{\partial^2\psi}{\partial x^2}, \quad \tau_{xy} = -\frac{\partial^2\psi}{\partial x \partial y} \tag{2.16}$$

Substituting cinematic Equations (2.10)-(2.12) in constitutive Equations (2.13)-(2.15), we obtain the following differential equations:

$$\frac{\partial u}{\partial x} = \frac{1}{E}\frac{\partial^2\psi}{\partial y^2} - \frac{\nu}{E}\frac{\partial^2\psi}{\partial x^2} \tag{2.17}$$

$$\frac{\partial v}{\partial y} = \frac{1}{E}\frac{\partial^2\psi}{\partial x^2} - \frac{\nu}{E}\frac{\partial^2\psi}{\partial y^2} \tag{2.18}$$

$$\frac{\partial u}{\partial x} + \frac{\partial v}{\partial y} = -\frac{1}{\mu}\frac{\partial^2\psi}{\partial x \partial y} \tag{2.19}$$

By differentiating Equation (2.17) in y twice, Equation (2.18) in x twice and Equation (2.19) first in x then in y, we obtain:

$$\frac{\partial^3 u}{\partial x \partial y^2} = \frac{1}{E}\frac{\partial^4\psi}{\partial y^4} - \frac{\nu}{E}\frac{\partial^4\psi}{\partial x^2 \partial y^2} \tag{2.20}$$

$$\frac{\partial^3 v}{\partial x^2 \partial y} = \frac{1}{E}\frac{\partial^4\psi}{\partial x^4} - \frac{\nu}{E}\frac{\partial^4\psi}{\partial x^2 \partial y^2} \tag{2.21}$$

$$-\frac{\partial^3 u}{\partial x \partial y^2} + \frac{\partial^3 v}{\partial x^2 \partial y} = -\frac{1}{\mu}\frac{\partial^4\psi}{\partial x^2 \partial y^2} \tag{2.22}$$

Substituting (2.20) in (2.22) we obtain:

$$\frac{1}{E}\frac{\partial^4\psi}{\partial y^4} + \left(\frac{1}{\mu} - \frac{\nu}{E}\right)\frac{\partial^4\psi}{\partial x^2 \partial y^2} + \frac{\partial^3\nu}{\partial x^2 \partial y} = 0 \tag{2.23}$$

Substituting (2.21) in (2.23), we finally obtain the following equation:

$$\frac{\partial^4\psi}{\partial y^4} + 2\frac{\partial^4\psi}{\partial x^2 \partial y^2} + \frac{\partial^4\psi}{\partial x^4} = 0 \tag{2.24}$$

Equation (2.24) represents the equilibrium condition in terms of Airy stress function and it is equivalent to $\nabla^2(\nabla^2\psi) = 0$, i.e. $rotrotE = 0$.

Westergaard found a method to solve a class of plane strain and plane stress problems. He defined a complex function by

$$Z(z) = ReZ + iImZ \tag{2.25}$$

with $z = x + iy$.

This function is required to be analytic, i.e. the derivative dZ/dz must be defined and continuous, for each z. The derivability of a function of a complex variable is guaranteed by the Cauchy-Riemann conditions, also known as monogeneity conditions, which express a necessary and sufficient condition for the function to be holomorphic. Given a generic function

$f : A \to \mathbb{C}$

$f(x + iy) = u + iv$

with x, y real variables and u, v real functions, the Cauchy-Riemann equations state that the function is holomorphic on $A \iff$ it is differentiable with continuous derivatives and verifying the following equations:

$$\frac{\partial u}{\partial x} = \frac{\partial v}{\partial y} \tag{2.26}$$

$$\frac{\partial u}{\partial y} = -\frac{\partial v}{\partial x} \tag{2.27}$$

Within a complex plane, if the function is called Z, the same conditions may be written as $i\frac{\partial f}{\partial x} = \frac{\partial f}{\partial y}$.

Considering the complex function $Z(z) = ReZ + iImZ$, where $z = x + iy$, and replacing u by ReZ and v by ImZ, the Cauchy-Riemann conditions are the following:

$$\frac{\partial ReZ}{\partial x} = \frac{\partial ImZ}{\partial y} = Re\frac{dZ}{dz} \tag{2.28}$$

$$\frac{\partial ImZ}{\partial x} = -\frac{\partial ReZ}{\partial y} = Im\frac{dZ}{dz} \tag{2.29}$$

For problems of fracture, i.e. for the case of Mode I cracks, Westergaard proposed the Airy stress function as follows:

$$\psi = Re\bar{\bar{Z}} + yIm\bar{Z} \tag{2.30}$$

where $\frac{d\bar{\bar{Z}}}{dz} = \bar{Z}$, $\frac{d\bar{Z}}{dz} = Z$, $\frac{dZ}{dz} = Z'$. By using equations (2.16), Westergaard obtained the stresses induced by the crack:

$$\sigma_x = ReZ - yImZ' \tag{2.31}$$

$$\sigma_y = ReZ + ImZ' \tag{2.32}$$

$$\tau_{xy} = -yReZ' \tag{2.33}$$

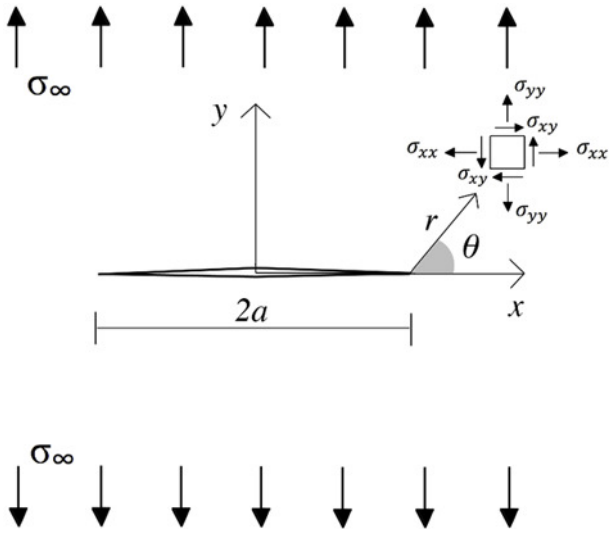

Figure 2.2: Straight crack within an infinite plate under biaxial tensile stress: stress field at the crack tip.

For the case of straight crack of length $2a$ along the x-axis in an infinite plate under biaxial tension σ applied at far distances from the crack (see Fig. 2.2), Westergaard gives the following solution:

$$Z(z) = \frac{\sigma}{[1-(a/z)^2]^{1/2}} \tag{2.34}$$

This analysis has certain limits. As and example, if the crack propagates rapidly, a dynamic-stress analysis is needed. However, Irwin shows that the stress distribution near the crack tip may be expressed independently of uncertainties of magnitude of the applied loads. Considering the Westergaard solution, he substitutes the variables

$$a + re^{i\theta} \tag{2.35}$$

and for the case of infinite plate under biaxial stress with straight mode I crack (see Fig. 2.2), he obtains the following stress fields:

$$\sigma_x = \left(\frac{EG}{\pi}\right)^{\frac{1}{2}} \frac{\cos\theta/2}{\sqrt{2r}}\left(1 - \sin\frac{\theta}{2}\sin\frac{3\theta}{2}\right) - \sigma \tag{2.36}$$

$$\sigma_y = \left(\frac{EG}{\pi}\right)^{\frac{1}{2}} \frac{\cos\theta/2}{\sqrt{2r}}\left(1 + \sin\frac{\theta}{2}\sin\frac{3\theta}{2}\right) \tag{2.37}$$

$$\tau_{xy} = \left(\frac{EG}{\pi}\right)^{\frac{1}{2}} \frac{\cos\theta/2}{\sqrt{2r}} \sin\frac{\theta}{2}\cos\frac{\theta}{2}\cos\frac{3\theta}{2} \tag{2.38}$$

G represents the energy exchange from mechanical or strain energy to thermal energy, occurring during crack propagation. It is associated with unit extension of the crack, and may be seen as the force which tends to extend the crack. Solutions of Equations (2.36),(2.37) and (2.38) are referred to a parabolic shape for the crack opening profile, near the crack tip. Irwin moves within an elastic frame, since he states that local stress relaxation and crack opening distortion by plastic flow do not change the loss of strain energy by an appreciable amount. The term $(EG/\pi)^{1/2}$ is named *stress intensity factor*, also known as K_I, for fracture mode I. By introducing K_I, he obtains:

$$\sigma_x = \frac{K_I}{\sqrt{2\pi r}} \cos\frac{\theta}{2}\left(1 - \sin\frac{\theta}{2}\sin\frac{3\theta}{2}\right) - \sigma \tag{2.39}$$

$$\sigma_y = \frac{K_I}{\sqrt{2\pi r}} \cos\frac{\theta}{2}\left(1 + \sin\frac{\theta}{2}\sin\frac{3\theta}{2}\right) \tag{2.40}$$

$$\tau_{xy} = \frac{K_I}{\sqrt{2\pi r}} \sin\frac{\theta}{2}\cos\frac{\theta}{2}\cos\frac{3\theta}{2} \tag{2.41}$$

The compact expression of Equations (2.39)-(2.41) is the following:

$$\sigma_{ij} = \frac{K_I}{\sqrt{2\pi r}} f_{ij}(\theta) \tag{2.42}$$

K_I represents the stress amplification occurring at the tip due to the presence of a crack, and it allows explaining why in brittle materials rupture occurs even for very low stress values. For a particular location of the crack, represented by r and θ, the stress intensity factor can be evaluated. This allows calculating the stresses near the crack tip through the linear elasticity theory, i.e. through Equations (2.39), (2.40) and (2.41), if the stress intensity factor is known. The values of G can be calculated experimentally by measuring local strain at certain positions.

Equation (2.42) has evidently some limits of application, since for very small distances from the tip, i.e. for $r \to 0$, the stress tends to infinite, which is physically not feasible. On the contrary, for large distances, i.e. for $r \to \infty$, the stress would tend to zero, and this is also not real. Fig. (2.3) shows the stress component σ_{yy} normal to the crack plane, for the case shown in Fig. (2.2).

Within an elastic problem, the stress must be proportional to external load. Hence, the stress intensity factor K_I must be proportional to the applied stress σ. Observing Equation (2.42), it is obvious that K_I must be proportional to the root square of a length. We consider the case of infinite plate, where the only length is the crack size. Therefore, the stress intensity factor takes the following form:

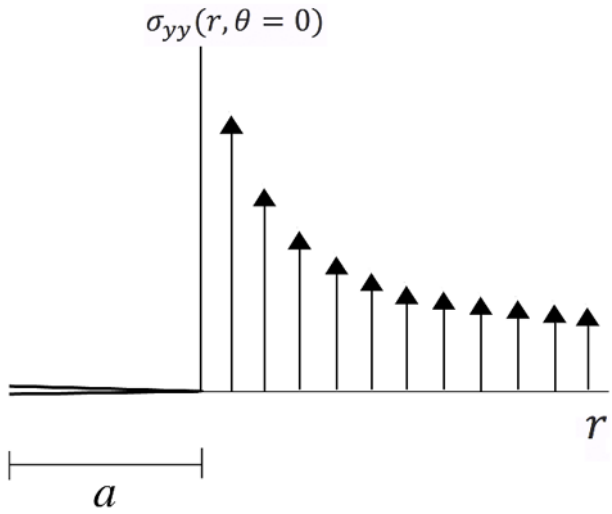

Figure 2.3: Stress field at the crack tip normal to the plane of the crack.

$$K_I = A\sigma\sqrt{a} \tag{2.43}$$

A is a dimensionless parameter depending on geometry. For the case of straight crack in infinite specimen under biaxial stress (see Fig. 2.2), $K_I = \sigma\sqrt{\pi a}$. This is also valid for the case of uniaxial stress normal to the crack plane. Since now, we have considered the ideal case of infinitely small crack compared to the plane dimension. For the real case of finite crack size, a correcting factor needs to be inserted for evaluating K_I. This factor, named geometry factor or shape factor Y, depends on the boundary conditions, i.e. on the geometry and on loading conditions. For instance, a bending test reveals a different value of the geometry factor compared to simple tensile tests.

Some cases of real cracks are semi-elliptical or quarter elliptical ones, respectively for edge and corner cracks. Elasticity theory through the work of Sneddon analyzed the case of a circular internal crack, named penny-shaped crack, within an infinite solid subjected to uniform tension, giving the following expression for the stress intensity factor: $K_I = (2/\pi)\sigma\sqrt{\pi a}$, i.e. $K_I \approx 0.637\sigma\sqrt{\pi a}$. For an embedded elliptical flaw, Irwin derived the following solution:

$$K_I = \frac{\sigma\sqrt{\pi a}}{\frac{3\pi}{8} + \frac{\pi a^2}{8c^2}} \left(\sin^2\phi + \frac{a^2}{c^2}\cos^2\phi \right)^{\frac{1}{4}} \tag{2.44}$$

For practical purpose, Equation (2.44) can be simplified for the case of semi-elliptical surface flaw, which is quite common in real brittle

materials. The stress in higher in correspondence to the minor axis, i.e. for $\phi = \pi/2$:

$$K_I = \frac{\sigma\sqrt{\pi a}}{\frac{3\pi}{8} + \frac{\pi a^2}{8c^2}} \tag{2.45}$$

For an edge crack, it was found that the value of K_I can be obtained by Equation (2.45) by using a correction factor, which is normally 1.12.

Hence, for a generic edge crack, the stress intensity factor takes the following form:

$$K_I = Y\sigma\sqrt{\pi a} \tag{2.46}$$

where Y is the so called dimensionless geometry factor, or shape factor. Crack systems in uniform loading differ only in the numerical factor Y. For an edge straight crack of length a in a semi-infinite specimen, the geometry factor is 1.12 (see Fig. 2.4).

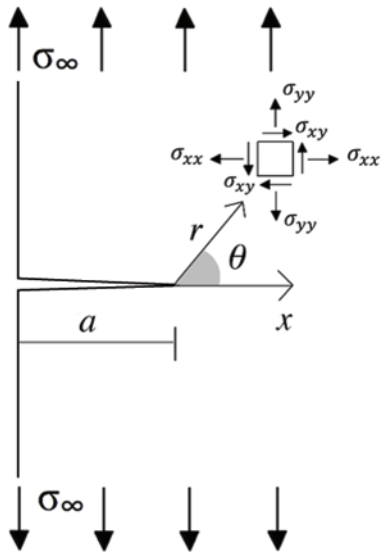

Figure 2.4: Edge straight crack of length a in a semi-infinite specimen.

A sharp crack induces a high stress concentration, which is directly related to the shape of the crack tip. In this case, the geometry factor takes a maximum value. It is easy to understand that a curved-front crack is much less dangerous than a sharp one. Indeed, for a penny shaped crack $Y = 0.637$. Since now we have considered the case of cracks subjected to tensile stress applied to the edges of the plate. Normally in real experiments specimens are subjected to bending tests, i.e. four-point or three-point bending tests, so that the loading condition

is different and the geometry factor must take account of this. For a four-point bending test, i.e. for a specimen subjected to two point forces, each of $P/2$, the maximum stress is given by the beam elasticity theory: $\sigma = 3Pl/4wd^2$ and this formula must be combined with the above-shown expression for K_I. As seen above, Griffith proposed a fracture criterion based on energetic principles, that is crack grows if the energy required to form new crack surfaces can be provided by the system. In a different way, but analogous, Irwin formulates a fracture criterion based on the applied stress. He states that crack propagates in an unstable way, i.e. fracture occurs, when the stress intensity factor reaches a critical value K_{Ic} known as *material toughness*, which represents the crack resistance of a brittle material and it is a material property. The stress intensity factor can reach this critical value whether the applied stress increases up to a maximum value σ_c or whether the crack length reaches a certain amplitude. This latter case implies the interaction between an even low stress and environment, i.e. chemical corrosion allows the crack growing until a critical length a_c. Hence, Irwin fracture criterion may be written as:

$$K_I \geqslant K_{Ic} \tag{2.47}$$

2.2.3 Equivalence between the two criteria

Irwin demonstrates that the two criteria, the tensional or local one formulated by him-self, and Griffith energetic or global one, are equivalent. In Griffith theory, the energy required for crack propagation must be delivered as a release of elastic energy. Griffith criterion may be written as:

$$\frac{\partial U_M}{\partial a} = \frac{\partial U_S}{\partial a} \tag{2.48}$$

Crack extension may occur when the energy release G is equal to the energy needed for crack extension, i.e. the energy needed for new crack surfaces formation:

$$G = \frac{\partial U_S}{\partial a} = -\frac{\partial U_M}{\partial a} \tag{2.49}$$

The negative sign indicates that by diminishing potential energy, in association with crack propagation, the energy release increases. The mechanical energy released during crack growth, i.e. G, is independent on loading configuration, as Lawn demonstrates (Lawn, 2004). It can be seen as a force analogue to the surface tension. Methods for evaluating G consist in analyzing the stress field at the crack tip. As seen above, a stress function is searched which satisfies the biharmonic equation which includes balance conditions, cinematic conditions and

constitutive laws, in the respect of the boundary conditions. From this stress function, it is possible to determine stress and displacement components. For infinitely narrow cracks, this analysis reveals some problems. The first analysis of a stress-function for these cracks are due to the work of the elasticians, as Westergaard and Muskhelishvili (Westergaard, 1939), leading to the Irwin solutions, with the hypothesis that the crack lips are stress-free. From the Airy stress-function, Irwin deduces the stress and displacement field:

$$\sigma_{ij} = \frac{K_I}{\sqrt{2\pi r}} f_{ij}(\theta) \tag{2.50}$$

$$u_i = \frac{K_I}{2E}\sqrt{\frac{r}{2\pi}} f_{ij}(\theta) \tag{2.51}$$

where σ_{ij} represents the distribution of the stress field and it depends on spacial coordinates. K_I determines the intensity of the local stress field and depends on the boundary conditions, i.e. on the applied load and on the specimen geometry. This solution has a singularity for $r = 0$, and this arises from the assumption that the crack is perfectly sharp. Equations (2.50) and (2.51) can be applied at distances not too small and not too large from the crack tip. K and G have been defined without using any criterion for crack extension.

The energy release rate is related to stress as follows:

$$G = \frac{\pi\sigma^2 a}{E} \tag{2.52}$$

G may be seen as the variation of total potential energy per units of crack extension, i.e. the variation of total potential energy associated with the process of opening of the crack of an amount of da. Griffith energetic approach implies that for $G \geqslant G_f$ crack propagates, where $G_f = {\sigma_c}^2\pi a/E$. Irwin tensional approach, on the other part, states that fracture occurs when $K_I \geqslant K_{Ic}$. Irwin demonstrates that the energy release rate and the stress intensity factor are related through the following expression:

$$G_c = \frac{{K_{Ic}}^2}{E} \tag{2.53}$$

for plane problems. This implies that the two fracture criteria are completely equivalent. Both G_f and K_{Ic} are material constant, since within a linear-elastic framework they do not depend respectively on the history of processes and on the loading histories. A demonstration of the equivalence may be found in some recent works on fracture mechanics (Broek, 1974; Lawn, 1983). Irwin criterion is more easily used for practical purposes since it is related to the applied stress and the testing geometry, which are variables known in experiments. By

introducing the stress intensity factor, Irwin allows considering all real cases.

2.3 Elasticity *versus* plasticity?

Since now, we have considered an ideal linear-elastic behaviour of brittle materials containing flaws. In real cases, in a small region around the crack tip, some plastic deformation and stress redistribution phenomena may occur. To consider the global behaviour linear-elastic or not depends on the size of the area around the crack tip where inelastic phenomena take place. This area is known as *process zone*. Considering the specific case of glass, which is considered perfectly linear-elastic until breakage, some recent works follow the hypothesis that a non-negligible process zone is formed in glass during crack propagation and they apply porous-plasticity models (Ferretti et al., 2011). In the present thesis, glass behaviour is considered as linear-elastic, since it follows some recent studies that experimentally revealed the existing of a process zone but of an amount of few nanometers, which can be neglected in a macro-micro analysis (Pallares et al., 2011). However, it is interesting to give a short glance of the theoretical models of non-linear fracture mechanics for generic brittle materials and for specific case of glass.

2.3.1 NLFM

Even for non-linear processes, fracture mechanics provides two approaches, the tensional one, i.e. local approach, and the energetic one, i.e. global approach. The tensional approach arises from the consideration that in brittle materials some damage and microcracking processes occur in a region around the crack tip, where defect, inclusions, voids and other imperfections induce forces that tend to close the crack and impede its propagation. This model is also known as cohesive fracture model, and it takes account of non-linear and dissipative microscopic phenomena occurring in the process zone around the tip. The size of the process zone is determinant in the analysis, since if it is small compared to the crack length, linear elastic model of LEFM can be applied. On the contrary, if the process zone is not small compared to the crack, it has to be properly modelled. The cohesive forces assume their maximum value at the tip, as shown in Fig. 2.5.

Several models were provided for simulating the process zone, as the one proposed by Baremblatt or Dugdale (Barenblatt, 1959). In recent years, many efforts have been made in this direction, and a description of the cohesive model has been recently provided. The main problem is to determine the length of the process zone, since this knowledge

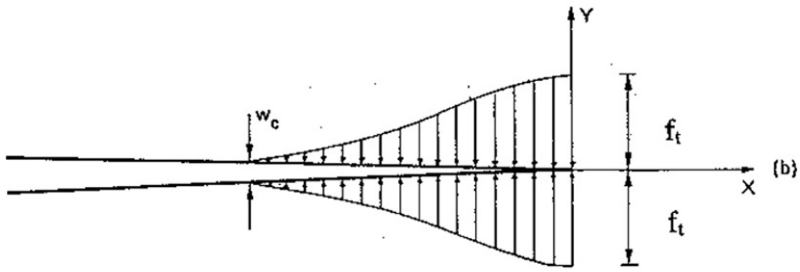

Figure 2.5: Cohesive forces near the crack tip.

allows framing the cracking problem in a linear-elastic theory or in a non-linear theory. Irwin proposed a method for evaluating the process zone in ductile materials (Irwin, 1957) and some works apply his studies to the case of quasi-brittle materials.

The second approach, that is the energetic or global approach, is based on the so-called $R-curve$. These models extend Griffith energetic criterion of LEFM for which fracture occurs when $G = G_f$ to the case of materials where the resistance R to crack extension is not constant. Fracture criterion becomes $G = R$.

Non-linear phenomena are normally induced by the presence of imperfection as voids, nucleations, microcracks. Depending on the size of these heterogeneities, the material can be considered as homogeneous or composite, i.e. discontinuous. Several micro-mechanical models have been proposed for evaluating mechanical properties of heterogeneous solids, as the homogenization techniques based on the Eshelby inclusion, who considers an inclusion in an homogeneous infinite elastic solid (see chapter 7).

2.3.2 Non-linear models for glass

As discussed above, a macroscopic analysis is not sufficient for describing glass behaviour, since its mechanical strength is highly affected by the presence of initial flaws of micrometer size. Hence, LEFM provides a more correct explanation for glass fracture behaviour, considering the strong interaction between the specimen scale and the scale of the defect. However, LEFM has some limits of applications, since in a material such as glass a complete analysis should take into account even the nanometer scale. Indeed, fracture is strictly connected with the breakage of interatomic bonds. In addition, all the chemical processes induced by the interaction with environment, occur at the level of the atoms. At this low level, linear elastic fracture mechanics fails, since

the proportionality between stress and strain from elastic theory implies that the stress assumes infinite values at the very crack tip. Real cracks are atomically sharp and propagate for successive rupture of the bonds. In addition, LEFM, i.e. continuum theory, considers that the region where separations occur is small, and this would imply a discrete analysis. Experiments on glass show that real fracture energy is much higher than the equilibrium surface energy of the theory, and this may be explained if other dissipative mechanisms around the crack tip are considered (Ferretti et al., 2011).

This is taken into account by two different approaches, in order to solve the problem of infinite stress at the crack tip. The first one is due to Barenblatt who considers the existence of surface cohesive forces which create a bridge across the crack lips (Barenblatt, 1959). In this model, the stress is finite at the crack tip or, equivalently, the opposite sides of the crack are smoothly connected at their ends. The second approach assumes that fracture is controlled by bulk dissipation properties. Hence, the applied load induces microvoids and microcracks in a small region around the tip which form the main crack, and this process is accompanied by the formation of a damaged zone. This is typical of ductile materials as metals or quasi-brittle materials, but in recent years several authors state that the process zone exists even in glass and ceramic materials, even if the spatial scales are lower. The formation of a plastic process zone has been witnessed by observations through atomic force microscope (AFM), which confirm the hypothesis that a plastic deformation takes part of the energy balance in the fracture process.

In each case, the uncertainties are about whether or not the crack is atomically sharp or whether the process of separation of the crack occurs at the very tip or in a wider region around it. The two approaches state that plastic process occurs respectively at the crack surface, through cohesive forces, and in a bulk neighborhood of the tip process zone. The question is still open and shows a high interest for all those authors who aim at correctly modelling glass fracture behaviour.

A recent work (Pallares et al., 2011) experimentally proves that nonlinear processes occur in a region of less than $10nm$, so for microscopic and macroscopic analysis, glass behaviour can be considered as linear-elastic.

2.4 Focal points

- LEFM takes origin from Griffith studies, who proposes an energetic fracture criterion, on the basis of mathematical theory of elasticity;

- Griffith criterion allows solving the incongruence between theory and experiments, which registered strength values relevantly lower;
- Griffith chooses glass as isotropic material obeying to Hooke's law, since its structure provides simpler analysis;
- Griffith theory goes beyond the limits of molecular theory and it identifies the presence of flaws of few μm as the cause of low strength;
- On the basis of previous studies by Inglis, Griffith provides a fracture criterion consistent with the real brittle behaviour;
- Crack advances and fracture takes place when the energy provided by the system is equal or exceeds the energy required for crack propagation;
- Later, Irwin proposes a tensional criterion for fracture, based on the concept of stress intensity factor, which represents the stress amplification at the crack tip and depends on flaw geometry and on boundary conditions;
- Irwin criterion represents the solution of an elastic problem, by introducing the Airy stress function;
- For the tensional criterion, crack advances when the stress intensity factor reaches a critical value, called material toughness;
- The two criteria, the energetic one and the tensional one, are demonstrated to be equivalent, by introducing the energy release rate concept;
- LEFM is framed within a perfectly linear-elastic context. However, in a small region around the tip, some irreversible processes take place;
- Some models consider non-negligible the non-linear mechanisms and even for glass non-linear models have been proposed;
- A recent work demonstrated that the non-linear zone around the crack tip is smaller than $10nm$, hence for a microscopic/macroscopic analysis glass can be properly considered as perfectly linear-elastic.

Chapter 3

Multi-physics coupling

3.1 Some preliminary definitions

In the previous section, the analysis of stresses at the crack tip implies that the material is embedded in vacuum. However, in most of real cases, materials are immersed in a chemically active environment, and this cannot be neglected. In a recent work, an effort has been made in order to include in fracture mechanics theory the chemical aspects (Lawn, 2004). In another work, absorption of environmental particles seems to play a relevant role by lowering the surface energy (Orowan, 1948).

Hence, in glass as in several other materials, some coupling mechanisms between different disciplines may occur leading to failure mechanisms that cannot be limited to the field of mechanics. Multi-physics coupling refers to all those cases where different physics interact, inducing complex phenomena and also implying the interaction between different scales. In fact, many of the elementary mechanisms occurring at the small scales have a consequence on macroscopic behaviour. The concept of coupling allows defining a *coupled system*. For system we refer to a set of entities which interact. A coupled system is a set of subsets which mutually interact through an interface. In a multiphysics system, each system corresponds to a different physics. Multi-physics coupling may assume two different forms. A *strong coupling* is a coupling where each subset, i.e. each physics, is strongly affected by the others. On the contrary, in a *weak coupling* only one physics strongly affects the other, and the reciprocal is not verified.

3.2 Examples of multi-physics coupling

Multi-physics coupling mechanisms are observed in several materials, as alloys, ceramics, glass. All the mechanisms occurring at the small scales have physical consequences on macroscopic behaviour. An example of elementary mechanism occurring in alloys is *dealloying*, consisting in a removal of one element from an alloy by corrosion processes. Alloys are considered as *bi-materials*, since one part of them is affected by corrosion and the other one is not. Corrosion mechanisms in alloys induce fragilization processes. The local modification of the composition, due to corrosion, corresponds to an evolution of material properties, and this has consequences on mechanical behaviour. Other elementary mechanisms are represented by voids, dislocations and cavities formation. It is clear that the interaction between different scales is strong. In alloys, an example of multi-physics coupling mechanism is the interaction between small-scale oxidation-corrosion and macro-mechanical behaviour. Mechanisms occurring at the level of the volume element affect structural response. As an example, the evolution of chemical composition, due to substrate oxidation, has a consequence on mechanics, as occurs in the phenomenon of *fluage*, since during oxidation the medium becomes porous. Some of mechanical consequences of this are decrease of elastic slope and decrease of rupture deformation. Another example of elementary mechanism is intergranular oxidation, which is a damage distributed in homogeneous way and which decreases tensile properties. Interaction between oxidation and deformation is known as cracking-assisted oxidation.

Temperature has a relevant role in multi-physics coupling mechanisms.

Another form of coupling occurs between electro-chemical potential and structure. Tests show that in areas subjected to tensile stress intergranular corrosion occurs. Hence, corrosion potentials are localized in function of the nature of the stress. This means that stress has an effect on surface electro-chemical potential.

Corrosion process has also consequences on structure mechanics. For instance, when a void is filled by an Hydrogen or Oxygen atom, a new thermal equilibrium holds.

Multi-physics coupling mechanisms also affect polymers, with consequences on durability and lifetime, since chemical modifications change mechanical properties. In particular, polymers are characterized by a strong coupling process between mechanical properties and environmental chemical degradation. During chemical degradation, a fragilization process occurs. Polymers composed by long molecules chains have high mechanical qualities while a short chain causes brittleness. Two phenomena of modifications of mechanical properties can be observed. The first one is a physical ageing, which induces reversible changes by

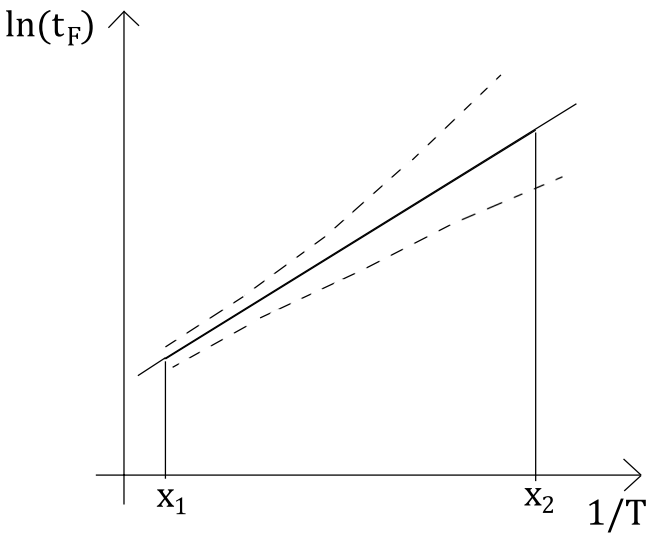

Figure 3.1: Arrhenius law for failure time as function of temperature (straight line).

modifying the mobility of chains and does not affect the chemical structure. An example of consequence is vitreous transition change, which implies that the polymer may change from rubber to glass state. Another consequence may be a decrease or increase of Young modulus or of yield properties. Some causes of physical ageing are molecules that enter inside the polymer, as water for instance. Water absorption may have consequences on visco-elastic properties.

The second type of mechanism is chemical ageing, which induces irreversible modifications of chemical structure and is a consequence of the environmental attack. In this case, material structure is modified irreversibly, and this type of ageing induces breakage in polymers. Some examples are thermal oxidation, that is interaction between temperature and Oxygen, or hydrolysis, that is interaction between temperature and H_2O molecules, or even photo-oxidation, induced by exposition to solar energy.

Fig. 3.1 shows that for thermal oxidation, Arrhenius[1] diagram is not valid anymore. Arrhenius law, represented by the straight line, shows the dependence of failure time t_F on absolute temperature T:

$$t_F = t_{F_0} exp(E/RT) \tag{3.1}$$

[1]Arrhenius chemical kinetics theory will be discussed in the next section.

Arrhenius approach is not good prediction when oxidation occurs.

Hydrolysis is an example of bonds rupture and chain scission increases with exposition time. Chemical ageing induces bonds breakage with a consequent fragilization process.

Fig. 3.2 represents some possible coupling effects.

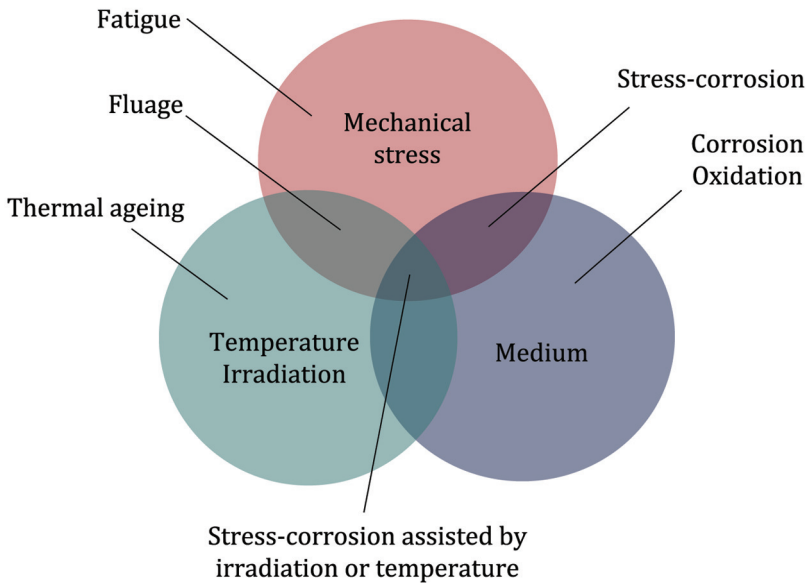

Figure 3.2: Example of multi-physics coupling between mechanics, material properties and environment.

Defect or void propagation is an example of microstructure evolution. At very low temperatures, the mobility of defects is very weak. These phenomena involve several spatial scales, and an effort in linking different scales is made by multiscale models. Microstructure deformations, as dislocation processes, have effect on macro-mechanical properties. Each mechanism, carrying a characteristic time, requires an adequate model and all different models need to be related.

3.3 Multi-physics coupling in glass

It is widely discussed that one of the strongest cause of glass failure is a coupling process between mechanical tensile stress and environment, also known as *stress-corrosion*, to which the next section will be dedicated. In particular, water molecules tend to fill the voids around the microscopic initial flaws and react with glass structure reducing

its strength. This corrosion effect is highly increased by temperature. Many recent works aim at understanding the ambiguous role of water at the very crack tip (Pallares et al., 2011; Wiederhorn et al., 2011). These works perform experimental studies at the nanoscale on silica glass, where environment corrosion is easier to observe, since there is not corrosion by Sodium molecules as in soda-lime silica glass, but only by water. Silica glass corrosion by water is represented by an *hydrolysis* reaction. At room temperature and with no stress, corrosion has very long term effects, i.e. several years.

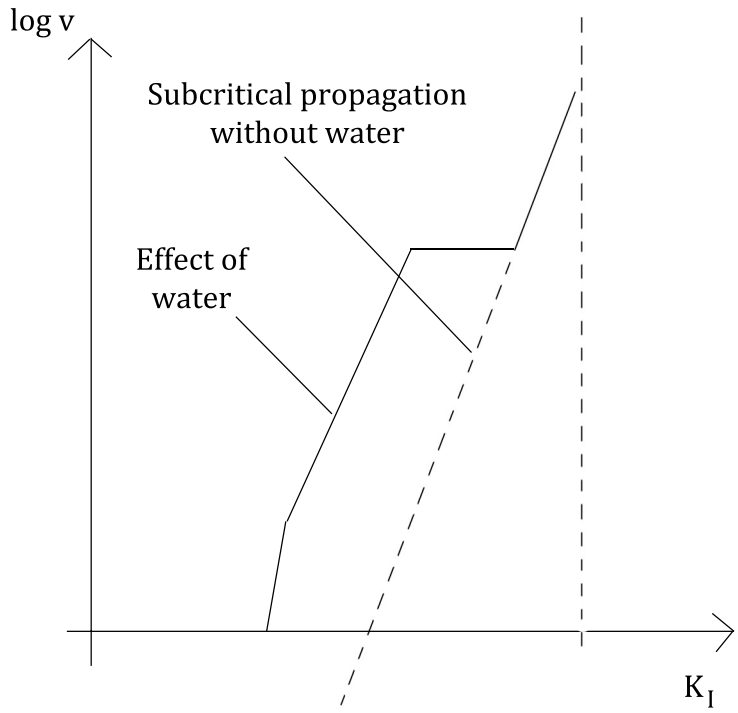

Figure 3.3: Crack propagation velocity *versus* stress intensity factor, in the presence of water.

Fig. 3.3 shows crack velocity, that is corrosion rate, *versus* stress intensity factor K_I. The dashed line would represent the inert condition of crack propagation with no water content in the environment. The continuous line represents the effect of water, which increases velocity by parity of stress. Around the process of water diffusion at the crack tip, there are different theories about whether or not the stress induces water penetration (Wiederhorn et al., 2011; Tomozawa, 1998). Another

coupling effect observed in glass is known as capillary condensation of water molecules inside the porous around the crack tip (Pallares et al., 2011). Physical water condensation, at the molecular scale, has relevant mechanical effects, by inducing a negative pressure that tends to close the flaw.

Water plays a central role also in crystalline solids, since the diffusion of Hydrogen at the scale of the grains induces a fragilization of the material. In a crystal, the Hydrogen decreases the surface energy, and this accelerates the formation of voids, leading to intergranular breakage. The mechanism of fragilization due to Hydrogen is affected by the heterogeneity of a material structure, at the scale of the grains. Crystals are composed by grains, so they have a microstructurale heterogeneity, which causes heterogeneity of mechanics fields.

Once stated that physical coupling process appears as a relevant mechanism in glass, it seems necessary to take it into account for a complete understanding of the phenomenon of microcrack propagation that leads to macroscopic fracture.

3.4 Focal points

- The analysis of stresses at the crack tip implies that the material is embedded in vacuum. However, in most of real cases, materials are immersed in chemically active environment;
- The interaction between mechanical stress and environmental attack is one example of multi-physics coupling mechanisms;
- These mechanisms imply a strong interaction between different physics and different spatial scales;
- Multiscale and multiphysics modelling allows considering this interaction;
- Multi-physics couplings are observed in alloys, polymers, ceramics, glass;
- Interaction between water absorption, inducing chemical degradation, and mechanical properties is an example of coupling effect;
- Temperature plays a relevant role since it accelerates coupling mechanisms;
- For a complete understanding of glass behaviour, it is necessary to consider these coupling effects, which in the case of glass are mostly represented by stress-corrosion mechanisms.

Chapter 4

Stress-corrosion in glass

4.1 Stress-corrosion mechanisms in glass

4.1.1 Subcritical crack propagation

Irwin fracture criterion from LEFM, as discussed in chapter 2, states that failure occurs, in brittle materials, when the stress intensity factor reaches material toughness K_{Ic}. However, in glass as in other materials, fracture may occur even for levels of the stress very lower than the critical one, i.e. for $K_I \ll K_{Ic}$. In this case, macroscopic failure is induced by subcritical microcrack propagation, which is a consequence of a combination between the stress amplification at the crack tip and a strong interaction with surrounding environment. This phenomenon is known in the literature as stress-corrosion and is widely illustrated in some recent works (Ciccotti, 2009; Gy, 2003). Stress-corrosion provides an explanation for a macroscopic phenomenon registered during tests, i.e. a *delayed failure* occurring in a glass element subjected to a constant stress even very low, as for example self-weight. Hence, exposure of glass to a chemically active environment reduces its strength.

Stress-corrosion chemical-physical reactions are triggered by water molecules contained in moist air or by liquid water when glass is plunged in a liquid. Due to the high hydrophilic nature of glass surfaces, water tends to chemically react with glass atomic structure in a small region around the crack tip. Even if the applied stress is low, the presence of the crack acts as stress concentrator at its tip, and this accelerates water-glass reactions. In stress-free states, one should wait several years for observing the effect of a chemical corrosion. Most of the works on stress-corrosion investigate mechanisms occurring in silica glass, which is mostly composed by SiO_4 tetrahedra, where Silicon and Oxygen atoms are connected by covalent bonds. The main chemical reaction occurring in silica glass in presence of water is a hydrolysis reaction:

$$Si - O - Si + H_2O \longleftrightarrow 2(Si - OH - Si) \tag{4.1}$$

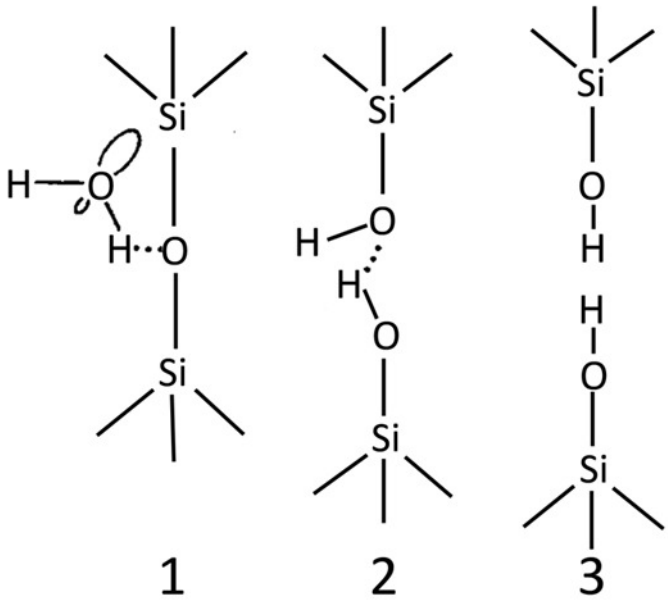

Figure 4.1: Water-glass reaction in silica glass.

Fig. 4.1 shows the typical reaction occurring in silica glass, whose simple structure and composition allow focusing on stress-corrosion complex mechanisms and provide a high resistance to corrosion. On the contrary, soda-lime silica glass, whose structure contains Silicon-Oxygen tetrahedra and several other molecules, has a low corrosion resistance, since corrosion comes not only from water molecules but also from other molecules as Sodium. However, this latter type of glass is the most common in building, and this work aims at investigating its response to stress-corrosion. In soda-lime silica glass, when a crack is formed, fresh fracture surfaces in contact with water undergo an ion exchange reaction, in which alkali ions in the glass exchange with Hydronium ions in the water, leaving hydroxyl ions behind to create a basic solution (Wiederhorn et al., 2011). As a consequence, the pH can get very high, also around 12, and it is known that solutions with a pH greater than 9 can corrode glass. On the contrary, silica glass contains no mobile ions and cannot have the crack tip stress field resulting from an ion exchange process. Tests indicate that the pH of silica glass in

water is ≈ 5, too low to cause corrosion. Hence, the only reaction is an hydrolysis reaction.

4.1.2 The central role of water in stress-corrosion reactions

First, it should be interesting to make a distinction between physical variables which play a role in stress-corrosion process. As mentioned above, water has a central role, since H_2O molecules tend to fill the micropores existing in proximity of the flaw apex, where they undergo a capillary condensation, assuming the form of liquid water (Pallares et al., 2011). Once the vapor has become water, it is able to chemically react with glass around the crack tip, and this reaction is highly stress-enhanced. Several works observe that stress-corrosion reaction is thermally activated. Hence, also temperature plays a relevant role, but in a different way compared to water, since it accelerates water-glass corrosion, where water is the main subject. In the literature, there are still open questions on how water enters inside the flaw. As will be discussed later, some recent theories provide an interesting explanation for which water penetration is enhanced by stress (Tomozawa, 1996). Water-glass interaction is still under investigation (Wiederhorn et al., 2011) as well as what really occurs at the microscopic scale (Charles and Hillig, 1962; Tomozawa, 1996). In addition, there are some divergences on the physical mechanisms occurring at the tip, since some theories state that water condensation tends to physically change the crack tip geometry (Charles and Hillig, 1962). On the role of water, some recent interesting works provide the hypothesis that water capillary condensation occurring inside the flaw tends to exercise a negative pressure, that is a tension, called *Laplace pressure*, which tends to close the lips of the flaw (Pallares et al., 2011; Wiederhorn et al., 2011).

Fig. 4.2 shows the effect of water capillary condensation, whose extension is a critical length L. Water undergoes condensation where the lips of the crack are at a distance lower than the critical distance H_c. There is a relation between critical length and critical height of condensation, as discussed in the same work (Pallares et al., 2011). As evident in the figure, water has the physical effect of making the crack lips closer, and this may have a different effect whether the state is stressed or stress-free. Indeed, crack sharpening due to Laplace pressure would induce a relevantly higher stress concentration at the tip, represented by K_I, when the solid is subjected to a tensile strength. Hence, capillary condensation would accelerate crack propagation in this case. On the contrary, in a stress-free state, Laplace pressure would induce a natural closure of the crack, inducing a phenomenon known in the literature as crack healing. Indeed, experimental tests show that specimens plunged in water with no stress application present a par-

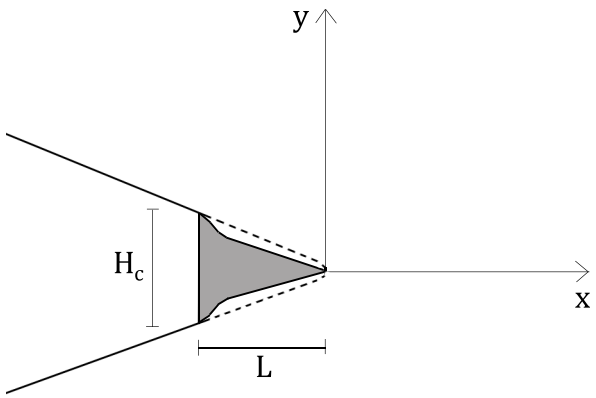

Figure 4.2: Water capillary condensation inside the microcrack (Pallares et al., 2011).

tial strength recovery, due to crack closure. This is a very interesting matter, and many questions are still open on whether this water penetration is induced by stress or not (Tomozawa, 1996; Tomozawa, 1998). This thesis concentrates on water-glass reaction in a stressed state.

4.1.3 Influence of temperature and pH on water-glass reactions

As it will be shown later, several experimental theories provide evidence of the influence of temperature and pH on stress-corrosion reactions (Wiederhorn and Bolz, 1970; Wiederhorn, 1971). It is well known that glass is susceptible to corrosion by solutions with a high pH, as mentioned before. Hence, corrosion rate increases when increasing pH. Similarly, corrosion reaction velocity strictly depends on temperature, since the process is thermally activated. In the following section, stress-corrosion will be framed within the chemical kinetics theory, where absolute temperature plays a central role. In a few words, independently on temperature, water molecules physically enter inside the flaw. As seen above, the physical effect is a negative pressure that tends to close the crack lips. In addition, water electric structure is able to react with glass SiO_4 tetrahedra, and this chemical reaction is enhanced by temperature. Simple tests show that specimens plunged in water, at different temperatures, register different strengths, i.e. different corro-

sion rates. The influence of temperature will be widely discussed in the following part, and is crucial within a design context.

4.2 Stress-corrosion theories

4.2.1 Chemical kinetics

Stress-corrosion main theory, which was formulated by Charles around 1960, takes its origin from the chemical kinetics framework for a general reaction, introduced by a work of Arrhenius of 1889 (Arrhenius, 1889). Given a general chemical reaction, reaction rate k strongly depends on temperature, and normally increases when increasing temperature. A general rule is that, at room temperature, k doubles or triples for each $10°C$ increase of temperature. In 1889, Arrhenius observed that for many reactions the rate k obeys to the following law:

$$k(T) = Ae^{-\left(\frac{E_a}{RT}\right)} \tag{4.2}$$

where A and E_a are constants characteristic of the reaction, R is the gas constant and T the absolute temperature. E_a is called Arrhenius activation energy, while A is a pre-exponential kinetic factor, with the same dimension of k. The exponential term is dimensionless, hence E_a has the dimension of $[RT]$, i.e. energy per mole and is usually expressed by kJ/mol or kcal/mol. Arrhenius law is derived by arguing that the temperature dependence of rate constants would probably resemble the temperature dependence of equilibrium constants. Van't Hoff equation describes temperature dependence of the ideal-gas equilibrium constant ${K_P}^o$, which is only function of T (Levine, 2009):

$$\frac{dln{K_P}^o}{dT} = \frac{\triangle H^o}{RT^2} \tag{4.3}$$

where $\triangle H^o$ is the standard enthalpy change for the ideal-gas reaction at temperature T. For gases, pure liquids and solids, a standard state of fixed pressure $P^o = 1bar$ is chosen, so that ${K_P}^o$ depends only on temperature. The general form for liquid and solid solutions depends both on temperature and pressure, and differentiating with respect to P gives:

$$\left(\frac{\partial lnK^o}{\partial P}\right)_T = -\frac{\triangle V^o}{RT} \tag{4.4}$$

where V^o is the solution volume. For an ideal gas, $\frac{dln{K_c}^o}{dt} = \frac{\triangle U^o}{RT^2}$, where ${K_c}^o$ is the standard concentration equilibrium constant and $\triangle U^o$ is the change in standard-state molar internal energy for the reaction.

The total energy of a body is $E = K + V + U$, where K and V are the macroscopic energies, respectively kinetic and potential, which are due to motion of the body through space. U is the internal energy, due to molecular motions and interactions. By analogy to Equations (4.2), (4.3) and (4.4), Arrhenius provided the following relation:

$$\frac{dlnk}{dt} = \frac{E_a}{RT^2} \tag{4.5}$$

By assuming that E_a is temperature independent and by integrating Equation (4.5), one obtains:

$$k = e^{-\left(\frac{E_a}{RT}\right)} e^c \tag{4.6}$$

where c is the integration constant and is equal to lnA. If a reaction responds to Arrhenius law, $log_{10}k$ *versus* $1/T$ is represented by a straight line. Let now spend a few words on the physical meaning of the term E_a. It represents the activation energy barrier, which has to be exceeded for the reaction to be triggered. From Arrhenius law, it is evident that a low activation energy implies a fast reaction. For a general kinetic process, the general definition of E_a, whether or not it depends on T, is:

$$E_a = RT^2 \frac{dlnk}{dT} \tag{4.7}$$

Equivalently, the kinetic factor A is equal to $ke^{(E_a/RT)}$. A physical interpretation for E_a is given by the following theorem: in a gas-phase elementary bimolecular reaction, $\epsilon_a = E_a/N_A$ is equal to the total average energy of the pairs of reacting molecules which are being involved in a reaction minus the total average energy of all the pairs of reacting molecules. An interpretation is that two molecules colliding require a certain minimum kinetic energy of relative motion for starting to break the bonds and form new products.

Arrhenius equation is valid for almost all the homogeneous elementary reactions and for several composite reactions. In his theory, both A and E_a are constant. More sophisticate theories provide a similar equation where the two terms depend on T as follows:

$$k \approx CT^m e^{-\frac{\triangle E_o}{RT}} \tag{4.8}$$

where $E_o = E_a - mRT$. As will be discussed later, stress-corrosion reaction occurring in glass may be derived by Arrhenius equation considering the case of temperature dependence of E_a.

4.2.2 Charles studies: the basis of stress-corrosion theories

In 1958, Charles formulated a theory that became the principal explanation for delayed failure phenomenon in soda-lime silica glass, through two contemporary works (Charles, 1958a; Charles, 1958b). In the first paper, he studies water vapor corrosion of soda-lime silica glass, by proposing a dissolution mechanism, where the initial phase of water corrosion is represented by an alkali ion self-diffusion that breaks the glass network. From experiments, Charles observes that a glass network expansion increases corrosion rate. Asymmetric expansion conditions around the flaw surface induced by the applied stress induce the growth of the defect in a preferred direction, causing a delayed failure effect. In previous studies, atmospheric water vapor was shown to be the most relevant factor in delayed failure (Baker and Preston, 1946). In his first work, Charles studies both chemical and mechanical aspects of delayed failure.

Chemical aspects

The effects of water vapor on alkali-silica containing glass are represented by an acceleration of the corrosion process, with a consequent loss of coherence and a strong volume expansion of corroded material. The entity of these effects depends on glass composition, temperature, exposure time. To validate his theory, Charles performed series of experiments on soda-lime silica glass specimens subjected to water vapor and to dry vapor at different temperatures and for different time intervals, observing a temperature and time dependence of the depth penetration of corrosion layer. After a certain time, penetration rate undergoes an acceleration and becomes the dominant process. This time increases when decreasing temperature, since at high temperature levels the corrosion process is fast and dominates failure mechanisms almost from the beginning. Glass is shown to be corroded both by water and water vapor, and alkali containing glass, when exposed to water vapor, even at low temperatures, undergoes decomposition. Charles analyzes the chemical reactions occurring between glass and water, where two structures play a dominant role. The first one is the unending silica network, the second one is the terminal structure which associates alkali ions to the silica network. Glass structure degradation is strictly dependent on terminal structures, and this justifies the different corrosion behaviour between pure silica glass and soda-lime silica glass. In describing dissolution reaction, Charles take account only of the terminal end associating Na^+ ions to the network, since they play a central role. The dissolution reaction may be expressed as follows: the first step is a hydrolysis reaction,

$$Si - O - Na + H_2O \rightarrow SiOH + Na^+ + OH^- \tag{4.9}$$

where a Na^+ ion migrates breaking an $O - Na$ bond, and to this follows that the free oxygen atom dissociates one water molecule by assuming an hydrogen ion, with the formation of a free hydroxyl ion OH^-. In a second step, the free OH^- ion creates a new bond with SiO_4 tetrahedra:

$$[Si - O - Si] + OH^- \rightarrow SiOH + SiO \tag{4.10}$$

The strong bond in silicon-oxygen tetrahedra breaks and an extreme of the broken bond becomes a silanol $SiOH$, while the other produces an end structure SiO^-, which is capable to dissociate another H_2O molecule:

$$SiO^- + H_2O \rightarrow SiOH + OH^- \tag{4.11}$$

Hence, the reaction between one silicon-oxygen tetrahedron and one water molecules creates two silanols $SiOH$. For each Na^+ ion dissociated from silica, an hydroxyl ion OH^- is formed, and this increases the pH of the corrosion layer, producing an acceleration of the corrosive process. The first step of the hydrolysis reaction acts as a trigger for alkali-silica glass dissolution in water vapor, and the reaction is temperature dependent, as shown in Fig. 4.3.

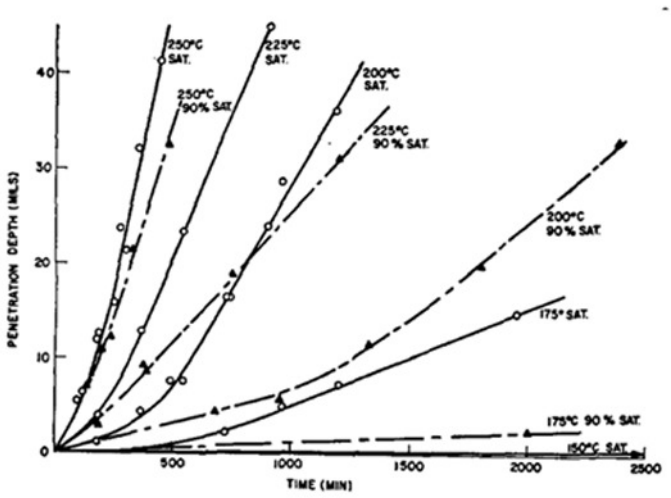

Figure 4.3: Temperature dependence of corrosion penetration in soda-lime glass (Charles, 1958a).

Corrosion of soda-lime silica glass in a steam phase is highly faster than corrosion in water phase, by parity of temperature, and this is due to the fact that in water phase a big dilution is possible with a consequent slower increase of pH.

Mechanical aspects

A part from the concentration of reactants, a relevant role in reaction rate of corrosion process is attributed to the structural state of glass. Density is strictly connected to corrosion processes. Indeed, low density glass structures, as the ones induced by elevate fictive temperatures[1], show expanded structures, while low fictive temperatures induce compacted structures. It is easy to understand that in expanded structures the number of Na^+ ions in the interstices between silica tetrahedra is relevantly higher inducing a low barrier energy E_a for diffusion, while in compact glass the number of Na^+ ions is reduced. This ion produces the major part of electrical, mechanical and chemical effects. Hence, the chemical activity of expanded glass is much higher compared to compact glass. Structural expansion may be induced not only by high fictive temperature but also by relevant triaxial tensile stresses of mechanical origin. Therefore, a stress state can induce Na^+ ions migration from the interstices with the above-shown chemical effects.

Finally, Charles explains why in an isotropic material as glass, crack tends to propagate in a preferred direction. This is due to the fact that asymmetric stress fields form around the defect, and these fields, in addition to corrosion mechanisms which are stress-dependent, induce crack propagation.

Charles stress-corrosion model

In the second of the two works presented in 1958, Charles illustrates a model for corrosion rate causing delayed failure [2]. Chemical reaction rate is affected by stress conditions around local areas and by temperature, pressure and composition of the surrounding environment. Self-diffusion of Na^+ ions in bulk glass is temperature dependent, and causes the low long term strengths of glass. In this work, Charles presents experimental results from four-point bending tests performed on soda-lime glass of known chemical composition (SiO_2 72%, Na_2O 17%, CaO 5%, Al_2O_3 and MgO), in a temperature range varying from $-170°C$ to $242°C$. He obtains delayed failure curves from different temperature, as shown in Fig. 4.4.

[1] The fictive temperature may be defined as follows: by instantaneously changing the temperature to the fictive temperature, material properties are in equilibrium.

[2] He continues writing about 'delayed failure'. The term stress-corrosion' will appear in a later work.

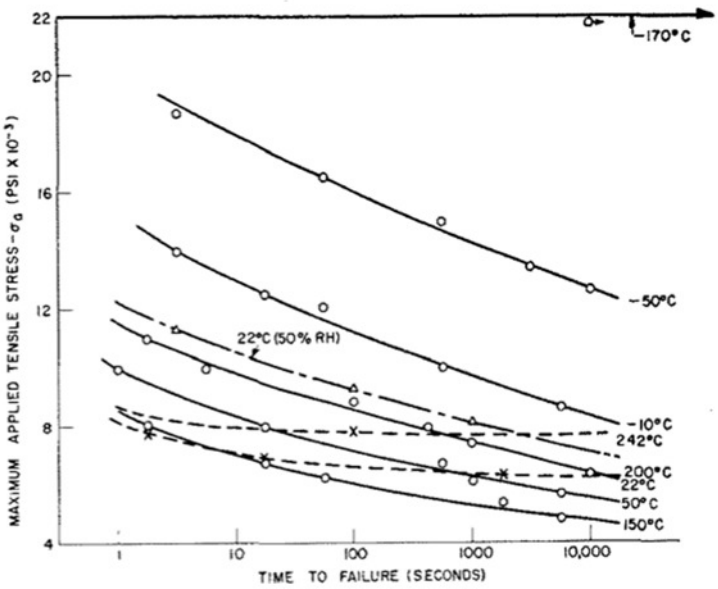

Figure 4.4: Delayed failure curves for soda-lime glass (Charles, 1958b).

At $T = -170°C$ no delayed failure is registered, since failure is independent of time. Charles refers to Inglis theory, where for an elliptic flaw tip the following relation states (Inglis, 1913):

$$\frac{\sigma_{tip}}{\sigma_A} = 2\Big(\frac{a}{\rho}\Big)^{\frac{1}{2}} \tag{4.12}$$

where σ_{tip} is the stress at the tip, σ_A the applied stress, a the flaw depth and ρ the radius of curvature of the tip. Through Griffith fracture criterion and Orowan developments (Griffith, 1921; Orowan, 1948) the critical stress is equal to:

$$\sigma_{cr} = \sigma_A 2\Big(\frac{a_{cr}}{\rho}\Big)^{\frac{1}{2}} \tag{4.13}$$

Charles bases on these theories by assuming that delayed failure is caused by a flaw propagating for corrosive mechanisms with constant and of atomic dimensions root radius. He assumes a simple general relation which expresses penetration rate of a flaw as function of the stress at the tip σ_{tip}:

$$v_x = f(\sigma_{tip}) + k_1, \quad T\,fixed \tag{4.14}$$

where v_x is the crack propagation velocity in x direction, which corresponds to the corrosion rate in the same direction, f is an unknown

function of the stress at the tip and k_1 is the zero-stress corrosion rate. For $\sigma_A = 0$, crack velocity v_x is equal to the zero-stress corrosion rate k_1 and assumes its minimum value. Charles makes then an important assumption, that is he supposes that the unknown function f is conform to an arbitrary power function of stress, within the high stress ranges around the flaw:

$$v_x = k_2(\sigma_{tip})^n + k_1, \qquad T\,fixed \tag{4.15}$$

where k_2 and n are constants.

This theoretically assumed law is shown to be consistent with experimental results and gives the basis of a power-law function that is commonly used in design predictions, as will be discussed in later sections. By using Inglis relation (see Equation (4.12)) and Griffith criterion (see Equation (4.13)) in order to avoid stress terms, and by assuming that temperature dependence of growth process of the flaw follows Arrhenius law, he obtains a law of crack velocity as function of temperature:

$$v_x(T) = A\Big[k_3\Big(\frac{a}{a_{cr}}\Big)^{\frac{n}{2}} + k_1\Big]e^{-\frac{E_a}{RT}} \tag{4.16}$$

since $\sigma_{tip}/\sigma_{cr} = (a/a_{cr})^{1/2}$. The assumption is on the one hand that the critical stress at the tip is constant within the temperature range, so it can be included in the constant term, and on the other hand that the activation energy can be applied both in a stress-activated corrosion and in a stress-free corrosion. For delayed failure to occur, stress-activated corrosion must exceed the ordinary zero-stress corrosion, and then crack velocity becomes:

$$v_x(T) \simeq B\Big(\frac{a}{a_{cr}}\Big)^{\frac{n}{2}} e^{-\frac{E_a}{RT}} \tag{4.17}$$

where $B = k_3A$. For n big, delayed failure effects are reduced, and for $n \to \infty$ crack growth occurs only when critical conditions are reached. From experimental results, n seems to be around 16, for delayed failure mechanisms.

In a later co-work presented with Hillig, Charles describes the kinetics of stress-corrosion, as a generalization of Arrhenius chemical theory (Charles and Hillig, 1962). If delayed failure is the macroscopic phenomenon observed, stress-corrosion represents the microscopic physical-chemical process causing delayed failure. In this interesting work, he postulates that the time dependent rupture of glass under stress and in a given environment is due to an alteration of the geometry of surface flaws, by corrosion or dissolution reaction. Some previous theories had focused on the effect of water on cracked surfaces, as the one assumed by Joffe in 1924, who postulates that uniform surface dissolution

blunts surface cracks (Joffe, 1924). Joffe shows that normally brittle alkali halides can behave in a ductile manner by immersion of the crystals of these salts in warm water during loading. He assumes that the original crystals contain microcracks on their surface, and water dissolves the cracked layer, by leaving a non-cracked surface, and this induces a strength increase. Then water has the effect of levigating the cracked surface. In further works, it was shown that the exposition to a chemical environment induces a strengthening of the crystal by an embrittlement (Parker, 1960).

Also Charles states that, in stress-free conditions, surface blunting reduces cracks and their effect of stress concentrators, with a consequent strength increase. In addition, Charles assumes that, on the contrary, when the cracked surface is subjected to tensile stress and the rate of chemical attack is sensitive to the stress state around the crack, the corrosion reaction induces a crack sharpening, that could lead to rupture. This was not clear before this work. Charles assumes a given dependence of corrosion rate on stress and he assumes that the stress distribution around the flaw is the one given by Inglis (see LEFM, chapter 2) and he proposes a mathematical model for stress-corrosion, considering glass as elastic isotropic. Charles models an ideally elastic isotropic solid reacting with environment, and this reaction is considered as thermally activated and in each point the reaction rate is determined by the local thermodynamic driving force and by local perturbations of the energy barrier that has to be exceeded for the reaction to occur. Hence, he states that the reaction rate is not controlled by transportation of the reactant on the reaction site and the local corrosion rate may be affected by the local stress state and by the excess of surface free energy. Charles model is in continuity with Arrhenius chemical kinetics (see previous section), since he expresses the activation energy E_a as function of applied tensile stress σ by using a Taylor expansion:

$$E_a(\sigma) = E_a(0) + \sigma \frac{\partial E_a}{\partial \sigma}|_{\sigma=0} + ... \tag{4.18}$$

where the term $\partial E_a/\partial\sigma$ has dimension of a volume and is termed activation volume V. $E_a(0)$ is the ordinary, zero-stress, Arrhenius energy and includes both the chemical potential difference driving the reaction and the energy barrier for the reaction species. Charles associates another term to the thermodynamic driving force, that is the molar free energy contribution $\triangle F$ associated with the curvature of the surface:

$$\triangle F = -\frac{\Gamma V_M}{\rho} \tag{4.19}$$

where Γ is the surface free energy, ρ the radius of curvature and V_M

the molar volume. Finally, Charles expresses the local corrosion rate normal to the crack interface as follows:

$$v = A' e^{-(E_a(0)+\Gamma V_M/\rho-\sigma V)/RT} \tag{4.20}$$

where A' is a pre-exponential kinetic factor. In this relation, v represents the corrosion rate and is a generalization of chemical kinetics k of the Arrhenius formula (see previous section) who expressed the rate of a general reaction in function of absolute temperature. It is evident that in this equation the dependence of velocity on stress is not a power law but an exponential law. Corrosion rate increases when increasing temperature, in a non-linear way, and it is equivalent to the crack propagation velocity. Hence, initial flaws propagate fast at high temperature levels, and this velocity is as higher as the activation energy lowers. In addition, the activation energy is reduced by the presence of the stress, and this justifies the sign of the σV factor. This means that, in a stressed state, the activation energy barrier that needs to be exceeded for the reaction to be triggered is lower than in an unstressed state, and so crack propagation is enhanced in the former case.

In a few words, Charles states that the combined action between stress and a reactive environment induces a change of flaw tip geometry, and this change determines local stress and local chemical potential. On the other side, local stress and local chemical potential determine a change in geometry. On the role of water at the crack tip, several investigations are still open. Both the power-law function (see Equation (4.17)) and the exponential function (see Equation (4.20)) are shown to be in agreement with experiments, so they can be considered as equivalent. Starting from Charles delayed failure or stress-corrosion studies, an experimental theory was formulated some years later by Wiederhorn, giving the basis of the main glass lifetime prediction models (Wiederhorn, 1967; Wiederhorn and Bolz, 1970; Haldimann, 2006; Overend and Zammit, 2012).

4.2.3 Wiederhorn experimental theory

Wiederhorn studies, consistent with Charles stress-corrosion theory, are based on experimental results focusing on the influence of relative humidity, temperature and pH of the environment surrounding a cracked glass surface. Also glass chemical composition is investigated, since experimental results show relevant differences between the different glasses. In collaboration with Evans, he shows that both power law and exponential law theoretically provided by Charles for crack propagation velocity as function of stress intensity factor are consistent with experimental data. As will be discussed in a further section, power law relation provides simpler calculation for lifetime predictions, and

for this reason it is the basis of current prediction models for glass. Wiederhorn studies show a relevant interest for physical processes that occur in stress-corrosion failures. His experimental theory has given a strong basis for the present thesis, whose focus is mostly on chemical-physical description of glass failure mechanisms.

In a first work, Wiederhorn focuses on the influence of water vapor on delayed failure, through an experimental investigation carried out by accurately measuring crack propagation velocity (Wiederhorn, 1967). From experimental results, crack velocity is found to be a complex function of stress and water vapor contained in the environment, since even small amounts of vapor react with glass under stress by causing a delayed breakage. As Charles had stated, reaction velocity with environment increases with stress. Two crack motions may be observed, the first one represented by a slow crack growth induced by chemical attack from environment occurring at the crack tip, i.e. sub-critical crack growth, the second one is an unstable growth occurring as the crack reaches its critical value, i.e. critical crack growth (see Griffith's theory, chapter 2). The two steps are shown in experimental results from tests performed on microscope slides of known composition (a specific soda-lime silica glass), where crack velocity v is measured as function of applied force and environment, under a constant stress. Fig. 4.5 shows crack propagation over time, for tests in air at relative humidity $RH = 50\%$.

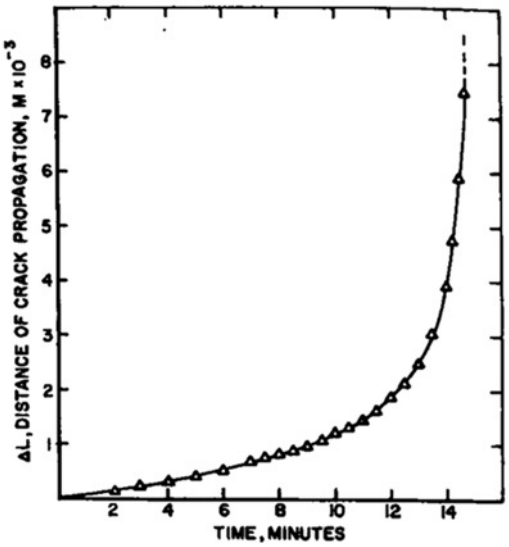

Figure 4.5: Crack propagation over time (Wiederhorn, 1967).

Through a series of experiments performed at different relative hu-

midity conditions and at room temperature, he also provides an explanation of the effect of water vapor on corrosion velocity, as shown in Fig. 4.6 (left) where crack velocity (on a logarithmic scale) is plotted *versus* applied force in function of water content in air. A distinction is made between air with $RH = 100\%$ and water, but the slopes of the curves are similar. Then he deduces that failure mechanism in water as in moist air is the same. Even if probably the chemical activity of water at the crack tip is different, it is possible to consider the two effects as the same effect. As will be discussed later, this thesis is based on experiments performed in water, and from Wiederhorn results it may be assumed that water corresponds to a relative humidity value of 100%. The curves of Fig. 4.6 (left) are obtained by interpolating experimental results by the method of least squares.

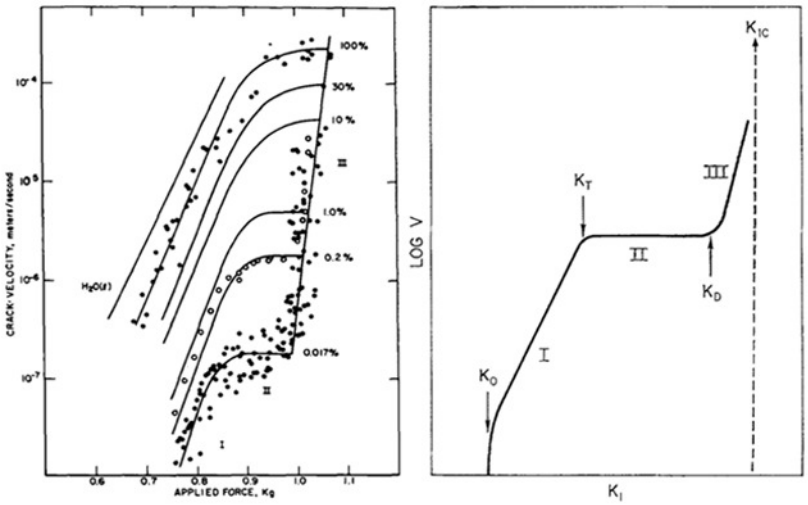

Figure 4.6: Crack velocity *versus* applied force at different levels of water content (left); different regions for crack velocity *versus* stress intensity factor (Wiederhorn, 1967; Evans, 1972).

From these experiments, Wiederhorn notices that crack motion is complex and it strictly depends on the amount of moisture in the environment. The trend of crack propagation velocity in function of stress, given by experiments, can be generalized by a graph where three different regions appear, as shown in Fig. 4.6 (right). In region I, crack velocity is dependent on applied force by an exponential law, that is $v = \alpha \exp\beta P$, where β is the slope of the curves. In Fig. 4.6 (left), the different curves show the same slope, which is then independent on relative humidity. On the contrary, the variation of the intercept α is independent of moisture. By decreasing relative humidity, crack

velocity decreases and the strength increases. Hence, in region I crack motion is limited by the rate of reaction of water with glass at the tip. Exponential dependence of region I is explained by the theory of Charles and Hillig (see the previous section). Wiederhorn assumes that in region I crack propagation is due to the corrosive attack of water vapor on glass at the crack tip. Down to the limit of region I, the crack is so small or the stress so law that no propagation is observed. In region II, crack velocity in nearly independent of the applied force, and this constant branch shifts depending on the water content. The assumption is that in this region crack velocity depends uniquely on water content, i.e. on the velocity of water transportation at the crack tip. Hence crack motion is limited by the rate of transport of vapor to the tip. In region III, crack velocity increases exponentially when increasing the applied force, but the slope of the curve is relevantly higher than the slope of region I. In order to explain this, Wiederhorn assumes that in region III crack motion mechanism is independent on water concentration in the environment, since the crack has reached a critical length, or equivalently the stress has reached its critical value, so that propagation is nearly instantaneous and does not depend on environment any more. Wiederhorn provides a chemical explanation for the three regions. From the theories of rate process, there are three possible limiting steps for the chemically enhanced fracture process: diffusion, chemisorption and chemical reaction. The latter two are expected to depend on the stress at the crack tip. If fracture were controlled by chemisorption or another chemical reaction, the crack velocity is expected to be exponentially dependent on the applied force (region I). By contrast, fracture controlled by the rate of water diffusion is expected to be independent on the applied force, while diffusion of gas reactants through surface does not depend on the stress state of the surface. Since in region II crack velocity is nearly independent on stress, one can deduce that in this region crack propagation rate is controlled by the rate of water diffusion to the crack tip. From his experimental studies, he obtains that, at constant load P, crack velocity in region I should depend on the partial pressure of water vapor to the n^{th} power as follows:

$$v = \gamma \left(\frac{p_{H_2O}}{p^o_{H_2O}} \right)^n \tag{4.21}$$

where p_{H_2O} is the partial pressure of vapor and $p^o_{H_2O}$ is the saturation pressure. The ratio in Equation (4.21) represents relative humidity of moist air. On a logarithmic plane, velocity dependence on RH is almost linear. For n, he found from experiments a range value of $0,5 \div 1$.

Basing on Charles and Hillig theory (see previous section), Wiederhorn develops an equation of combined rate which takes account of

experimental data of both regions I and II. However, there are some discrepancies between theory and experiments, probably due to an uncertainty on chemical reaction at the tip and on processes of transport at the tip.

Other tests performed investigating the effect of temperature show a consistency with Charles Equation (4.20) (Wiederhorn, 1967). From these tests, Wiederhorn provides an experimental equation by neglecting the terms of surface energy, which are small compared to the others, and simply obtains:

$$v = v_0 e^{-(E_a - V\sigma)/RT} \tag{4.22}$$

which describes properly results in region I. Since E_a is a function of environment, Equation (4.22) can be extended in order to take into account also the moisture content in environment. The activation energy may be expressed as the difference in the chemical potential between reactants and product of corrosion:

$$E_a = {\mu_B}^* - \mu_B - n\mu_{H_2O} \tag{4.23}$$

where μ_B^* is the chemical potential of the activated state, μ_B the chemical potential of an initial bond, μ_{H_2O} the chemical potential of water and n is the number of water molecules required for the initial bond B to be broken. He assumes that water behaves as a perfect gas:

$$\mu H_2O = RT[\Phi(T) + ln p_{H_2O}] \tag{4.24}$$

where $\Phi(T)$ is a function of temperature. By substituting the Equations (4.23) and (4.24) in the expression for crack velocity, Wiederhorn obtains the following relation for crack motion:

$$v = v_0 (p_{H_2O})^n e^{-[\mu_B^* - \mu_B - nRT\Phi(T) - \sigma V]/RT} \tag{4.25}$$

In this way, the two dependencies of crack velocity, i.e. corrosion rate, on water vapor and on temperature are separated. Water condensation is governed by Kelvin equation:

$$ln\left(\frac{p_o}{p}\right) = -\frac{2\Gamma V}{\rho RT} \tag{4.26}$$

Few years later, Wiederhorn presents several experimental results from tests performed on six glasses, investigating the influence of temperature on corrosion velocity, that is on crack propagation (Wiederhorn and Bolz, 1970). Tests were carried out by plunging the specimens in water, in order to provide constant conditions of moisture. By measuring crack velocity as function of stress intensity factor K_I (from LEFM, chapter 2), glass composition and absolute temperature T, he

obtains for each test the activation energy E_a and the activation volume V. Results are consistent with Charles and Hillig stress-corrosion theory. Silica glass shows the highest resistance to corrosion, while soda-lime silica glass the lowest one, and this is due to the sodium ions. Tests were performed at 2°, 25°, 40°, 60° and 90°C. The 2°C temperature was reached with ice floating in water while the high temperatures by heating a coat around the box containing water. Temperatures were controlled at $\pm 1°C$. A similar procedure is proposed for this thesis, as will be shown later. The independent variable is the stress intensity factor for fracture mode I, K_I, which is proportional to the stress at the crack tip and which allows eliminating defect dimension a and testing geometry Y as experimental variables. Tests performed at the same temperature (25°C) in water ($RH \approx 100\%$) show the differences between four glasses (see Fig. 4.7).

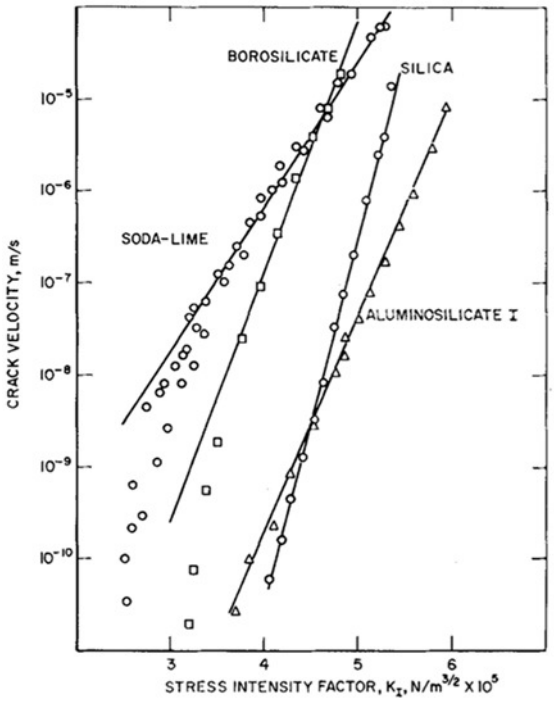

Figure 4.7: Crack velocity as function of K_I for four glasses (Wiederhorn and Bolz, 1970).

Hence, glass chemical composition plays a relevant role in stress-corrosion mechanisms and on crack growth rate.

As for the influence of temperature, Fig. 4.8 shows experimental results for tests on soda-lime silica glass specimens, for three different

temperatures. The slope of the curves is more or less the same, while the intercept changes with temperature.

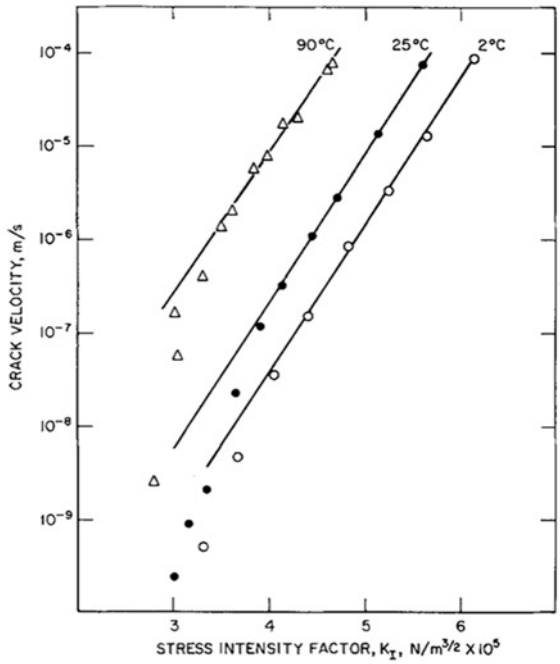

Figure 4.8: Influence of temperature on crack velocity in soda-lime silica glass (Wiederhorn and Bolz, 1970).

Moreover, the exponential dependence of velocity on K_I, which characterizes fracture region I, belongs to a smaller range of velocity when increasing temperature. Fig. 4.9 shows temperature behaviour for soda-lime silica glass (left) and pure silica glass (right).

In silica glass, the curves are more compact and with a higher slope and for higher levels of K_I. From experimental results, Wiederhorn obtains information on the processes activated during stress-corrosion. His experimental data fit the empirical equation

$$v = v_0 e^{-(E_a - bK_I)/RT} \tag{4.27}$$

where v is crack velocity, v_0, E_a and b are experimental constants, which he determines empirically by the method of the least squares. Table represented in Fig. 4.10 shows the influence of chemical composition on these parameters.

Silica glass, compared to soda-lime glass, has higher values of activation energy E_a, and this implies a higher resistance to stress-corrosion,

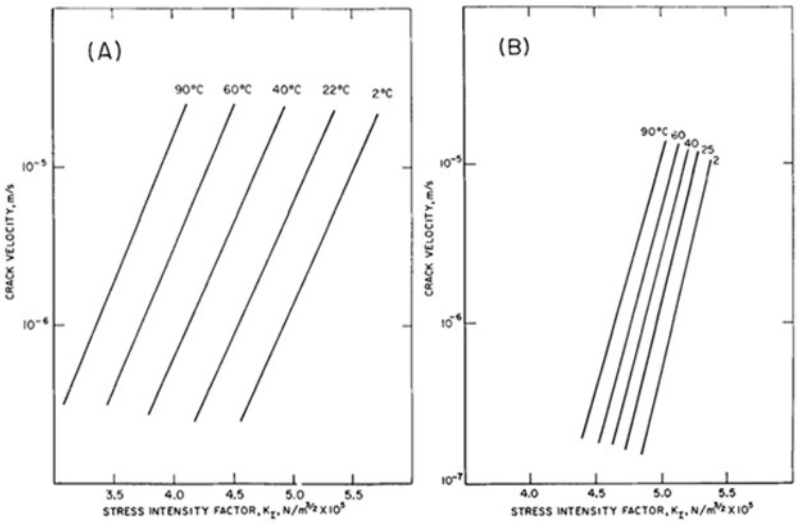

Figure 4.9: Crack velocity *versus* K_I for soda-lime silica glass (left) and silica glass (right) (Wiederhorn and Bolz, 1970).

see previous section. In a further chapter, it will be shown that the empirical parameters of Equation (4.27) depend not only on chemical composition but also, under a deeper glance, on environmental variables. Silica glass has a lower value for v_0 which is a kinetic factor and implies that crack propagates more slowly. Wiederhorn investigates the influence of macroscopic flaws, while glass strength depends on the presence of small surface flaws, even smaller than $10\mu m$. Experimental results agree with Charles and Hillig theory. All chemical reactions are activated processes. So, also stress-corrosion is an activated process, and the activation energy for the process is stress-sensitive, and the reaction is faster where the stress fields are higher. Hence, water reacts more rapidly at the crack tip where the stresses are higher.

Charles and Hillig provided a quantitative theory for stress-corrosion, where $v = v_0 \exp(-E_a + V\sigma - \Gamma V_M/\rho)/RT$. This formula is valid for a two-dimensional Griffith crack, where $\sigma = 2K_I/\sqrt{\pi\rho}$. For high stresses, a sharpening occurs and ρ decreases down to a limit given by glass structure. This means that down to a certain limit, the term $\Gamma V_M/\rho$ is a constant independent of stress, and Charles equation becomes:

$$v = v_0 e^{\frac{(-E_a^* + 2VK_I/\sqrt{\pi\rho})}{RT}} \tag{4.28}$$

where $E_a^* = E_a + \Gamma V_M/\rho$, both terms non dependent on stress. By defining a parameter b such as $V = b\sqrt{\pi\rho}/2$ Wiederhorn simply obtains $v = v_0 \exp(-E_a^* + bK_I)/RT$. Hence, for high stresses, Wiederhorn

Glass	E^* (kcal/mol)* (J/mol)	b (mks units)	ln v_0
Silica	33.1±1.0 (1.391 E5)	0.216±0.006	−1.32±0.6
Aluminosilicate I	29.0±0.7 (1.212 E5)	.138±0.003	5.5±0.4
Aluminosilicate II	30.1±0.6 (1.262 E5)	.164±0.003	7.9±0.3
Borosilicate	30.8±0.8 (1.288 E5)	.200±0.005	3.5±0.5
Lead-alkali	25.2±1.2 (1.056 E5)	.144±0.006	6.7±0.6
Soda-lime silicate	26.0±1.1 (1.088 E5)	.110±0.004	10.3±0.5

*Values given in J/mol in parentheses.

Figure 4.10: Values for the three parameters from tests performed on six different glasses (Wiederhorn and Bolz, 1970).

experimental equation is equivalent to theoretical equation formulated by Charles and Hillig.

Wiederhorn gives also a chemical interpretation for stress-corrosion, considered as a stress-enhanced chemical reaction between water and glass (Wiederhorn, 1971). In this theory, crack propagation is influenced by the crack tip ion OH^- concentration. This hypothesis is supported by the observation that experimental results are related to pH measurements in glass and water. Measurements show that pH varies with glass composition from 5 to 12, and this suggests a high variation of pH at the crack tip.

The steps are the following: 1) chemical reaction occurs where the stress is higher (tip of the crack); 2) crack grows due to the chemical reaction; 3) crack reaches its critical length. Charles had stated that hydroxyl ions attack glass network by leading to breakage of the siloxane bonds (Charles, 1958a), and glass is supposed to be susceptible to corrosion by high pH solutions. Wiederhorn provides an experimental study on the relation between fracture process in glass and hydroxyl ion concentration in water, and he confirms the hypothesis that in stress-corrosion process hydroxyl ions have a relevant role. The parameters which characterize the crack tip environment are a high ratio crack surface-to-void inside the flaw and a leaching action of the environment on fresh fracture surfaces, which are formed during crack propagation. Leaching experiments are performed by putting distilled water (pH = 6 to 6,5) through ground glass, by accurately measuring pH during water penetration. Water-glass reaction is observed as well as the dependence of pH on temperature and on glass-to-void ratio.

The pH seems to change relevantly with glass composition, more than with temperature. The registered wide range of pH corresponds to a wide range of environments at the crack tip. Fig. 4.11 shows the effect of temperature on pH, and results are consistent with Arrhenius plot.

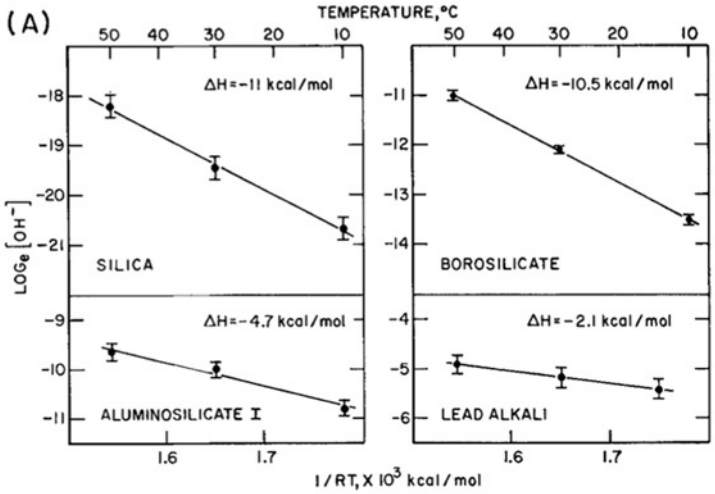

Figure 4.11: Effect of temperature on pH of ground glass (Wiederhorn, 1971).

The relation between pH and temperature has the following form: $\ln(OH^-) = -\alpha/RT$, that is OH^- =exp$(-\alpha/RT)$. Where there is a high concentration of alkali ions, pH strongly depends on chemical concentration. Glass corrosion increases when increasing hydroxyl ion OH^- concentration. Charles suggests that hydroxylis reaction controls the rate of breakage of atomic bonds during crack growth, hence OH^- ion concentration at the tip is relevant to determine glass resistance to delayed failure. Hydroxyl ion concentration at the tip is determined by chemical reactions between glass components and chemical species in solution which have been leached from glass. In highly alkali glasses, the exchange between mobile alkali ions in glass and hydroxyl ions in solution induces a strong concentration of hydroxyl ions at the tip. Ion exchange is a type of hydroxyl reaction, and the pH at the tip depends on the effective concentration of alkali-ions. The dependence of hydroxyl-ion concentration on temperature can be affected by several processes. Experiments confirm the relation

$$OH^- = Ae^{-\frac{\triangle H}{RT}} \tag{4.29}$$

where A depends on the concentration of reactants and $\triangle H$ is the slope of the curve OH^- *versus* $1/RT$. Fresh surfaces created by the

fracture process play a relevant role in defining pH at the tip. From the theory of chemical reactions one can derive the kinetic equations that describe crack motion. If the bond-breaking reaction at the tip depends on OH^-, the rate of chemical reaction v can be related to $[OH^-]$ and to the effective concentration of siloxane bonds $[C]$ at the tip:

$$v = \Big(\frac{kT}{h}\Big)[OH^-]^n[C]e^{-(\frac{\triangle G^\ddagger}{RT})} \tag{4.30}$$

where k is the Boltzmann constant, h is the Planck constant, n is the order of velocity limiting the chemical reaction and $\triangle G^\ddagger$ is the change in free energy. He finally obtain the theoretical equation

$$v = B[OH^-]^n e^{\frac{-\triangle E^\ddagger + (\sigma \triangle V^\ddagger/3) - (\Gamma V_M/\rho)}{RT}} \tag{4.31}$$

which has the same form of the experimental Equation (4.25). Hence, chemical theory is consistent with results on crack velocity expressed by the empirical law. The conclusion is that corrosion rate of a glass surface in a stress-free condition is enhanced by the presence of hydroxyl ions on the surface, and crack velocity is equivalent to corrosion rate. He finally relates results on crack velocity with crack tip environment, confirming the hypothesis that OH^- ions play a role in the fracture process. He theoretically arrives to the crack motion equation and proves that it is equivalent to the one experimentally founded.

Parallel to chemical considerations, Wiederhorn, in collaboration with Evans, provides an empirical equation that has been used for years in predictive models for glass (Evans, 1974; Evans and Wiederhorn, 1974). In a previous work, Evans analyses crack velocity as function of stress intensity factor, referring to Wiederhorn studies. Slow crack growth in ceramic materials can be described by crack velocity and stress intensity factor for a given microstructure and corrosive species. The relation between v and K_I for each system depends on concentration of corrosive species (water) in the environment and on temperature and it is independent of crack length and testing conditions. Evans provides a simple scheme of the three regions of crack propagation, as shown in Fig. 4.6 (right), from Wiederhorn experimental results on water vapor. Looking at the figure, K_0 represents a slow crack growth limit, which in other works is known as threshold and is called K_{th}, while K_{Ic} is the critical value that stress intensity factor reaches after subcritical crack propagation due to stress-corrosion (regions I and II). After K_I reaches its critical value, also known as material toughness, the crack propagates in an unstable way and rupture is almost instantaneous. Evans shows as the exponential law that describes crack behaviour in region I, as stated by Charles and Wiederhorn (see Equations (4.20) and (4.27)) leads to difficult calculations, in deriving failure time. Hence, for prediction purposes, he shows that

another relation between v and K_I is required, also giving a good fit to experimental results. The logarithmic relation as the one used by Charles in 1958 (Charles, 1958c), that is $v = k(\sigma_{tip})^n \exp -E_a/RT$ provides good approximation of experimental data, and a simpler form is given by Evans, keeping v proportional to K^n as follows:

$$\frac{v}{v_0} = \left(\frac{K}{K_0}\right)^n \tag{4.32}$$

for $K > K_0$. As exponential law, also power law gives a correct fit to experimental data and can be used for design purposes.

In a further work, Evans and Wiederhorn provide an analytical accurate lifetime prediction based on experimental tests. In ceramic materials, testing is determinant for giving predictions. As Evans had stated few months before, in region I crack velocity can be expressed as a power function of K_I:

$$v = AK_I^n \tag{4.33}$$

and it will be discussed in the following section that this power law relation is the basis of the major part of current design models for structural glass.

4.3 Focal points

- In glass, subcritical crack growth may occur, as consequence of stress-corrosion mechanisms;
- Stress-corrosion is the explanation of macroscopic phenomenon known as delayed failure;
- Corrosion process by environment is stress-activated and depends on water content, pH and temperature;
- Soda-lime silica glass has a low resistance to corrosion, compared to pure silica glass, and this is due to the presence of Sodium ions;
- Water plays a central role in stress-corrosion, and investigations on its complex effect as well as on the role of stress are still open;
- The chemical-physical effect of water has a different consequence if the crack is exposed to tensile stress or not;
- The main stress-corrosion theory is formulated by Charles basing on the chemical kinetics theory;

- Charles studies provide two equivalent relations for corrosion rate, a power-law and an exponential law, which both are shown to fit experimental data;
- Wiederhorn provides an experimental theory on stress-corrosion consistent with Charles studies;
- Power-law relation is the basis of the main glass lifetime prediction models, since it provides simpler calculations.

Chapter 5

Stress-corrosion and lifetime

5.1 Static fatigue and lifetime curve

Stress-corrosion involves physical-chemical mechanisms occurring at the very small scale (from nanometer to micrometer scale). At a small scale, these mechanisms affect microcrack propagation velocity, as discussed in the previous section. The macroscopic and visible effect of stress-corrosion, which can be empirically registered, is a reduction of material failure time, that is material lifetime. A glass element, loaded in vacuum, would show a lifetime relevantly longer than a glass element tested in a normal environment as moist air. As already mentioned, a macroscopic phenomenon related to lifetime reduction and induced by stress-corrosion is delayed failure, that is a glass element subjected to a constant stress does not fail instantaneously but after a time delay. This means that the applied stress does not reach the critical value, that would break glass immediately, but can also be very low, since it is combined with the attack of environment at the crack tip. Stress-corrosion is also the onset of a macroscopic mechanism known in the literature as *static fatigue*, which is equivalent to delayed failure. Static fatigue represents a strength decrease over time, and the term *fatigue* does not refer to cyclic loading as in metals does. The strength decrease over time is clearly an effect of the interaction between stress and a chemically active environment. The longer is the exposition of a glass element to the environment, the shorter is its lifetime.

In my opinion, it is important to make a distinction between the different mentioned mechanisms. In the literature, many authors write about stress-corrosion, delayed failure, subcritical crack growth and static fatigue as about the same phenomenon. However, the point of

view is not exactly the same. Stress-corrosion is a micro-physical process, consisting in an interaction between a tensile stress and a chemical reaction occurring between glass and environment. This interaction induces propagation of preexisting cracks even if the stress is far from its critical value. Hence, stress-corrosion is the onset of subcritical crack propagation. This latter, occurring at the scale of the flaw, induces a reduction of failure time and is the cause of the two macroscopic phenomena, delayed failure and static fatigue, which are equivalent one to each other.

In the literature, static fatigue curves, i.e. curves of failure stress (strength) *versus* time (load duration), were provided by Mould and Southwick in 1959 (Mould and Southwick, 1959). These curves are built on the basis of experiments carried out on soda-lime silica glass specimens (microscope slides) immersed in distilled water at room temperature, after subjecting the specimens to different surface abrasion treatments. Cracks with different geometries produced differing static fatigue curves at room temperature, but the authors provide a single *universal fatigue curve* by dividing the strength values for each abrasion by the low-temperature[1] strength for the same abrasion and plotting it versus a reduced time. From experimental data, glasses with different kinds of surface damage show not only different strengths but also different ratios of long-to-short time strengths, which represent different rates of static fatigue. The aim of this work was to evaluate the effect of flaw geometry on strength and static fatigue. For each type of abrasion, strength *versus* load duration is plotted, as shown in Fig. 5.1 (left). Strength is high for short-time loads and decreases when increasing load.

Other tests performed in liquid nitrogen at low-temperature provided strength values in the absence of static fatigue. Each strength value σ obtained by the first tests is divided by the corresponding low-temperature strength σ_N based on the data of tests in liquid nitrogen, by using an adjusting parameter. By plotting the ratio σ/σ_N *versus* load duration, the differences in the static fatigue curves are reduced, as shown in Fig. 5.1 (right). The horizontal line of the figure represents load duration for a given ratio σ/σ_N corresponding to 0.5. For each static fatigue curve, the duration corresponding to this ratio is called $t_{0.5}$. By shifting horizontally the curves of Fig. 5.1 (right) so that all the values of $t_{0.5}$ coincide, the authors obtained a single static fatigue curve, shown in Fig. 5.2.

Static fatigue curve has a relevant interest in design, since it enables predicting how long a glass element will last, under a constant stress condition, for a given environment and for known glass chemical composition. In this thesis, static fatigue curve will be named lifetime

[1] The low-temperature strength is independent of load duration, as resulting from the tests.

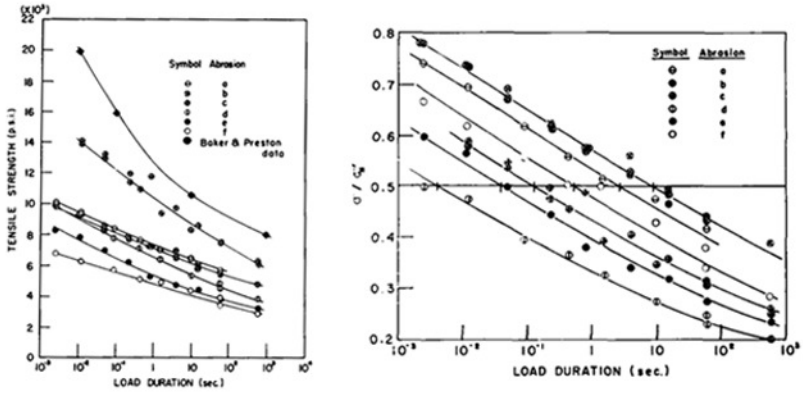

Figure 5.1: Strength *versus* loading time (left) and normalized stress *versus* time (right) (Mould and Southwick, 1959).

curve. Within a design context, it is important to be able to predict a glass element lifetime. Also Wiederhorn provided static fatigue curves for different glass compositions, as shown in Fig. 5.3 (Wiederhorn and Bolz, 1970).

Equivalently, for a glass element to last a given time, static fatigue curves allow knowing the corresponding value of stress that needs to be applied. In glass lifetime prediction, both theory and experimental investigation play a relevant role. Testing allows eliminating some variables from calculation and theory provides predictions on long times (even years) that cannot be considered within a test.

In order to analytically obtain a lifetime equation, whose parameters need to be experimentally calibrated, it is necessary to start from the micromechanism which is the basis of delayed failure or static fatigue phenomena. The propagation velocity of the microdefect corresponds to time derivative of defect dimension:

$$v = \frac{da}{dt} \tag{5.1}$$

At this point, two possibilities are given. The first approach makes use of the exponential law given by Charles (see Equation (4.20), chapter 4) and Wiederhorn (see Equation (4.27), chapter 4), where crack velocity is function of stress and environmental variables. The second possible approach starts from the simpler power-law relation formulated by Evans and Wiederhorn (see Equations (4.32) and (4.33), chapter 4) on the basis of Charles studies of 1958 (Charles, 1958a,b,c). The major part of predictive models, also in recent years, is based on the power-law relation, since it provides simpler integration, but it is now important

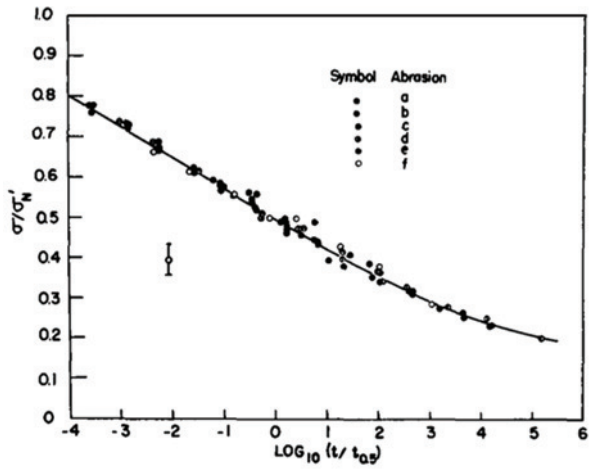

Figure 5.2: Universal static fatigue curve (Mould and Southwick, 1959).

to remember that both expressions are correct since they fit well experimental results, and we can consider them as perfectly equivalent.

5.2 Lifetime curve: current prediction models

5.2.1 Current models based on power-law

Some recent models aim at evaluating glass lifetime, starting from the above-shown theoretical framework. In 1984, Mencik proposed a lifetime model for a general loading history $\sigma(t)$ and for a range where subcritical crack growth occurs, basing on the power-law relation, that is $v = v_0(K_I/K_0)^n$ (Mencik, 1984). K_0 is an arbitrary constant and v_0 and n are parameters characterizing the influence of environment on material. Considering that crack velocity is the time derivative of crack length, i.e. $v = da/dt$ and by using the formula for stress intensity factor from LEFM (see chapter 2), i.e. $K_I = \sigma Y\sqrt{a}$, by integrating through variable separation for a time interval $[0, \tau]$ corresponding to a defect dimension range $[a_i, a_{(\tau)}]$ and for a general loading history $\sigma = \sigma(t)$, he obtains:

$$\int_0^{\tau} {\sigma_{(t)}}^n \, dt = \frac{{K_0}^n}{v_0 Y^n} \int_{a_i}^{a_{(\tau)}} a^{-\frac{n}{2}} \, da \tag{5.2}$$

By solving integration of the right side of Equation (5.2), one obtains:

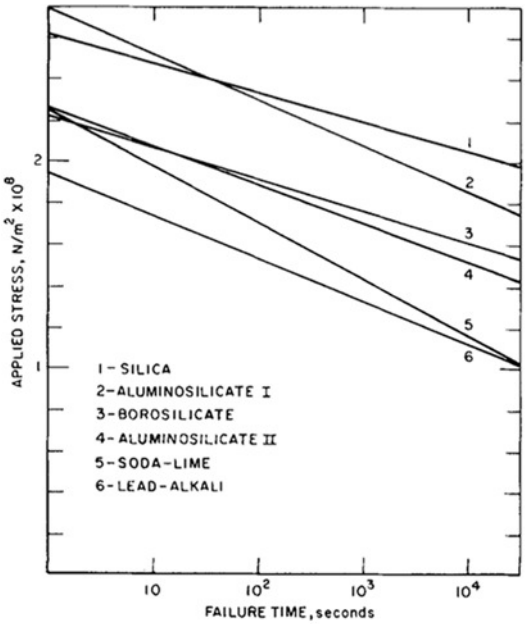

Figure 5.3: Static fatigue curves for different glasses (Wiederhorn and Bolz, 1970).

$$\int_0^{\tau} {\sigma_{(t)}}^n \, dt = \frac{2{K_0}^n}{v_0 Y (n-2) a_i^{\left(\frac{n-2}{2}\right)}} \left[1 - \left(\frac{a_i}{a_{(\tau)}} \right)^{\frac{n-2}{2}} \right] \tag{5.3}$$

The right side of Equation (5.3) depends only on material and on environment. The left side depends only on stress, loading time and environment. Mencik states that two loads induce the same crack propagation, that is the same failure, when the following relation is respected:

$$\int_0^{\tau_1} {\sigma_{1(t)}}^n \, dt = \int_0^{\tau_2} {\sigma_{2(t)}}^n \, dt \tag{5.4}$$

for n constant. Since now, he has considered a generic loading history. He defines an equivalent static stress $\overline{\sigma}$:

$$\overline{\sigma} = \left[\frac{1}{\tau} \int_0^{\tau} {\sigma_{(t)}}^n \, dt \right]^{\frac{1}{n}} \tag{5.5}$$

that is the constant stress that would cause the same crack growth of a loading history $\sigma_{(t)}$ when acting in the same time interval.

For practical purpose, equivalent stress can be expressed as follows:

$$\overline{\sigma} = g^{\frac{1}{n}} \sigma_{ch} \tag{5.6}$$

where σ_{ch} is a chosen characteristic value of the loading history, and g is a coefficient depending on the type of loading:

$$g = \frac{1}{\tau} \int_0^\tau \left[\frac{\sigma_{(t)}}{\sigma_{ch}} \right]^n dt \tag{5.7}$$

Mencik gives different values of g for the main types of single and cyclic loads (Mencik, 1984). For a linear loading history, that is for the case of $\sigma_{(t)} = \dot{\sigma} t$, where $\dot{\sigma}$ is the constant stress rate, he gives the following value for g:

$$g = \frac{1}{n+1} \tag{5.8}$$

and in this case σ_{ch} corresponds to the maximum value σ_{max} that is reached during loading, that is failure strength. By using $\overline{\sigma}$, any type of load can be converted to the static case, which is the simplest one. Relation expressed in Equation (5.8) may be simply demonstrated. For $\sigma_{(t)} = \dot{\sigma} t$, g may be expressed as follows:

$$g = \frac{1}{(\sigma_{ch})^n \tau} \int_0^\tau (\dot{\sigma} t)^n \, dt \tag{5.9}$$

Considering that $\dot{\sigma}$ is assumed constant, Equation (5.9) becomes:

$$g = \frac{\dot{\sigma}^n t^{(n+1)}}{(\sigma_{ch})^n \tau (n+1)} \tag{5.10}$$

and by substituting $\dot{\sigma}$ with σ/t one obtains $g = 1/(n+1)$.

Through Mencik experimental theory, it is possible to obtain lifetime predictions, and many recent glass design models are based on it (Haldimann, 2006; Overend and Zammit, 2012). In 2006, a model was proposed basing on empirical power-law, which is advantageous for practical use. This model makes use of the fracture mechanics formula $K_{I(t)} = \sigma_{(t)} Y \sqrt{\pi a_{(t)}}$ and considers Irwin tensional criterion (see LEFM, chapter 2) which states that fracture occurs when $K_I \geqslant K_{Ic}$. Critical conditions are reached if the load reaches its critical value or equivalently if the defect reaches its critical length. From the critical conditions, one may obtain the critical stress $\sigma_{c(t)}$:

$$\sigma_{c(t)} = \frac{K_{Ic}}{Y \sqrt{\pi a_{(t)}}} \tag{5.11}$$

as well as the critical crack length $a_{c(t)}$:

$$a_{c(t)} = \left(\frac{K_{Ic}}{\sigma_{(t)} Y \sqrt{\pi}} \right)^2 \tag{5.12}$$

Both σ and a depend on time, hence also σ_c and a_c are time-dependent. The critical stress σ_c is also known as *inert strength*, and it represents the strength of a material when no subcritical crack growth occurs. This model also starts from the power-law relation (see Equation (4.32), chapter 4), substituting the constant K_0 with material toughness K_{Ic}:

$$v = \frac{da}{dt} = v_0 \left(\frac{K_I}{K_{Ic}} \right)^n \tag{5.13}$$

The model is valid for $K_I > K_{th}$, hence it does not consider crack growth threshold. Power-law requires that the $v(K_I)$ curve is plotted on a logarithmic plane, while in Evans and Wiederhorn theory it was plotted on a semi-logarithmic plane. As Mencik had previously shown, by integrating by variable separation Equation (5.13) and considering a time range $[0, t_F]$, where t_F is material failure time, i.e. material lifetime, one obtains:

$$\int_0^{t_F} {\sigma_{(t)}}^n \, dt = \frac{2{K_{Ic}}^n}{(n-2)v_0(Y\sqrt{\pi})^n {a_i}^{(n-2)/2}} \left[1 - \left(\frac{a_i}{a_F} \right)^{(n-2)/2} \right] \tag{5.14}$$

where a_i is the initial defect dimension (for $t = 0$) and a_F is the crack dimension at failure (for $t = t_F$). In Wiederhorn studies, the value of n was found around equal to 16 (Evans and Wiederhorn, 1974). For such a value, and considering that $a_F \gg a_i$ since we are considering a stress-corrosion regime where subcritical crack growth occurs, Equation (5.14) is simplified as follows:

$$\int_0^{t_F} {\sigma_{(t)}}^n \, dt = \frac{2{K_{Ic}}^n}{(n-2)v_0(Y\sqrt{\pi})^n {a_i}^{(n-2)/2}} \tag{5.15}$$

This is the classic relation used in current design for glass, which enables evaluating lifetime, given a stress history and by knowing initial crack geometry. This relation has some limits of application, since the assumption that $a_F \gg a_i$ loses validity in inert conditions, that is when the loading time is too short or crack velocity too low.

Considering Mencik relation between a loading history and an equivalent constant stress, i.e. $\int_0^{t_F} {\sigma_{(t)}}^n \, dt = \overline{\sigma}^n t_F$, one may obtain the following expression for failure strength *versus* failure time:

$$\overline{\sigma}_{(t_F)} = \left(\frac{2{K_{Ic}}^n}{(n-2)v_0(Y\sqrt{\pi})^n {a_i}^{(n-2)/2}} \right)^{\frac{1}{n}} {t_F}^{-\frac{1}{n}} \tag{5.16}$$

Failure strength $\overline{\sigma}$ is the static stress that a crack may undergo for a time interval t_F, i.e. lifetime, for a given initial crack, whose dimension a_i and shape Y are known, and for given environmental conditions.

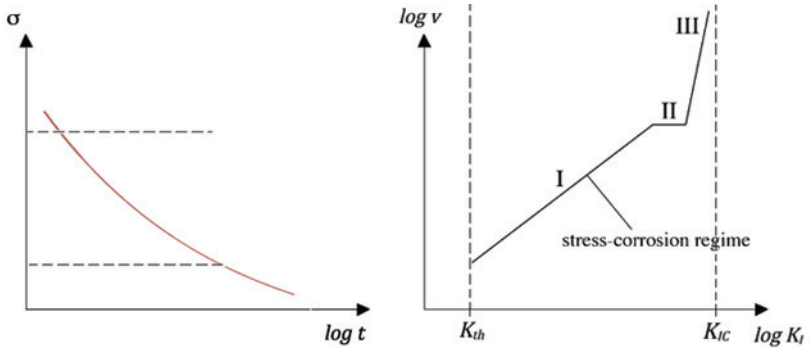

Figure 5.4: Static fatigue curve (left) compared with the three physical regions of $v(K_I)$ (right).

Equivalently, failure time as function of failure stress σ_F and defect geometry is expressed as follows:

$$t_{F(\sigma_F)} = \left(\frac{2{K_{Ic}}^n}{(n-2)v_0(Y\sqrt{\pi})^n {a_i}^{(n-2)/2}} \right) {\sigma_F}^{-n} \tag{5.17}$$

Equation (5.17) shows a high sensitivity of failure time to defect dimension variation. A sensitivity analysis can be easily provided showing that even for small variations of a_i, that is even for few micrometers, failure time undergoes relevant changes. Indeed, experimental investigation shows that depending on the edge finishing, that is responsible for crack dimension, failure time of glass specimens tested at the same conditions is different. Some edge finishings, as polishing or grounding, induce crack lengths of the order of few decades of micrometers, while water-jet cutting finishing causes defects even more than 100 times larger. Hence, as stated by Griffith in his theory of rupture, the conditions of glass surface play a central role in material strength.

In the mentioned models, a correspondence between lifetime curve and the three regions of crack propagation velocity (see chapter 4) is lacking, as shown in Fig. 5.4.

In an even more recent work, the above-mentioned lifetime prediction model has been enriched by considering the two limit values, that is subcritical crack growth threshold and inert conditions (Overend and Zammit, 2012), giving the following relation:

$$\overline{\sigma}_{(t_F)} = \left[\left(\frac{2{K_{Ic}}^n}{(n-2)v_0(Y\sqrt{\pi})^n {a_i}^{(n-2)/2}} \right) \left(\frac{1-(\frac{a_i}{a_F})^{(n-2)/2}}{1-(\frac{a_{th}}{a_i})^{(n-2)/2}} \right) \right]^{\frac{1}{n}} {t_F}^{-\frac{1}{n}} \tag{5.18}$$

where a_F is the length that the crack reaches when the stress intensity factor assumes its critical value:

$$a_F = \left(\frac{K_{Ic}}{\sigma Y \sqrt{\pi}} \right)^2 \tag{5.19}$$

and equivalently a_{th} is the crack length when the stress intensity factor is at the threshold limit:

$$a_{th} = \left(\frac{K_{th}}{\sigma Y \sqrt{\pi}} \right)^2 \tag{5.20}$$

Fig. 5.5 shows the curve taking account of both limits.

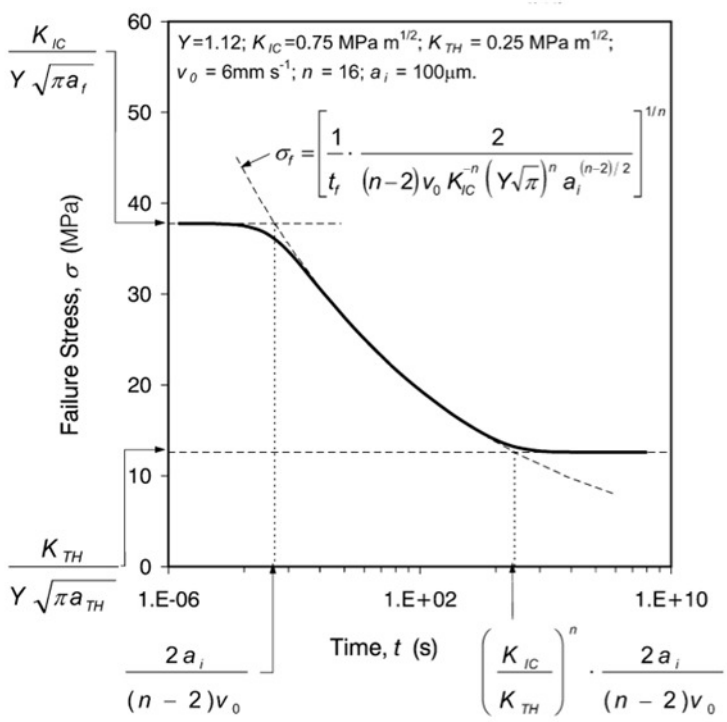

Figure 5.5: Static fatigue curve including inert and threshold conditions (Overend and Zammit, 2012).

5.2.2 Empirical parameters and limits of power-law

In Equation (5.13), crack velocity as function of stress intensity factor is known only if the two parameters n and v_0 are known. The two parameters represent the dependence of crack velocity v on environment,

but they are empirically provided. In a previous work, Wiederhorn had found from experimental investigation that n was around 16, for standard conditions. A more recent work provides tables with the values of the two parameters for different conditions of relative humidity and temperature, as shown in Fig. 5.6 (Haldimann, 2006).

Environment	n (–)	v_0 (mm/s)	S (m/s)·(MPa m$^{0.5}$)$^{-n}$
water*	16.0	50.1	5.0
air, 50% relative humidity*	18.1	2.47	0.45

Failure mode	n (–)	v_0* (mm/s)
all	16.8	1.78
edge failure	15.5	0.548
surface failure	**17.70**	**10.7**

* calculated with $Y = 1$

Environment	n (–)	v_0 (mm/s)	S (m/s)·(MPa m$^{0.5}$)$^{-n}$
Laboratory testing and 'Summer conditions'	16.0	4.51	0.45
'Winter conditions, melting snow, 2 °C'	16.0	8.22	0.82

Environment	n (–)	v_0 (mm/s)		Test setup (Source)
Water	26 ±7	$3.7 \cdot 10^7$		dynamic fatigue tests
Water	18 ± 1	19 ± 4		cyclic fatigue tests, as-indented and annealed
Water	20.1 ± 0.7	28.8 ± 6.4	*	dynamic fatigue tests
	19.9 ± 0.7	6.4 ± 1.4	†	
'normal' environment (air, 27 °C, 65% RH)	19.7 – 21.2	0.2 – 0.4		direct optical measurement
	21.8	2.6		4PB - dynamic fatigue, natural flaws
	21.1	2.4		4PB - dynamic fatigue, indentation flaws

* as-indented † annealed

Figure 5.6: Some values for the two parameters provided by the literature (Haldimann, 2006).

These values are taken from different experimental works, and one can notice that a direct correspondence of n and v_0 with the environmental variables is lacking. In other words, the two parameters are not expressed as function of temperature and relative humidity. From the tables, it is clear that the kinetic parameter v_0 is higher in water, since this latter accelerates crack velocity. On the contrary, n is higher in moist air than in water and this can be explained through a numerical verification. The same work provides a wide description of the quantification of the two parameters. However, we have seen that relative humidity and temperature play a relevant role in stress-corrosion mechanisms and strongly affect glass failure time. In my opinion, it seems reductive to use tables given by other works for a correct lifetime prediction, since a table combining all the feasible cases of temperature and relative humidity has not been given by any work of the literature. For a scientific interest, considering that glass failure process involves interesting physical-chemical mechanisms, it should be convenient to express failure time, or equivalently failure strength, as direct function of environmental variables. This has certainly a design justification

also, if we consider that in recent years structural use of glass has been spreading in different geographic regions for increasingly larger climatic ranges. As already mentioned, most of the predictive models follow the above-shown procedure, basing on power-law empirical relation. It will be now proposed a methodology which aims at providing glass lifetime curve basing on physical relations, i.e. starting from Wiederhorn exponential relation of Equation (4.27) (see chapter 4), and by calibrating the parameters of the problem in function of environment.

5.3 Failure time as function of environment

Since the literature does not provide values for the two empirical parameters n and v_0 covering all the possible combinations of temperature and relative humidity, this work aims at expressing failure time as explicit function of environment. For this purpose, Wiederhorn exponential law is used, where temperature and relative humidity are expressed as variables. The model starts from the following relation:

$$\frac{da}{dt} = (RH)^n v_0 \, e^{-\frac{E_a}{RT}} \, e^{\frac{bK_I}{RT}} \tag{5.21}$$

By separating variables one obtains:

$$dt = \frac{da}{(RH)^n v_0 e^{(-E_a/RT)}} \; e^{-\frac{bK_I}{RT}} \tag{5.22}$$

Considering the relation

$$dK_I = \frac{\sigma Y \sqrt{\pi}}{2\sqrt{a}} \, da \tag{5.23}$$

Equation (5.22) becomes

$$dt = \frac{2\sqrt{a} \quad dK_I}{\sigma Y \sqrt{\pi} (RH)^n v_0 e^{(-E_a/RT)}} \; e^{-\frac{bK_I}{RT}} \tag{5.24}$$

but since $\sqrt{a} = K_I / \sigma Y \sqrt{\pi}$, it gives

$$dt = \frac{2K_I \, dK_I}{(\sigma Y \sqrt{\pi})^2 (RH)^n v_0 \, e^{-E_a/RT}} \; e^{-\frac{bK_I}{RT}} \tag{5.25}$$

By defining the initial value of stress intensity factor $K_{I1} = \sigma Y \sqrt{\pi a_i}$, the equation becomes

$$dt = \left(\frac{2a_i}{(RH)^n \, K_{I1}^2 \, v_0 e^{-E_a/RT}} \right) K_I \, e^{-\frac{bK_I}{RT}} \, dK_I \tag{5.26}$$

Analytical integration is made on the one hand with respect to time, on the other hand with respect to stress intensity factor, which

also evolves during crack propagation since it depends on defect shape and length, which are both time dependent variables:

$$\int_0^{t_F} dt = \frac{2a_i}{(RH)^n\, K_{I1}^2\, v_0\, e^{-E_a/RT}} \quad \int_{K_{I1}}^{K_{Ic}} K_I\, e^{-\frac{bK_I}{RT}}\, dK_I \tag{5.27}$$

The integral on the right side of Equation (5.27) has the form $\int x\, e^{-\alpha x}\, dx$ and the analytical solution is $-e^{-\alpha\, x}(1+\alpha\, x)/\alpha^2$. Hence, the integration leads to

$$t_F = \frac{2a_i}{(RH)^n\, K_{I1}^2\, v_0\, e^{-E_a/RT}} \left(-\frac{e^{-\frac{bK_I}{RT}}(1+\frac{b}{RT}K_I)R^2T^2}{b^2} \right) \Bigg|_{K_{I1}}^{K_{Ic}} \tag{5.28}$$

The assumption is that, in a stress-corrosion regime, the critical value of stress intensity factor K_{Ic} is relevantly higher compared to initial value K_{I1}, which is function of the initial value of the preexisting crack when glass is not loaded yet. For K_{Ic} very high, the term $e^{-\frac{bK_I}{RT}}$ tends to zero and can be neglected. Hence, failure time is given in function only of initial conditions:

$$t_F = \frac{2a_i\, R^2T^2}{(RH)^n K_{I1}^2\, b^2\, v_0\, e^{-E_a/RT}\, e^{bK_{I1}/RT}} \left(1 + \frac{bK_{I1}}{RT}\right) \tag{5.29}$$

Considering that the factor bK_{I1}/RT is $\gg 1$, and considering that the term $v_0\, e^{-E_a/RT}\, e^{bK_{I1}/RT}$ represents initial crack velocity, when $t = 0$, that we can call v_1, a relation is obtained for failure time as function of initial stress conditions, initial defect geometry and environmental variables, i.e. temperature and relative humidity:

$$t_F = \frac{2a_i RT}{(RH)^n K_{I1} v_1 b} \tag{5.30}$$

and the explicit equation, by using fracture mechanics formula for K_{I1}, takes the following form:

$$t_F = \frac{2a_i RT}{(RH)^n Y\sqrt{\pi a_i}\, b\, v_0\, e^{-E_a/RT}\, \sigma_F\, e^{b\,(\sigma_F\, Y\sqrt{\pi a_i})/RT}} \tag{5.31}$$

This relation is practically useful since it allows evaluating failure time by knowing the initial defects contained in glass edges through microscopic investigation. By observing Equation (5.31), some interesting comments may be made about the influence of environmental

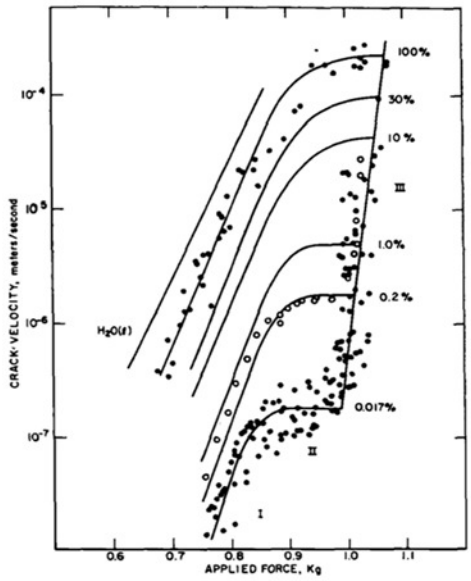

Figure 5.7: Water content influence on crack velocity (Wiederhorn, 1967).

variables. Failure time seems to decrease when increasing relative humidity, and since Wiederhorn experimental data provide a value for the exponential factor n equal to 1, this dependence is more or less linear.

By observing once again Wiederhorn experimental results for tests at different levels of moisture (see Fig. 5.7), by increasing water content in air, crack velocity increases, and the linearity is not directly observed only because the ordinates are represented on a logarithmic scale.

The dependence of crack velocity, and then of failure time, on temperature is more complex, since by observing the compact form of Equation (5.31) temperature is also included in the term v_1 as exponential factor. An explicit expression may be written in order to observe the dependence on temperature, by keeping constant the other variables and parameters:

$$t_F = \alpha T e^{\frac{\beta}{T}} \tag{5.32}$$

For $T \to \infty$, failure time would tend to zero, and this is due to the exponential factor. Hence, temperature dependence may be represented as a curve, as shown in Fig. 5.8 (left) where glass chemical composition, applied stress and relative humidity are considered as known.

When temperature increases, failure time decreases, in a non-linear

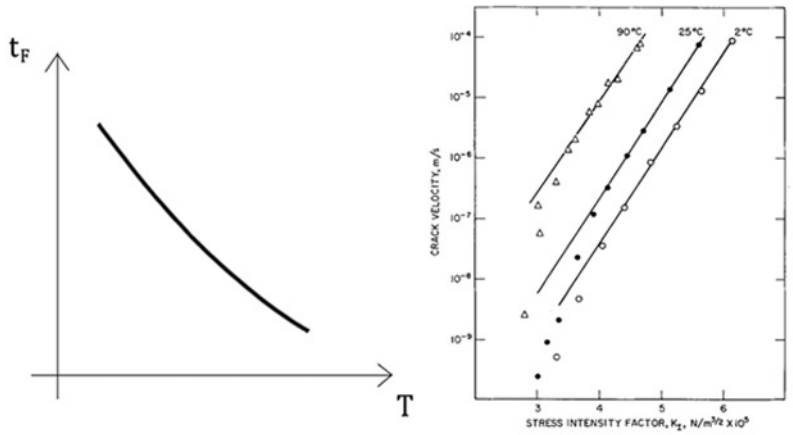

Figure 5.8: Influence of temperature on failure time (left) and on crack velocity (right).

way, and equivalently crack velocity increases, as already shown through Wiederhorn results in the previous section. Equation (5.31) of failure time cannot be analytically inverted, but it admits inverse function, since it is a decreasing function of stress. An indirect expression of strength in function of failure time can be obtained:

$$\sigma_F \, e^{b\,(\sigma_F\, Y \sqrt{\pi a_i})/RT} = \frac{2a_i RT}{t_F\,(RH)^n Y \sqrt{\pi a_i}\, b\, v_0\, e^{-E_a/RT}} \tag{5.33}$$

A curve of strength *versus* failure time can be constructed by numerical inversion, obtaining a lifetime curve directly function of physical environmental variables. The expression of failure time, without considering relative humidity, was already found by Wiederhorn. However, an interesting effort has been made in this work in order to give to this expression a prediction value. This is possible only if the three parameters E, b and v_0 are properly calibrated. Indeed, in the literature, Wiederhorn studies provide values for the three parameters only for one environmental condition, corresponding to water at $25°C$. For lifetime equation to be predictive, one should be able to apply it for different cases and conditions, through parameter calibration. For this purpose, it was firstly necessary to understand the physical and chemical nature of those parameters, and this will be discussed in the following section.

5.4 Focal points

- Stress-corrosion induces a strength decrease over time, which is known as static fatigue;
- Static fatigue curve has a prediction value and may be built on the basis of both exponential law and power-law relations;
- Recent prediction models express failure time on the basis of empirical parameters which refer to the influence of environment;
- A correspondence between the parameters and the two environmental variables, temperature and relative humidity, is lacking;
- The present work aims at expressing glass lifetime as explicit function of physical variables, starting from Wiederhorn exponential law;
- As expected, failure time linearly decreases with relative humidity and non-linearly decreases when increasing temperature;
- The literature provides values for the chemical-physical parameters only for one environmental condition;
- A complete prediction requires the calibration of the parameters as function of environment, on the basis of experimental investigation.

Chapter 6

Prediction lifetime curve

6.1 Chemical physical parameters: dependence on chemistry and on environment

As already discussed, Wiederhorn provided values for the three parameters for six different glasses, as shown in the table of Fig. 4.10 (see chapter 4) (Wiederhorn and Bolz, 1970). A strong variation in values is observed when varying glass chemical composition. The commonly used soda-lime silica glass has a low value of the activation energy, and this means that it has a low resistance to corrosion, since by parity of stress crack propagation velocity is higher. This is due to the presence of sodium ions, which enhance corrosion process by altering the pH.

However, it was observed that these parameters do not depend only on chemistry. Indeed, tests performed on soda-lime silica glass small specimens, that will be described soon, register a failure time for a given environmental condition. The glass tested is very similar to the glass used by Wiederhorn. Hence, by parity of chemical composition, by using the values of the three parameters provided by Wiederhorn for soda-lime silica glass and by inserting them in lifetime Equation (5.31) (see chapter 5), failure time theoretically calculated should correspond to the value registered during tests. However, a divergence is observed between the two values, and this implies that the meaning of E_a, b and v_0 is more complex. In addition, since the tests performed for this work have not the same environmental conditions of the tests performed by Wiederhorn, it may be deduced that the three parameters strictly depend on environmental conditions.

By observing Wiederhorn experimental results shown in Fig. 6.1 it is possible to make some interesting considerations. In the figure on the left, by varying water content, the slope of the curves v *versus* K_I is constant, while the interception with the $y - axis$ changes. By

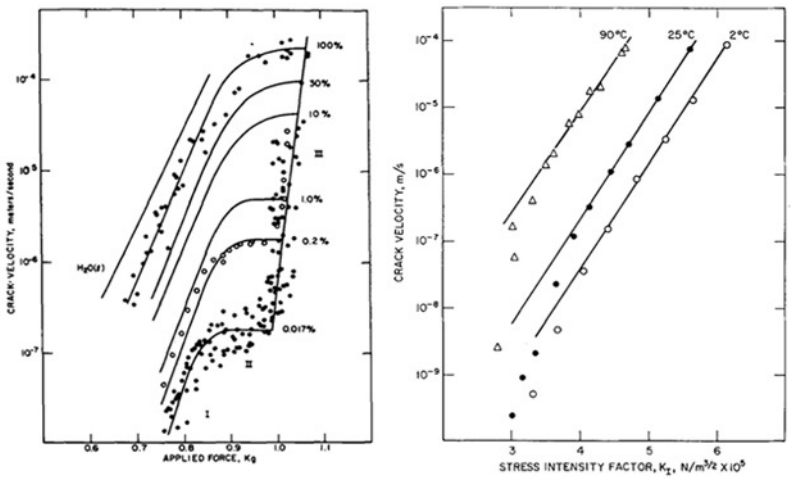

Figure 6.1: Influence of relative humidity (left) and temperature (right) on crack velocity (Wiederhorn, 1967; Wiederhorn and Bolz, 1970).

representing Wiederhorn exponential law (see Equation (4.25), chapter 4) on a semi-logarithmic scale, one may obtain the following relation:

$$\ln v = \left[\ln (RH)^n + \ln v_0 - \frac{E}{RT}\right] + \frac{b}{RT} K_I \tag{6.1}$$

The slope of the curves is represented by the factor b/RT and since it is constant, this implies that b is independent of RH. The intercept is represented by the factor in square brackets in Equation (6.1), which contains the two parameters E_a and v_0 as well as the physical variable RH it-self. The assumption is that the most relevant variation of the intercept is due to variations in relative humidity. Hence, this assumption leads to consider that the two parameters E_a and v_0 have a weak dependence on relative humidity. However, this phenomenon will be the object of future investigations.

The influence of temperature on empirical parameters has been investigated and appears relevant. In order to understand dependence on temperature, a value for relative humidity has been chosen equal to 1, corresponding to water, so that Wiederhorn exponential law is simplified as follows:

$$v = v_0 \, e^{\frac{-E_a + bK_I}{RT}} \tag{6.2}$$

In this way, it is possible to observe the dependence of the three parameters on temperature. In Equation (6.1), the slope of the curves is represented by the factor b/RT. By observing Fig. 6.1 right, showing

Wiederhorn results for different temperatures on a semi-logarithmic plane, the slope of the curves is more or less the same. This means that b/RT is constant and this implies that b linearly scales with temperature, by parity of glass chemical composition. The intercept is represented by the factor $\ln v_0 - E_a/RT$ and it increases when increasing temperature. This means that E_a and v_0 depend on temperature, in a non-linear way. In particular, considering that crack velocity increases with temperature, the signs of the factor representing the intercept mean that v_0 increases when increasing temperature. E_a could both increase or decrease since it is divided by temperature, which also changes. It is sure that the factor E_a/RT is expected to decrease when increasing temperature.

6.2 Experimental parameter calibration

Once the dependence of empirical parameters on chemistry and physical variables is clear, it is possible to calibrate them experimentally. It would be physically interesting to provide the three parameters as function of temperature and relative humidity, as follows:

$$E_a = E_a(T, RH), \qquad b = b(T, RH), \qquad v_0 = v_0(T, RH) \tag{6.3}$$

In order to do this, the way could be to perform a series of tests by varying glass chemical composition, environmental variables and applied stress, through an adequate experimental instrumentation that would allow measuring instantaneously crack propagation velocity and the evolution of the stress intensity factor over time, as the crack propagates changing length and shape. However, it will be proposed a simple methodology referring only to initial flaw geometry by making some simplifying assumptions and basing on simple four-point beam-bending tests. Parameter calibration will be provided for one glass composition and one environmental condition, and a lifetime prediction curve will be given for those conditions. Experimental tests will be used joint to Wiederhorn theory, providing an alternative prediction which is explicit function of environment.

6.2.1 Experimental program

The experimental program has been carried out at Steel Structures Laboratory Icom at EPFL, in Lausanne. A water-jet cutting machine, shown in Fig. 6.2, allowed obtaining more than 300 specimens from one soda-lime silica glass panel.

The specimen geometry is $100mm \times 10mm \times 3.8mm$, and the focus is on edge flaws, which propagate under beam-bending. On each specimen, the range corresponding to constant maximum value of bending

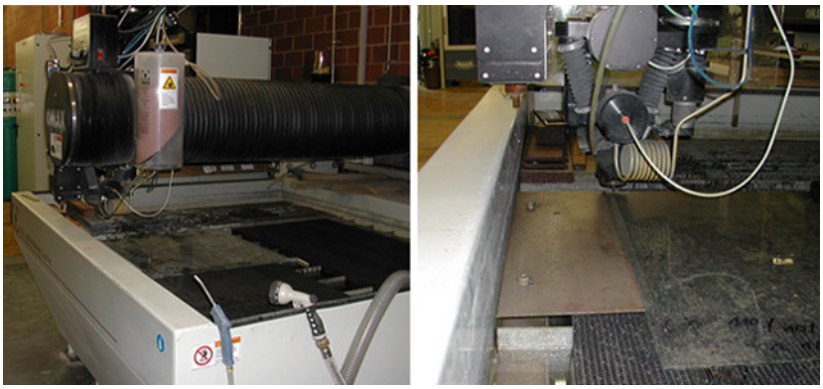

Figure 6.2: Water-jet cutting machine, EPFL, Lausanne.

moment was signed, and only breakage taking place in that range was considered in the analysis (see Fig. 6.3).

Tests were performed by applying a constant stress using an universal machine *Thümler* Z3-Z50 (capacity 5kN) controlled by the software ZPM v4-5 and registering failure time for each specimen. Testing setup is shown in Fig. 6.4.

Some microscopic investigations allowed measuring a mean value for the edge defect initial length, corresponding to $450\mu m$. Indeed, the edge finishing used in order to accelerate testing setup induced very large rounded flaws, which highly reduce specimen strength, but this was not relevant since the focus of this work is the influence of environmental variables. Some recent works show the different values of strength induced by different edge finishing (Lindqvist et al., 2011). Microscopic investigation has been made using an optical microscope $OlympusBX5$ equipped with a digital camera $LeicaDFC420$. Images were captured under $20\times$ objective (see Fig. 6.5).

Linear elastic fracture mechanics was used in order to evaluate a mean value for the geometry factor Y. Considering a half penny-shaped crack, a value of 0.637 was found. In the literature, a standard value of 1.12 is used for lifetime prediction, but this work found relevant the influence of both dimension and shape of the defects and so a correct estimate was needed. By observing Equation (5.31) of failure time (see chapter 5), that is lifetime equation, t_F appears relevantly sensitive to small variations of initial dimension a_i and shape Y of the flaws. Indeed, even varying the defect length of few MPa induces strong variations in failure time. Sensitivity on defect population seems even stronger compared to the dependence on environmental variables, but as already said this work did not focus on edge flaws strength. However, as will be shown, the stronger is the influence of environment, the lighter the

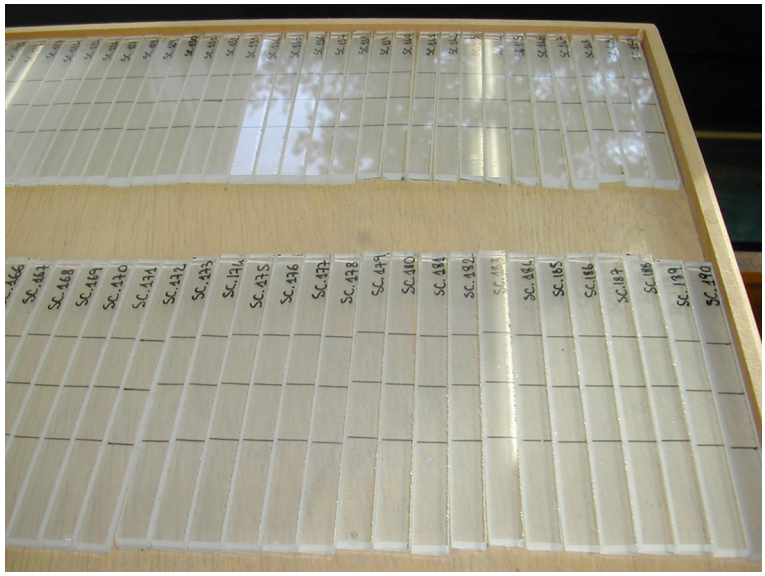

Figure 6.3: Soda-lime silica glass specimens.

sensitivity to defects. For instance, by increasing temperature or relative humidity during tests, the result dispersion due to defect variation in length or shape is relevantly reduced.

Series of four-point beam-bending tests were performed under constant stress both in air and water, as shown in Fig. 6.4. In air, relative humidity and temperature were kept constant at respectively $44 \pm 1\%$ and $20 \pm 1°C$. In water, tests were performed for three different temperatures, 65, 20 and $10°C \pm 1°C$. For tests in water, temperature was kept constant using an insulating box (see Fig. 6.4 (right bottom)).

Table 6.1 shows the series of specimens tested and Tables 6.2 and 6.3 show the registered mean failure time μt_F, giving also standard deviation σ_x and normalized standard deviation σ_x/μ, showing respectively the influence of relative humidity and temperature.

For an increase of relative humidity from 44% to water, average failure time is reduced of 92.85%, and this is consistent with Wiederhorn experimental results (Wiederhorn, 1967). However, Table 6.2 shows a very high dispersion of the experimental results; this aspect will be discussed at this end of this section.

For each test, failure time was measured as the time of application of constant load, as shown in Fig. 6.6 (top).

Fig. 6.6 (bottom) shows a broken specimen, revealing a single fracture pattern. Indeed, specimens broke in a short time, due to the large edge flaws induced by the water-jet cutting finishing. Other edge fin-

Table 6.1: Testing conditions.

Series	N.Specimens	F [N]	σ_A [MPa]	RH [%]	T [$^\circ C$]
1	17	126	31.13±0.3	44±1	20±1
2	17	122	31.10±1.3	44±1	20±1
3	22	103	25.58±1.3	44±1	20±1
4	21	103	25.18±0.5	water	20±1
5	9	103	25.46±0.8	water	65±1
6	13	103	25.92±1.2	water	10±1
7	5	92	23.51±0.5	water	20±1
8	6	82	20.80±0.1	water	20±1

Table 6.2: Influence of relative humidity on failure time.

Series	RH [%]	T [$^\circ C$]	σ_A [MPa]	$\mu(t_F)$ [sec]	$\sigma_x(t_F)$ [sec]	$\sigma_x/\mu(t_F)$
3	44±1	20±1	25.58±1.3	879.89	1021.67	1.16
4	water	20±1	25.18±0.5	62.89	42.95	0.68

Table 6.3: Influence of temperature on failure time (tests in water).

Series	T [$^\circ C$]	σ_A [MPa]	$\mu(t_F)$ [sec]	$\sigma_x(t_F)$ [sec]	$\sigma_x/\mu(t_F)$
6	10±1	25.92±1.2	77.33	72.11	0.93
4	20±1	25.18±0.5	62.89	42.95	0.68
5	65±1	25.46±0.8	2.39	1.71	0.71

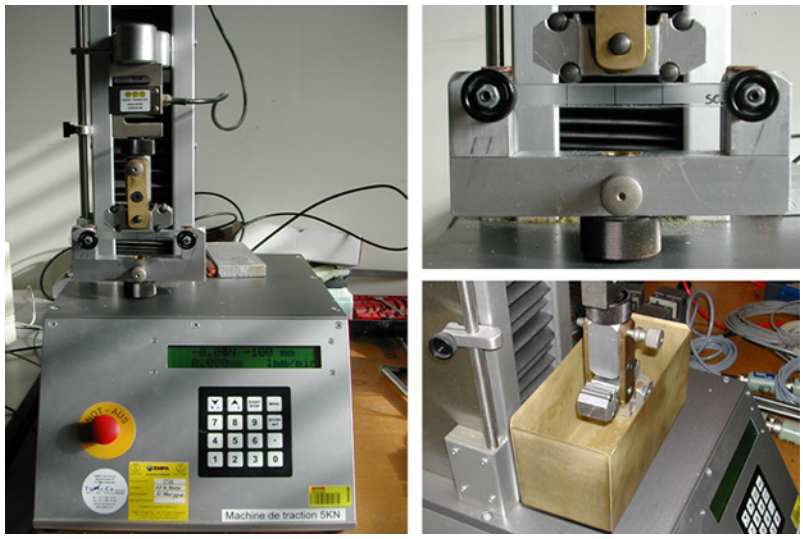

Figure 6.4: Testing setup (left); tests performed in air (right top) and water (right bottom).

ishings, inducing defects of the order of few decades of MPa, cause multiple fracture pattern due to the interaction between different small flaws.

As shown in Table 6.1, three series of tests were performed in air, respectively series 1, 2 and 3, for three different levels of stress, by parity of glass chemical composition, temperature ($20 \pm 1°C$) and relative humidity ($44 \pm 1\%$). The application of a constant load of $103N$ induced failure time even of more than one hour, and this load value was chosen in order to test specimens in water, where failure time was supposed to be relevantly shorter. Hence, under a load of $103N$, three series of specimens, that is series 4, 5 and 6, were tested in water by varying temperature, respectively at 20, 65 and $10 \pm 1°C$.

At a later stage, other two series, that is series 7 and 8, were tested in water at $20 \pm 1°C$ under two lower stress values, in order to observe the trend of strength over time by parity of environmental conditions.

By comparing series 3 for air at $20 \pm 1°C$ and series 4 for water at $20 \pm 1°C$, an information is obtained on the influence of water content on stress-corrosion process, as shown in Table 6.2. Specimens tested in moist air showed a mean failure time of 879.89 seconds, while specimens tested in water broke in around 62.89 seconds. The behaviour is considered linear, referring to the assumptions described in chapters 4 and 5. Fig. 6.7 shows the two mean values of failure time as function of relative humidity, and the trend of the curve is assumed from the

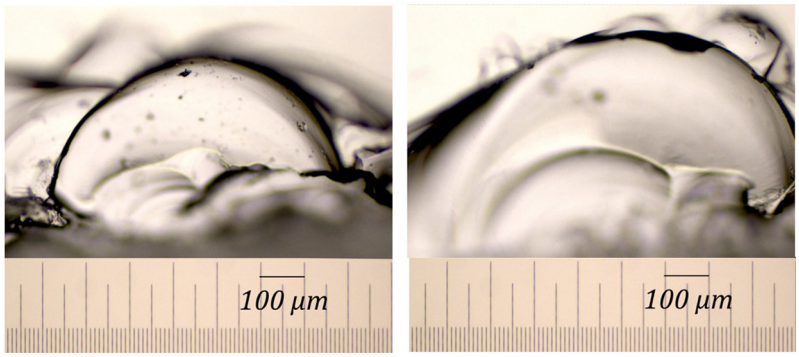

Figure 6.5: Microscopic observation of edge flaws.

theory (see chapters 4 and 5).

However, it can be now observed in the figure that dispersion of series 3, relative to tests in air, is higher compared to dispersion of series 4, for tests in water. This is due to the fact that dispersion is induced by defect variability caused by the water-jet cutting finishing used for accelerating testing setup, but it seems that increasing the influence of environmental variables, in this case relative humidity, leads to a relevant reduction of sensitivity of failure time on defect geometry. This is an interesting theme that could be the object of future works. Concerning result dispersion one could also notice from the tables that some series are composed of few specimens, since some of them broke for thermal shock and other for fracture taking place out of maximum moment range.

As to the influence of temperature, by comparing the three series 4, 5 and 6 tested in water at 20, 65 and $10 \pm 1°C$ under the same stress value, by parity of relative humidity, it is possible to observe the trend of failure time in function of temperature, as shown in Fig. 6.8.

For $T = 10°C$, tests register a mean failure time of 77.33 seconds. For $T = 20°C$, mean failure time is 62.89 seconds and for $T = 65°C$ it results 2.39 seconds. This is shown in Table 6.3. It is evident that the trend is non-linear.

Results referring to the influence of temperature have been compared to the curves provided by Wiederhorn for three other temperatures, 90, 25 and $2 \pm 1°C$. Comparison with Wiederhorn is shown in Fig. 6.9 (right).

On the left side, Wiederhorn experimental data are shown as already described in chapter 4. On the right, dots representing the tests are compared with Wiederhorn curves. In order to represent experimental results on a plane of crack velocity *versus* stress intensity factor, it

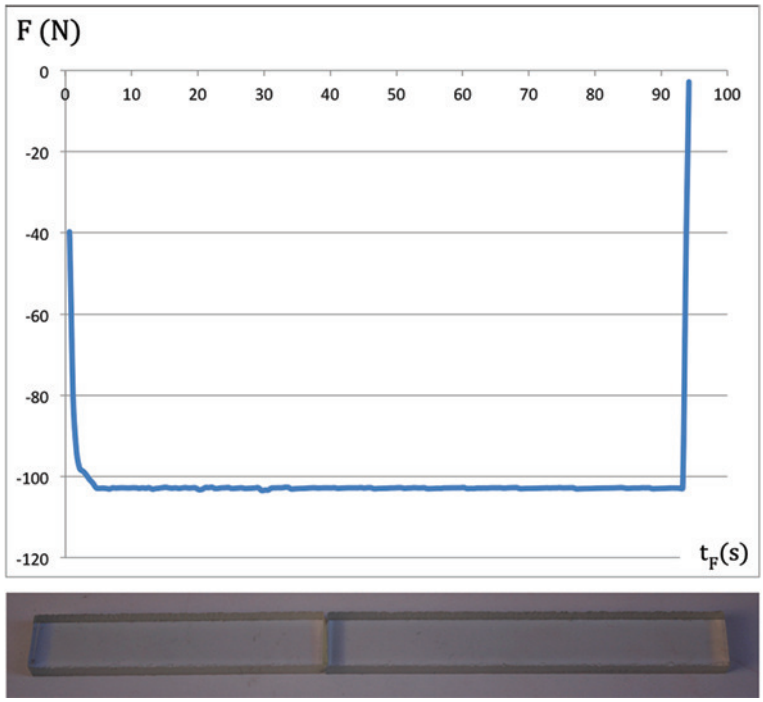

Figure 6.6: Applied load over time (top); broken specimen (bottom).

was necessary to measure both v and K_I. The stress intensity factor was obtained by fracture mechanics formula (see chapter 2), that is $K_I = \sigma Y \sqrt{\pi a}$, considering a half penny-shaped crack and converting bending moment in tensile stress obtaining a shape factor equal to 0.637. As already said, a mean value of defect length was measured through microscopic investigation, corresponding to $450\mu m$. A mean value of crack velocity was calculated for each specimen as follows:

$$v_m = \frac{h}{t_F} \tag{6.4}$$

where h is the specimen height, since crack velocity was not instantaneously measured. This approximation, in this case, is correct, since the applied stress is very close to the critical value, and tests have a short duration, varying from few seconds to few hours. Crack behaviour is at limit of stress-corrosion regime and stress intensity factor can be considered as constant. On the contrary, if the stress had been relevantly lower, then it would have been necessary to instantaneously measure crack propagation velocity as well as the evolution of the stress intensity factor over time. Indeed, for very slow crack growth,

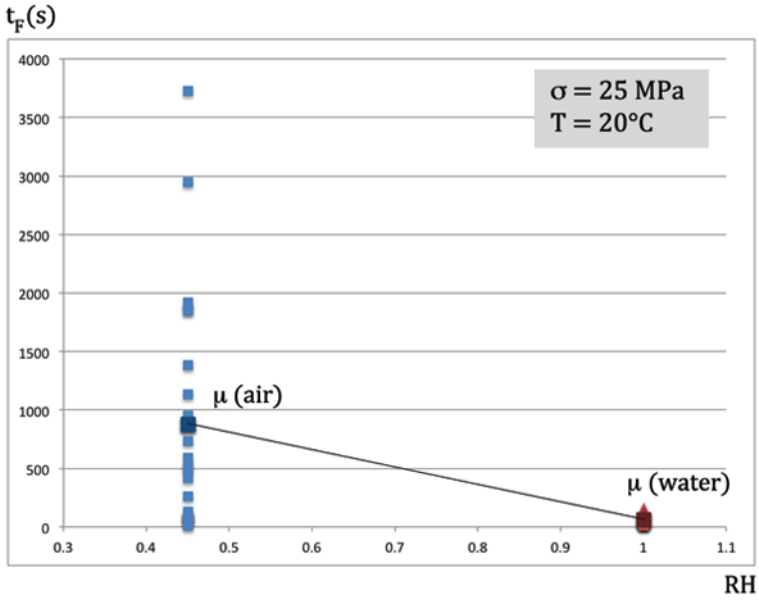

Figure 6.7: Registered failure time in function of relative humidity (tests in air and water).

the defects evolves by changing length and shape, and this induces a modification of K_I factor that cannot be neglected. In this case, a different experimental instrumentation would be required, allowing observing crack growth at a smaller scale.

Observing Fig. 6.9 (right), experimental results are consistent with Wiederhorn curves and theory, since, by parity of applied stress, crack velocity increases when increasing temperature, in a non-linear way.

6.2.2 Parameter calibration

A first glance on experimental results allowed registering a consistence both qualitative and numerical with physical theories on stress-corrosion (see chapter 4), where crack propagation velocity is strongly affected by environmental variables T and RH.

A deeper glance has permitted to make use of experimental results in order to calibrate the three parameters E_a, b and v_0. As already said, since a more accurate instrumentation was not available, it was possible to calibrate parameters referring only to one glass chemical composition and one specific environmental condition. Glass tested is soda-lime silica glass and the chosen environment is water at $20°C$.

The first assumption is that, by parity of glass chemical composi-

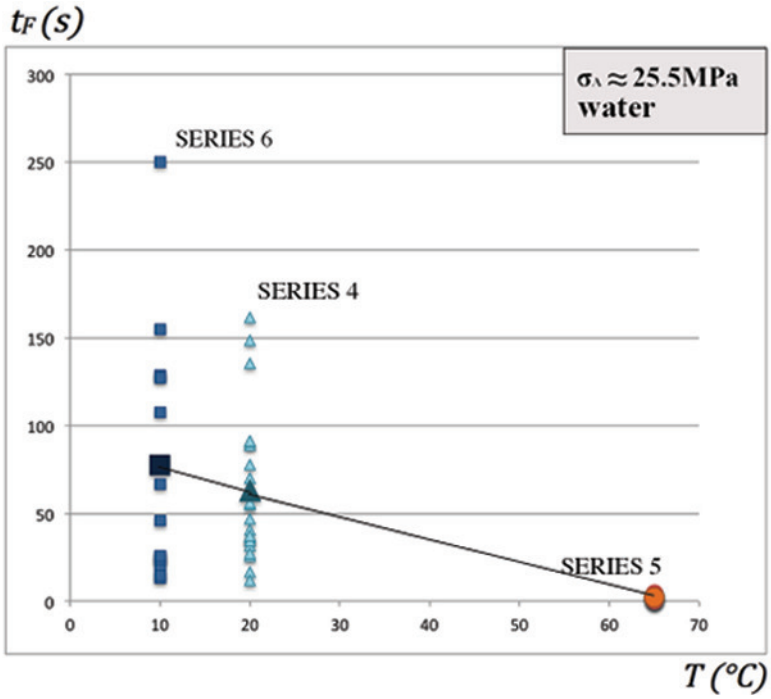

Figure 6.8: Registered failure time in function of temperature (tests in water).

tion, the slope of the curves $v(K_I)$ is constant, by varying temperature (see chapter 4). The glass tested is similar to the glass used by Wiederhorn and then the slope of the curves is known. By Wiederhorn data, the factor b/RT is 4.43×10^{-5} (Wiederhorn and Bolz, 1970). From this factor, it is possible to obtain the value of b for $T = 20°C$, corresponding to 0.0913. In addition, by knowing the slope of the curve, starting from the dot representing mean value for specimens tested in water at $20°C$ it was possible to obtain the trend of the curve, as shown in Fig. 6.10.

This allowed obtaining the interception with the $y - axis$ for $T = 20°C$, giving information on v_0 and E_a.

The second assumption is that v_0 has a lower influence compared to E_a and b, since in Wiederhorn equation it does not belong to the exponential term. Hence, the value provided by Wiederhorn for v_0 for $T = 25°C$ (see chapter 4) was used for tests at $T = 20°C$. In this way, the intercept allowed obtaining the value of the activation energy E_a. Table 6.4 gives the three values obtained for water at $T = 20°C$.

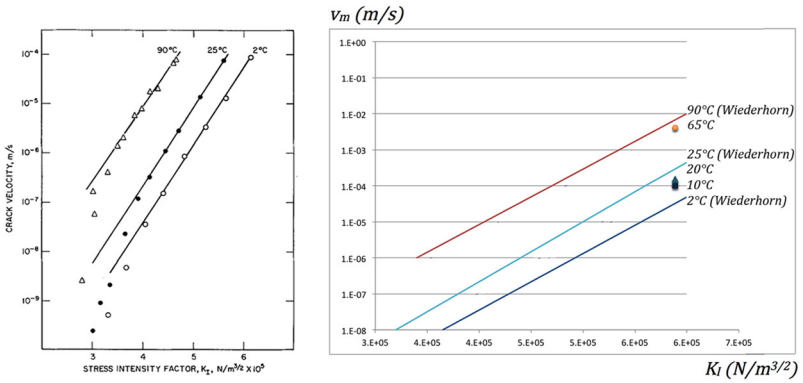

Figure 6.9: Wiederhorn results on temperature influence (left); experimental results for three different temperatures compared with Wiederhorn curves (right).

Table 6.4: Values of the three empirical parameters for water at $20°C$.

E_a	b	v_0
J/mol	mks	m/s
1.13×10^5	0.0913	29732

6.3 Lifetime curve for soda-lime silica glass in water at $20°C$

Once the three parameters have been calibrated for the chosen environmental condition, it is possible to construct a prediction lifetime curve, referring to soda-lime silica glass and to that environment. Considering the indirect Equation (5.33) (see chapter 5) representing strength as function of failure time, by fixing the initial values of defect shape factor Y and length a_i, given an environmental condition corresponding to $RH \approx 100\%$ and $T = 20°C$, by inserting the three parameters found E_a, b and v_0, a curve of strength *versus* time is obtained, as shown in Fig. 6.11.

The figure shows a relevant dispersion of results, and this can be explained as consequence of both variations in defect shape and length and variations in specimen height. The reason is that the edge finishing used for accelerating testing setup induced large flaws with a high variability in dimension. Both length and shape are influent, since by parity of dimension, a sharp crack would induce a higher stress concentration compared to a rounded flaws. Real flaws induced by industrial edge finishing, as polishing or grounding, are usually sharper and smaller that

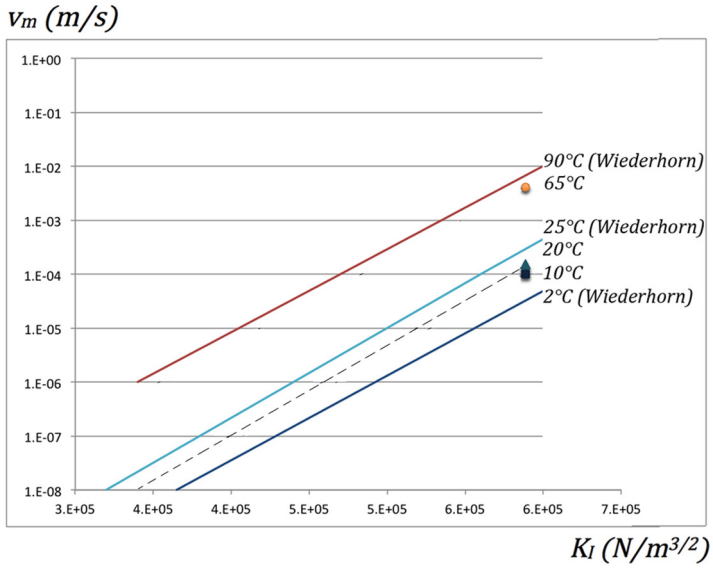

Figure 6.10: Trend of the curve for water at $T = 20°C$.

the ones obtained by the water-jet cutting machine. Hence, the problem of sensitivity on defects and of result dispersion could be avoided just by using another edge finishing providing smaller flaws with a lower variability in dimension.

Lifetime curve has a high prediction value and an interesting physical meaning, since it allows estimating failure time of a structural glass element subjected to a certain stress and exposed to given environmental conditions.

6.4 Future aims

As already said, the obtained lifetime curve refers to one glass and one environmental condition. An interesting aim would be to obtain a series of lifetime curves for different glasses and different combinations of relative humidity and temperature. In order to do this, one should consider that failure time depends on RH and T even through the three parameters E_a, b and v_0, which also depend on physical variables. Hence, a complete prediction would imply to perform series of tests varying glass chemical composition, stress, temperature and relative humidity obtaining the three parameters as function of environment and then physically founded prediction curves.

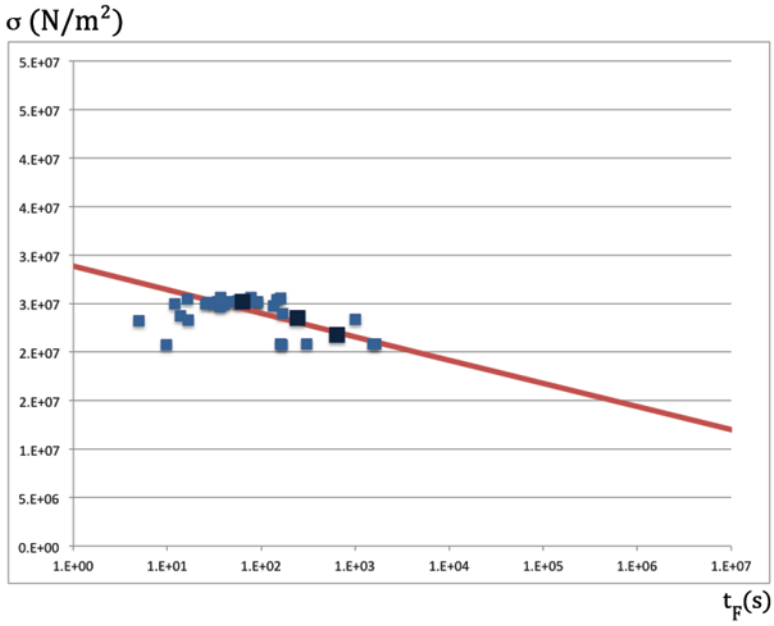

Figure 6.11: Experimental dots consistent with lifetime curve, for water at $T = 20°C$.

6.5 Dynamic fatigue in glass: a consequence of stress-corrosion

As already shown, static fatigue, i.e. strength decrease over time, is a consequence of stress-corrosion mechanisms. The strong influence of environment, which takes place at the nanoscopic and microscopic scale and involves both chemical and physical processes, explains also another macroscopic phenomenon, that is a dependence of strength on applied stress-rate $\dot{\sigma}$. In some works, this is known as dynamic fatigue, from Charles studies parallel to his theories on stress-corrosion and static fatigue (Charles, 1958c). The term dynamic fatigue does not refer to loading cycles or to inertial forces but to the evolution process of crack advance over time.

As shown for the static fatigue curve, also dynamic fatigue curve can be obtained starting both by power-law relation and by Wiederhorn exponential law. By power-law, considering the dependence of stress intensity factor on time, that is $K_I(t) = \sigma(t)Y\sqrt{\pi a(t)}$, one obtains:

$$\frac{da}{dt} = \frac{v_0 \sigma(t)^n Y^n [\pi a(t)]^{\frac{n}{2}}}{K_{Ic}^n} \tag{6.5}$$

Assuming that the loading history is linear, that is stress-rate is constant, strength can be expressed as $\sigma(t) = \dot{\sigma}t$, so that Equation (6.5) becomes:

$$\frac{da}{dt} = \frac{v_0 \dot{\sigma}^n t^n Y^n [\pi a(t)]^{\frac{n}{2}}}{K_{Ic}^n} \tag{6.6}$$

By integrating by variable separation, the following relation is obtained of strength as function of stress rate:

$$\sigma_F = \left[\frac{2a_0^{(n-2)/2} K_{Ic}^n (n+1)}{(n-2) v_0 Y^n \pi^{n/2}} \right]^{\frac{1}{n+1}} \dot{\sigma}^{\frac{1}{n+1}} \tag{6.7}$$

or more synthetically

$$\sigma_F = A \dot{\sigma}^{\frac{1}{n+1}} \tag{6.8}$$

This last result was given by Charles in a work considering also the influence of environmental variables (Charles, 1958c). As already done for static fatigue, also in this case strength *versus* stress-rate can be expressed starting from Wiederhorn exponential law. By numerical inversion, an indirect relation of strength as function of stress-rate is obtained:

$$\sigma_F^2 \, e^{b\sigma_F Y \sqrt{\pi a_i}/RT} = \frac{2a_i RT}{(RH)^n Y \sqrt{\pi a_i} b v_0 \, e^{-E_a/RT}} \, \dot{\sigma} \tag{6.9}$$

Also in this case, the curve assumes predictive value if the empirical parameters are calibrated. By using the values found in the previous section, a curve of strength as function of stress-rate is obtained, for water at $20°C$, as shown in Fig. 6.12.

Dots refer to mean values of tests performed in water varying the applied stress rate, and are consistent with the curve theoretically found.

Hence, a simple methodology has been proposed for evaluating the two curves representing static fatigue and dynamic fatigue phenomena, considering the strong influence of environment. Even if this procedure is more complex, it is physically interesting for the reasons explained above.

6.6 Focal points

- Physical-chemical parameters are shown to depend on both glass chemical composition and environment;

- Dependence of parameters on temperature, which seems to be higher, has been investigated in this thesis;

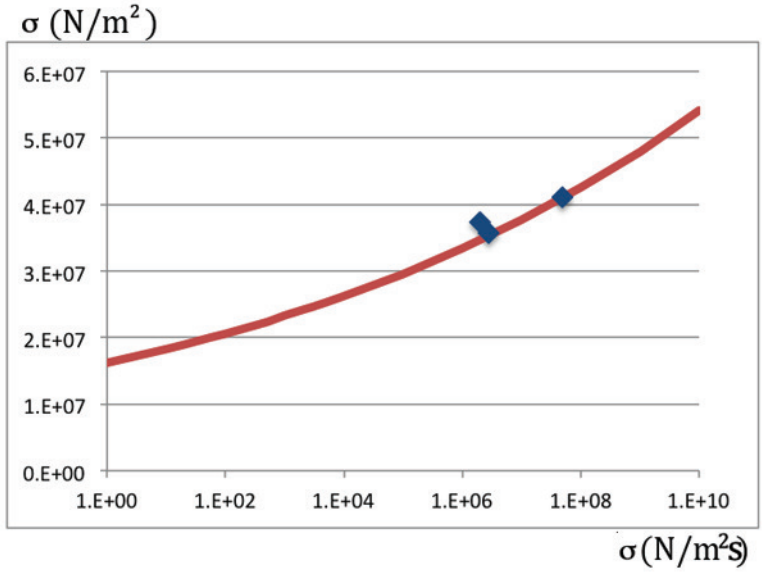

Figure 6.12: Experimental dots consistent with strength *versus* stress-rate curve, for water at $T = 20°C$.

- Experimental investigation has permitted to calibrate the three parameters for one glass type and one environmental condition;
- Tests have been performed in air and water at different temperatures, observing the influence of physical variables and a consistence with stress-corrosion theories;
- Parameter calibration allows obtaining a lifetime curve for one glass and one environment corresponding at water at $20°C$;
- Equivalently, parameters have been used in order to obtain a curve of strength *versus* stress-rate, observing the phenomenon of dynamic fatigue, another consequence of stress-corrosion;
- It would be physically interesting to perform an experimental investigation in order to obtain the three parameters as function of relative humidity and temperature, not limiting to one environmental condition.

Chapter 7

Future aims and conclusions

7.1 Modelling stress-corrosion failure mechanisms

This thesis has highlighted the fact that failure mechanisms in glass are strongly affected by the phenomenon of stress-corrosion. As in other multi-physics coupling mechanisms, described in chapter 3, also stress-corrosion implies a strong interaction between different spatial scales and different physics.

Future developments of this work may concern two directions. On the one hand the aim is to express chemical-physical parameters of Wiederhorn experimental theory as function of environmental variables. This would be permitted by a more accurate experimental investigation through a more sophisticate instrumentation. On the other hand, the purpose is to provide an analytical physical-mathematical model which could describe subcritical crack growth in a stress-corrosion regime.

Modelling will probably start by a single flaw, by including at the crack tip corrosion potential from environment, up to model propagation of different flaws mutually interacting. Considering the small scale of the defect, it is evident that a possible way would be to formulate a microstructured continuum model. Glass could be modelled as isotropic linear-elastic continuum containing a microstructure (defects) which evolves over time as effect of mechanical parameters (stress) and environmental variables (relative humidity and temperature).

The deep glance taken in this work at the micro-physics dominating stress-corrosion allowed identifying the variables which play a relevant role in the phenomenon and that could be included in the model.

Some examples of continua with microstrucure models are given by

the literature (Eringen, 1966; Capriz, 1989; Gurtin, 1994; Herrmann, 2002). Some of them are based on Eshelby inclusion model, where an ellipsoidal inclusion within an infinite matrix is considered. Eshelby solution includes several specific cases of inclusions, as also crack. Eshelby mechanics is characterized by configuration changes and may be applied in fluid dynamic, referring to current configuration. As mentioned at the beginning of this thesis, glass may be seen as a highly viscous solid, carrying properties of both fluids and solids. Hence, a model based on configurational mechanics could be proper. Gurtin proposed a model based on configurational forces in order to explain dissipative phenomena (Gurtin, 1994). One of these phenomena is the advance of a crack in a brittle material. In his theory, additional forces, additional elastic tensor and additional balance need to be considered. By considering glass as dissipative material, due to crack propagation, and by following these models one should consider that the reference configuration evolves through a reorganization which dissipates energy. Cauchy continuum model does not take into account small scales phenomena, as micro-cracking. Hence, subcritical crack growth in glass should be modelled only considering additional variables. In addition, scale effects need to be considered. Scale effects imply that, by changing from one scale to another, material properties may change qualitatively. For instance, glass homogeneity is valid only at the big scale, while at the microscopic scale, or even more at the atomic scale, it looses validity. At the small scale, microstructure is fundamental. For this reason, modelling stress-corrosion requires to make use of an enriched Cauchy model, considering the evolution of the microstructure. The question is whether this microstructure is represented by the flaw or whether by atomic irregularities. One other question is how this microstructure should be modelled.

7.2 Conclusions

Although the existing mentioned modellings, analytical models describing stress-corrosion mechanisms are still lacking, and in my opinion to be able to model this complex phenomenon is not only a scientific aim but also a design purpose.

This thesis has presented on effort in understanding stress-corrosion mechanisms. On the one hand, a simple method has been proposed for evaluating failure time as function of environmental conditions. The reason of this effort arises from both a deep scientific interest about the influence of temperature and relative humidity on stress-corrosion, and design needs, given that structural glass is being used in an increasingly wide range of climatic conditions. This work is just beginning and needs further efforts along both directions outlined above. In partic-

ular, the lifetime equation will be generalized in order to include the inert strength and the threshold conditions, as done in the literature. Further investigations about microscopic aspects need to be carried out. Further considerations are also required about the influence of geometry of the defect apex and of stress on water supply. Some useful information is found in literature but this field is still very open.

On the other hand, this work has permitted to identify the physical variables which play an interesting role in stress-corrosion mechanism. It is my opinion that starting from glass phenomenology and basing on experimental investigation is a necessary step to be able to correctly model the observed phenomenon, considering the complexity and the number of variables involved.

Bibliography

[1] Arrhenius, S. (1889), *On the Reaction Rate of the Inversion of Non-Refined Sugar upon Souring*, Z Phys. Chem. 4, 226-248.

[2] Auradouis, H., Vandembroucqt, M., Guillott, C. and Bouchaudtt, E. (2002), *A Model for the Stress Corrosion Fracture of Glass*, Trans. ASME, Phil. Maalg., 3221-3228.

[3] Baker, T.C. and Preston, F.W. (1946), *Fatigue of Glass under Static Loads*, J. Appl. Phys. 17 (3), 170.

[4] Barenblatt, G. I. (1959), *On Equilibrium Cracks Formed in Brittle Fracture. General Concepts and Hypotheses. Axisymmetric Cracks.* J. Appl. Math. and Mech. (PMM), 23 (3), 622-636.

[5] Broek, D. (1974), *Elementary Engineering Fracture Mechanics*, Leyden. Noordhoff Int. Publ.

[6] Capriz, G. (1989), *Continua with Microstructure*, Springer, New York.

[7] Charles, R.J. (1958a), *Static Fatigue of Glass I*, J. Appl. Phys., 29 (11), 1549-1553.

[8] Charles, R.J. (1958b), *Static Fatigue of Glass II*, J. Appl. Phys., 29 (11), 1554-1559.

[9] Charles, R.J. (1958c), *Dynamic Fatigue of Glass*, J. Appl. Phys., 29 (12), 1657-1662.

[10] Charles, R.J. and Hillig, W.B. (1962), *The Kinetics of Glass Failure by Stress-Corrosion*, In: Symposium on mechanical strength of glass and ways of improving it. Florence, Italy. September 25-29, 1961. Union Scientific Continental du Verre, Charleroi, Belgium, 511-527.

[11] Ciccotti, M. (2009), *Stress-Corrosion Mechanisms in Silicate Glasses*, J. Phys. D: Appl. Phys. 42, 1-29.

[12] Eringen, A.C. (1966), *Theory of Micropolar Fluids*, J. Math. Mech. 16, 1-18.

[13] Evans, A.G. (1972), *A Method for Evaluating the Time-Dependent Failure Characteristics of Brittle Materials - and its Application to Polycrystalline Alumina*, J. Mat. Science 7, 1137-1146.

[14] Evans, A.G. (1974), *Slow Crack Growth in Brittle Materials under Dynamic Loading Conditions*, Int. J. Fract. 10 (2), 251-259.

[15] Evans, A.G. and Wiederhorn, S.M. (1974), *Proof Testing of Ceramic Materials - an Analytical Basis for Failure Prediction*, Int. J. Fract. 10 (3), 379-392.

[16] Ferretti, D., Rossi, M., Royer-Carfagni, G. (2011), *An ESPI Experimental Study on the Phenomenon of Fracture in Glass. Is it Brittle or Plastic?*, J. Mech. Phys. Solids 59, 1338-1354.

[17] Griffith, A.A. (1921), *The Phenomena of Rupture and Flow in Solids*, Phil. Trans. R. Soc. Lond. A 221, 163-168.

[18] Gurtin, M.E. (1994), *The Nature of Configurational Forces*, Department of Mathematical Sciences. Paper 497.

[19] Gy, R. (2003), *Stress-Corrosion of Silicate Glass: a Review*, J. Non-Cryst. Solids 316, 1-11.

[20] Haldimann, M. (2006), *Fracture Strength of Structural Glass Elements - Analytical and Numerical Modelling, Testing and Design*, EPFL, 79-95.

[21] Hillig, W.B. (2006) *The C-H Delayed Failure Mechanism Revisited*, Int. J. Fract. 139, 197-211.

[22] Hillig, W.B. (2007), *Model of Effect of Environmental Attack on Flaw Growth Kinetics of Glass*, Int. J. Fract. 143, 219-230.

[23] Inglis, C.E. (1913), *Stresses in a Plate due to the Presence of Cracks and Sharp Corners*, Trans. I.N.A., Vol. XLIV, page 15, 219-241.

[24] Irwin, G.R. (1957), *Analysis of Stresses and Strains near the End of a Crack traversing a Plate*, Trans. ASME, J. Appl. Mech. 24 (3), 361-364.

[25] Joffe, M.W., Kirpitschewa, U.M.A. and Lewitzky (1924), Z. Physik 22, 286.

[26] Kienzler, R. and Herrmann, G. (2002), *Fracture Criteria based on Local Properties of the Eshelby Tensor*, J. Mech. Res. Comm. 29 (6), 521-527.

[27] Lawn B.R. and Marshall, D.B. (1980), *Flaw Characteristic in Dynamic Fatigue: the Influence of Residual Contact Stresses*, J. Am. Ceram. Soc. 63 (9-20), 532-536.

[28] Lawn, B.R. (1983), *Physics of Fracture*, J. Am. Ceram. Soc. 66 (2), 83-91.

[29] Lawn, B.R. (2004), *Fracture of Brittle Solids*, Cambridge Sol. State Science Series.

[30] Levine, I.N. (2009), *Physical Chemistry*, McGraw-Hill, New York.

[31] Lindqvist, M., Vandebroek, M., Louter, C. and Belis, J. (2011), *Influence of Edge Flaws on Failure Strength of Glass*, Glass Performance Days Proceedings, 126-129.

[32] Maugin, G.A. (1993), *Material Inhomogeneities in Elasticity*, Chapman and Hall, London.

[33] Mencik, J. (1984), *Rationalized Load and Lifetime of Brittle Materials*, J. Am. Ceram. Soc. 67, C-37-C40.

[34] Michalske, T.A. and Freiman, S.W. (1983), *A Molecular Mechanism for Stress Corrosion in Vitreous Silica*, J. Am. Ceram. Soc. 66 (4), 284-288.

[35] Mould, R.E. and Southwick, R.D. (1959), *Strength and Static Fatigue of Abraded Glass under Controlled Ambient Conditions: II*, J. Am. Ceram. Soc., 42, 582-592.

[36] Orowan, E. (1948), *Fracture and Strength of Solids*, Reports on Progress in Physics XII, 185-232.

[37] Overend, M. and Zammit, K. (2012), *A Computer Algorithm for Determining the Tensile Strength of Float Glass*, Eng. Struct. 45, 68-77.

[38] Pallares, G., Grimaldi, A., George, M., Ponson, L. and Ciccotti, M. (2011), *Quantitative Analysis of Crack Closure Driven by Laplace Pressure in Silica Glass*, J. Am. Ceram. Soc. 94 (8), 2613-2618.

[39] Parker, E.R. (1960), *Status of Ductile Ceramic Research*, Am. Soc. Testing Mats., 52.

[40] Ronchetti, C., Lindqvist, M., Louter, C. and Salerno, G. (2013), *Stress-Corrosion Failure Mechanisms in Soda-Lime Silica Glass*, Eng. Failure Analysis, to be published.

[41] Ronchetti, C. and Salerno, G. (2013), *Structural Glass Lifetime Prediction Model based on Environmental Variables*, COST Action TU0905, Mid-term Conference on Structural Glass, Poreč, 205-214.

[42] Tomozawa, M. (1998), *Stress Corrosion Reaction of Silica Glass and Water*, Phys. Chem. Glasses 39 (2), 65-69.

[43] Veer, F. (2010), *Corrosion effects on Soda-Lime Glass*, Proc. of Challenge Glass 2 - 2010 - TU Delft, Netherlands.

[44] Westergaard, H.M. (1939), *Bearing Pressures and Cracks*, J. Appl. Mech., 61, A49-A53.

[45] Wiederhorn, S.M. (1967), *Influence of Water Vapor on Crack Propagation in Soda-Lime Glass*, J. Am. Ceram. Soc. 50 (8), 407-414.

[46] Wiederhorn, S.M. and Bolz, L.H. (1970), *Stress-Corrosion and Static Fatigue of Glass*, J. Am. Ceram. Soc. 53 (10), 543-548.

[47] Wiederhorn, S.M. and Townsend, P.R. (1970), *Crack Healing in Glass*, J. Am. Ceram. Soc. 53 (9), 486-489.

[48] Wiederhorn, S.M. (1971), *A Chemical Interpretation of Static Fatigue*, J. Am. Ceram. Soc. 55 (2), 81-85.

[49] Wiederhorn, S.M., Fett, T., Rizzi, G., Fünfschilling, S., Hoffmann and M.J., Guin, J.P. (2011), *Effect of Water Penetration on the Strength and Toughness of Silica Glass*, J. Am. Ceram. Soc. 94 (S1), S196-S203.